Investigation of Different Clutch Material for Minidor, Force Three Wheeler

Rediet Tadiyos Feleke

A thesis submitted to Department of Mechanical Engineering

School of Mechanical, Chemical, and Material Engineering

Office of Graduate Studies

Adama Science and Technology University

November 2022

Adama, Ethiopia

Investigation of Different Clutch Material for Minidor, Force Three Wheeler

Rediet Tadiyos Feleke

Advisor Dr. G.M. Sayeed Ahmed

A thesis submitted to Department of Mechanical Engineering

School of Mechanical, Chemical, and Material Engineering

Office of Graduate Studies

Adama Science and Technology University

November 2022

Adama, Ethiopia

DECLARATION

I hereby declare that this Master Thesis entitled “Design and Simulation of Single Plate Minidor, Force Three wheeler clutch” is my original work. That is, it has not been submitted for the award of any academic degree, diploma or certificate in any other university. All sources of materials that are used for this thesis have been duly acknowledged through citation.

Redet Tadiyos Feleke ______________ ___________________

Name of student Signature Date

RECOMMENDATION

I/we, the advisor(s) of this thesis, hereby certify that I/we have read the revised version of the thesis entitled “Design and Simulation of Single Plate Minidor, Force Three wheeler clutch” prepared under my/our guidance by Rediet Tadiyos Feleke submitted in partial fulfilment of the requirements for the degree of Mater’s of Science in Automotive Engineering. Therefore, I/we recommend the submission of revised version of the thesis to the department following the applicable procedures.

Dr. G.M. Sayeed (PhD)	______________________	_______________
Advisor	Signature	Date
_________________________	______________________	_______________
Co-advisor	Signature	Date

APPROVAL PAGE OF MSc THESIS

I/we, the advisors of the thesis entitled "Design and Simulation of Single Plate Minidor, Force Three wheeler clutch" and developed by Rediet Tadiyos Feleke; hereby certify that the recommendation and suggestions made by the board of examiners are appropriately incorporated into the final version of the thesis.

Dr. G.M. Sayeed (PhD)	______________________	_______________
Advisor	Signature	Date
________________________	______________________	_______________
Co-advisor	Signature	Date

We, the undersigned, members of the Board of Examiners of the thesis by Rediet Tadiyos Feleke have read and evaluated the thesis entitled "Design and Simulation of Single Plate Minidor, Force Three wheeler clutch" and examined the candidate during open defense. This is, therefore, to certify that the thesis is accepted for partial fulfilment of the requirement of the degree of Master of Science in Automotive Engineering

________________________	______________________	___________________
Chairperson	Signature	Date
________________________	______________________	___________________
Internal Examiner	Signature	Date
________________________	______________________	___________________
External Examiner	Signature	Date

Finally, approval and acceptance of the thesis is contingent upon submission of its final copy to the Office of Postgraduate Studies (OPGS) through the Department Graduate Council (DGC) and School Graduate Committee (SGC)

______________________	_________________	________________
Department Head	Signature	Date
______________________	_________________	________________
School Dean	Signature	Date
______________________	_________________	________________
Office of Postgraduate Studies, Dean	Signature	Date

ACKNOWLEDGMENT

First, I would like to thank almighty God for giving me everything. The successful completion of a thesis mostly requires help and cooperation from other people. Here, I would like to express my heartiest gratitude to my Advisor Dr. G.M Syeed (Phd) for his generous support, guidance, and continuous encouragement throughout this thesis work. I would like to thank my beloved family for their support and appreciation throughout the completion of this paper. I would also like to thank Mr. Garbe Chekulu and Mr. Adane Gashu for their technical guidance and valuable comments. Finally, I would like to thank my friends and colleagues for their support and constructive advice.

TABLE OF CONTENT

Content page

LIST OF TABLES

LIST OF FIGURES

ACRONYMS

CFD	Computational Fluid Dynamics
CVT	Continuous Variable Transmission
FEM	Finite Element Method
FEA	Finite Element Analysis
HAST	Highly Accelerated Stress Testing
IC	Internal Combustion
NVH	Noise, Vibration and Harshness
PID	Proportional Integral Derivative
PPCA	Pressure Plate Cover Assembly
RMS	Root Mean Square
RSM	Response Surface Methodology
TWV	Three-Wheeled Vehicles
THB	Temperature/Humidity Bias
3D	Three Dimensional

SYMBOLS

σ	Strength
ρ	Density
E	Elastic modulus
Q gen. f	Heat generated from the flywheel,
Q gen. c	Heat generated from the clutch disc
Q gen .p	Heat generated from the pressure plate
Vs/ ωs	Sliding speed
K	Thermal conductivity
c	Specific heat
n	Number of contact surface
R_m	Mean radius of the friction surface
r_o	Outer radius
r_i	Inner radius
W	Load
C	Pressure intensity
P_{avg}	Average pressure
μ	Coefficient of friction
F_s	Safety factor
ε	Relative error
V	Total volume of wear debris produced
L	Sliding distance

ABSTRACT

Three-wheeler is the most popular and favorite road transport user's way and has an important role for transporting people, goods and property, short distances all around the world. The number of three-wheeler in Ethiopia is growing significantly every year to meet the needs of passengers. In Ethiopia, passengers are usually use three-wheeler for traveling because of its availability and economically inexpensive. Three-wheeler, usually named as Minidor, Force Bajaj, are gaining popularity in our country Ethiopia due to the assembling company were found around central Ethiopia, Mojo. ***.*** *These vehicles give short distance transportation, there is frequent speed variations. Increasing the engine speed too high engages the clutch causing excessive clutch plate wear and slippage occurs due to loading condition the pressure contact between the contacts surfaces that occurs due to the axial force applied the diaphragm spring. This thesis work focuses on Investigation of Different Clutch Material for Minidor (Force) Three Wheeler. By re modelling the Minidor (Force) three wheeler clutch using CATIA V5, then performing dynamic test on the clutch model using LS DYNA software. After performing dynamic test identifying the critical zones of clutch on the three wheeler to make modification on the identified critical zone of the clutch, and then test the effect of the modified clutch for better performance. From the result it has been obtained 11.03% temperature reduction and the amount of wear debris removed is 0.00319mm*^{3} *lining of clutch have been improved from existing Minidor clutch by the modification made. The investigation of clutch lining material FE simulation regarding effect on human health is very fruitful results as thermal test. Force three wheeler should be fitted with the modified clutch futures implemented on this thesis work.*

Keywords*: Dynamics, Investigation, Modification, Resonance, Significance, Simulation*

CHAPTER ONE

INTRODUCTION

1.1. Background of the Study

Clutch is one of the essential components in automobiles. It is located between the engine and the gearbox. The main function of the clutch is to initiate the motion or increase the velocity of the vehicle by transferring kinetic energy from the flywheel. Clutches has designed to transfer maximum torque with minimum heat generation. During engagement and disengagement, the two clutch discs has the sliding motion between them (Sagar, 2022).

Single plate clutch has mainly used in lightweight vehicles for transmitting torque from an engine to the input shaft. As per the name of this Clutch, it just has a single Clutch plate.

Single Plate Clutch system comprise of flywheel, clutch disc plate and friction material, pressure plate, clutch cover, diaphragm spring and the linkage necessary to operate the clutch. The clutch engages the transmission gradually by allowing a certain amount of slippage between the flywheel and the transmission input shaft. However, the slipping mechanism of the clutch generates heat (Mahendra, 2018)

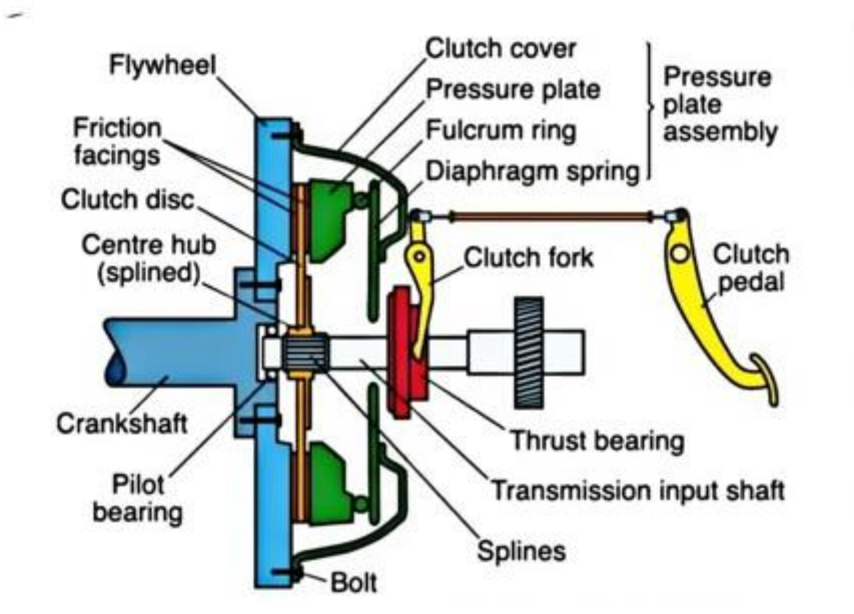

Figure 1.1. Single plate clutch

https://images.app.goo.gl/orcyVuDBB4cQgMic9/ www.automobileinformer.com

The clutch disc is a coupling between the engine and transmission. It has used to transmit torque when tightening and to block torque transmission when loosening. Common pads are prepared from organic materials that give coefficients of resistance more than 0.27. If the temperature of the two pad is too high, gas evolution has observed which lubricates the pad area and reduces this coefficient of friction. This causes the clutch to slip and prevent the clutch from transmitting engine torque.

Clutch works on the principle of friction. When two friction surfaces are brought in contact with each other and pressed they are united due to the friction between them (Ravikiran and Sarje, 2015). The friction between the two surfaces depends upon the area of the surfaces, pressure applied on them and co-efficient of friction of the surface material. The two surfaces can be separated and brought into contact when required. One surface is considered as a driving member the other as a driven member. The driving member is kept rotating, when the driven member is brought in contact with the driving member it also rotates. When the driven member is separated from the driving member it does not rotate (Pooja et al., 2014).

Mechanical engagement generates frictional heat at the contact surfaces due to sliding between the surfaces. Thermal deformation of the friction surface of friction discs, plates and flywheels have caused by high heat and pressure distribution on the friction surface. Excessive thermal overload on the friction surface can cause casting distortion, wear and surface cracking due to excessive heat dissipation. In this fourth case, premature failure of the clutch can lead to malfunction of the clutch system, resulting in vehicle torque not being transferred to the road, leading to end-user complaints. Below the bursting pressure plate section.

For that reason, it is compulsory to identify the temperature exchange at the contact faces to prevent premature failure of the clutch system. Clutch failure and damage due to excessive frictional heat and thermal fluctuations of the clutch pressure plate and flywheel are common to all types of clutches. Failure modes due to pressure and heat distribution have been identified by several researchers (Zhao et al., 2016).

1.2. Statement of the Problem

As we see, the transportation system Bajaj or three wheelers are expanding in most towns even in rural areas of Ethiopia. They give short distance transportation system. So now and then there is braking or accelerating. The overall parts of automotive, besides engines, there are more crucial parts that engineers need to look into consideration. Suspension, brake, electrical, hydraulic and gear are all the crucial systems in the automotive areas. Each of all system has their own functionality that brings life to the automation industries. Clutch is the toughest working part of vehicle with a manual transmission. One or more friction discs have joined or pressed against a flywheel using springs. Clutch plates found in three wheelers are made of asbestos. . When the clutch pedal is depressed, the spring pressure is released pushing or pulling the diaphragm of the pressure plate. Thus, the friction plate is released and allowed to rotate freely. The clutch plate used to increase or decrease the speed of a vehicle. However, increasing the engine speed too high engages the clutch. This, in turn, causes excessive clutch plate wear and slippage occurs due to loading condition the pressure contact between the contact surfaces that occurs due to the axial force applied the diaphragm spring.

1.3. Objective

1.3.1. General Objective

The general objective is investigation of different clutch disk material for Mindor, Force three-wheeler

1.3.2. Specific Objective

The specific purpose of this study is:

- To investigate the existing clutch material
- To isolate the drawback of the existing material
- To check different clutch material
- To compare with the existing material
- To select the best material

1.4. Scope and Limitation of the Study

This study basically concentrates on studying the lining material effect of clutch disc by considering during Minidor, Force TD 499 LC 15^{o-}DI three wheeler transportation at maximum speed by using existing clutch as well as new ones at engaging condition. This study doesn't consider the effects grooves depth and thickness during heat dissipation. CATIA was used for designing the components and LS_DYNA for numerical analysis to study dynamic simulation in this work. Finally, the newly designed clutch system is compared with the conventional one.

1.5. Significance of the Study

This study has aimed to give better riding comfort by reducing vibration effect of Bajaj on the driver and passenger by improving the clutch spring material and suggesting which load and speed is better and minimize sound pollution caused by noise and vibration of the car. In addition, minimize the hazard caused by asbestos by choosing the suitable material.

1.6. Organization of the Study

This thesis organized in to five chapters. In the **first chapter**, background and justification of thesis work and the objectives to be achieved, are discussed. In **chapter two**, a review of literature relevant to this thesis work, which has been investigated by different researchers, is given. Materials and Methods used to complete this work are discussed in **chapter three**. Next, in **chapter four** finite element methods and conditions are discussed. Three dimensional finite element analysis is done by ANSYS and LS DYNA workbench. Also different dynamic and thermal boundary and conditions are discussed in detail. In **chapter five** results of the analysis are summarized and discussions are made based on the outputs of the finite element method. In addition, comparison of existed and modified results is made. Finally, **chapter six** gives conclusion achieved from this thesis work and proposed future work in this field of study.

CHAPTER TWO

LITERATURE REVIEW

2.1. Introduction

To gain a deeper understanding of this research issue, It is important to review some links and test different software used in this area. Therefore, in order to understand the concepts, principles, and methodologies that are important for the development of knowledge-based systems, I refer to related literature such as books, articles, and other sources taken from the Internet.

2.2. Clutch Design Parameters

RSM has applied in this experiment. In this work, Design Explorer was used to integrate the FEM and experimental design to optimize the design of the damping clutch disc, obtain a target damping curve, and lower the stresses that occur during operation that exist in this approach (Thacker & Vijayaragavan, 2018).

In this article, they investigated the outcome of disc radius on heat flow and temperature distribution in friction clutches. The friction clutch is an essential mechanical element that transfer torque from the engine to the transmission. Therefore, a good approximation of the heat fluctuation and temperature at the clutch disc surfaces is important for better clutch design to prevent thermal stress-induced failures. High temperature creates thermal stresses on contact surfaces. High thermal stress creates a number of defects such as surface cracking and permanent set, ultimately leading to friction material failure rather than expected clutch life. For this reason, examining the factors and their effects on the disc radius of the generated heat is the key to enumerating heat flow and temperature content of clutch friction materials. The effect of (R) on axial force, inner and outer radii, circumferential speed and torque was also investigated. For numerical analysis, MATLAB and ANSYS were used (Oday, 2012).

In this article, they developed a system for testing automotive clutch discs. Due to the large disturbance torque and high requirements for control accuracy, a composite sliding controller based on a Kalman filter have been proposed to control the system. Simulations show that the algorithm has high long-term accuracy, tracking accuracy and high response speed compared to synthetic PID. The Kalman filter controller can suppress random noise and power frequency interference. The measurement results show that the test system is stable and reliable with improved accuracy and efficiency (Tang, 2012).

In this study, a process of convective dissipation accompanies the energy transfer during operation of the friction clutch on the friction surface. In order to improve the operation of the friction clutch, it is important to analyze the maximum temperature rise of the friction surface. Various design options for clutch disc grooves are analyzed using CFD and FEA methods to find the optimal design that provides good airflow around the grooves and can withstand the significant loads generated during mating. As a result, a new clutch disc design featuring a conical groove shape has proposed. Results show that the new design has improved convection between the air and the friction surface, reducing the maximum temperature rise (Porwal et al., 2018).

2.2.1. Requirement

Clutch materials have used in automobiles, railroads, coaches, motorcycles, construction equipment, and the agricultural industry to control speed and gearshifts in a wide variety of vehicles, from tractors to racing cars. Regardless of size or specific parts, there are general recommendations for clutch materials. These materials must be durable and able to withstand the effects of abrasion such as scratches and abrasions. Shift gears generate heat as a by-product, so these materials must accommodate thermal expansion, remain constant over a wide temperature range, and have high heat capacity, good thermal properties, and conductivity. These systems are inherently resilient to high pressures and their ability to withstand high contact pressures is essential to their function. Clutch devices may be exposed to the environment and must be able to withstand moisture, dust, and other environmental factors while providing consistent clutch engagement and disengagement. Many, but not all, components are frequently subject to friction. These specialized components should exhibit all of the above properties while maintaining a high coefficient of friction, which is the ratio of the frictional forces between two bodies in contact with each other. These friction materials are often rough or textured to add friction and increase efficiency. Compressing the clutch pedal or lever generally also compresses a plurality of springs connected to the pressure plate. This pulls the plate and associated clutch disc away from the flywheel, which has bolted to the engine's crankshaft.

This separation stops the clutch disc from rotating and internally separates the central hub of the disc from the input shaft. The driver can then change gears or coast. After shifting, releasing the pedal reengages the clutch disc with the flywheel. The clutch system works to ensure consistent clutch engagement and disengagement. Steel, cast iron, aluminum, and ceramics are common for high-stress, low-friction components such as pressure plates. Asbestos was once the most popular choice for high-friction items, but health concerns have led coupling manufacturers to look for alternatives.

Fives of ceramic, copper, steel, iron, minerals, cellulose, aramid, chopped glass, rubber, and brass are all used in the production of composite clutch materials. These fusions are useful in that they retain the quality, abrasion resistance, and strength of all the powders and fibers used in their formation. These bonding materials are often attached to the metal base via rivets or strong adhesives. Hands-on experience, chemistry, and materials technology are constantly advancing the design of clutch materials. These advancements in result, lower maintenance and operating costs, longer lifespans, improved functionality, and improved overall customer satisfaction.

Design of a single-disc membrane clutch for medium and heavy vehicles. This should have be considered when designing the clutch,

I. The contact surfaces generate friction between the contact surfaces that can withstand and sustain the load at moderately low pressures.
II. Frictional heat must be dissipated quickly and the tendency to seize must be minimized.
III. The surface must be reinforced with a material of sufficient hardness to ensure a sufficiently constant pressure.
IV. Appropriate friction material must be selected to form the contact surface.
V. Couplings must not require external forces to maintain contact and must protect protruding parts. Coupling components should be designed with all these essential parameters in mind (Luniya, 2019).

2.3. Clutch material analysis

Five different materials are used in modern clutch designs (Akshay, 2018):

- "Organic" clutch material, a mixture of fiberglass and other materials (sometimes including brass) molded or woven into the friction surface.
- Kevlar, these are synthetic fibers that guarantee a very durable (and very forgiving) clutch friction lining.
- A ceramic clutch material, usually a mixture of silicon dioxide and various metals and additives, was sintered or brazed to the clutch disc.

- Feramic coupling material. It is very similar to ceramic materials, except that it has a much higher proportion of metal.
- Feram Alloy is a new and excellent alternative to feramic and ceramic coupling materials.

In this study, the stresses of an automotive single plate clutch has analyzed as a function of the material used. Structural analysis of the clutch has performed using the finite element method for an example oppressive vehicle, the Toyota KUN 25. First, the input data for numerical analysis were calculated. Numerical analysis has performed with the ANSYS software package. The result is the value of the stresses and deformations present in the clutch during vehicle operation. In this work, clutch discs for automotive clutch assemblies have designed using different materials and simulated in ANSYS software for comparison. Cermet friction material has selected from these lining materials. The temperature rise between the friction disc and the flywheel was a major cause of clutch wear, but minimized by proper material selection. Good contact pressure also reduces sliding wear (Narayan et al., 2018).

In this work, they considered the material performance of the clutch disc. During engagement, the pressure on the facings caused an enormous amount of wear, quickly degrading the clutch disc material. The idea was to comprehend the behavior of materials and their wear and friction criteria. In this study, a composite clutch disc was tested. Composites were of polymer, ceramic and metal matrix types. Composite materials have used due to their good coefficient of friction and wear resistance. It was important to identify coupling materials with heat-resistant pick friction coefficients (μ) and to determine the optimal composites with low wear rates under various temperature, capacity, and speed conditions. Clutch discs have modeled and analyzed using Creo and FEA software. Experimental studies of discs have performed using a "pin to disc" device to determine the degree of wear and coefficient of friction. As a result, it was found that AL6061 has a extremely low friction coefficient, but a very large amount of wear. Due to the necessity of the clutch disc material S, fiberglass has a significantly higher factor of friction around 0.2 and a very small abrasion volume of 45mm^3 compared to the aluminum matrix. This means that S glass fiber is good for the material of the clutch disc (Bhorkade & Kakade, 2020).

This study focused on the design and analysis of diaphragm springs used to generate the clamping force. The single disc clutch design has created for Force Motors New Vehicle and based on theoretical calculation result. CATIA V5.0 software has used to design the diaphragm springs. To determine the stress distribution; structural analysis was performed on the model.

During analysis, the design has checked for safety and results have compared with theoretical calculations and results. HYPERMESH software has used for static calculations. The results show that the spring material has theoretical and analytical values that are safe for stress analysis, and both values are within 10% of tolerance. Therefore, the theoretically calculated height is accepted, and a deflection slightly above the limit (spring height) is a value does not affect the function of the spring (Rupnar et al., 2016).

Materials such as Kevlar 49 has considered replacing the currently used friction disc material. Theoretical calculations has used to design clutch disc. The single plate clutch has designed and modeled using CREO 2.0 software. Static and dynamic analysis has performed using ANSYS 15.0. As a result, plots of equivalent stresses, strains and total strains of various friction materials for the clutch friction disk have obtained. Uniform wear theory has used for the analysis. Assessment of material usage to identify suitable materials for friction discs completed (Ilie & Cristescu, 2022).

In this article, we investigated ways to reduce premature failure of damper springs subjected to static and cyclic loading conditions by analyzing the driven plate assembly (D.P.A.) of a clutch that failed frequently during service. Engine power has transferred to the structure through the clutch. Malfunction of this essential part in operation could bring down the entire application. This analysis has performed on the active plate of a clutch used in a TATA vehicle. Here numerous conditions about clutch failure under high loads. The damper springs in the drive plate assembly typically fail during operation due to repetitive loads. Because of this**,** they designed and modeled the damper spring in Pro-E and analyzed it in the FEA package, but the actual design has modified to lower the failure value. The actual spring model results show that the determined shear deformation is very close to the theoretical shear stress. Find different values of Max from his FEA analysis of the modified model. Shear stress, maximum deformation and safe spring life. Increasing the wire diameter from 5.385 to 5.893mm significantly reduced the shear stress value from 1339MPa to 856MPa for model 1 and improved the maximum safe life between 3116 and 14880. The strength of the spring is affected by the difference in the spring wire diameter, and at pick diameter the spring may lose its elasticity and become unsuitable for use (Banker et al., 2020).

2.4. Previous Work

Design demonstration and finite element analysis of automotive clutch design. The design consists of a clutch disc, a pressure plate and a disc spring. The materials of the three parts are low carbon steel, cast iron GS-70-02 and spring steel. Structural analysis of each part has performed. Graphs of equivalent stress, total deflection and factor of safety were find and examined. Finite element analysis was performed in pre-processing, solution, and post-processing. The analysis used permanent wear theory. Solid Works Office Premium and ANSYS programs have used for design and analysis. The outcomes shows that the proposed friction clutch construction was good throughout investigation of stress and deformation of dry friction clutch system (Rupnar et al., 2016).

The optimization of rigid clutch disc geometry and design elements using FEM had been described. A numerical method has presented to calculate the stress and vibration properties of rigid clutch discs. Two types of rigid clutch discs have studied a reference model and a newly proposed model. The effect of the newly proposed ideal have contrasted with existing models. Optimization of rigid clutch disc geometry and design elements using FEM has been described. A numerical method has presented to calculate the stress and vibration properties of rigid clutch discs. Two types of rigid clutch discs have studied, a reference model and a newly proposed model. The outcome of the newly proposed idea were contrasted with existing one (Abdullah et al., 2013).

Illustration of numerical parameters of the mechanical properties of dry contact slip at the brake pad interface have studied. Determination and picturing of structural deformation due to sliding contact between disk and pad has demonstrated. Stress evolution at rotating disc and ring bodies has calculated using a mesh model. A convergence examination has planned to value the effect of the grid on the validity of the numerical answer. Using the developed model, the effect of design variables on the results has evaluated by the finite element method. They investigated the effects of fine mesh, lining substance, elastic modulus of lining substance, friction coefficient, and disc rotation velocity on the calculation results (Belhocine & Omar, 2016).

A variety of materials are selected and the suitability of two conventional and one unconventional materials used for couplings is evaluated. It has been shown that non-traditional materials (composites of aluminum matrix and ceramic particles) can be used in bonded parts to improve mechanical and thermal properties (Glodova et al., 2014).

A clutch assembly has designed and a finite element analysis has performed on the clutch assembly. Equivalent stress, total deflection and factor of safety diagrams are obtasined and the design is optimized to achieve a safe coupling design, as described in another study (Purohit et al., 2014).

The clutch thermal model has changed to computer code for engine control unit (ECU) implementation. Clutch thermal overload protection has been shown to extend drivetrain life, especially for dry clutch discs, without changing drivetrain mechanical components (Gunes, 2015).

Research on the design and physical analysis of single-plate clutches. Understanding thermos elasticity is important when designing friction clutches. A stress analysis of an automotive single-disc clutch has shown. Use software to try to minimize stresses and forces on the clutch disc. Software pro-e and ANSYS have used for modeling and analysis. Depend on the values, they rich the equivalent stress result for the assumed loading situation is less than the allowable stress for the particular situation. Therefore, they found a clutch design that is well designed, efficient and reliable. (Vishal et al., 2013).

Using the unit wear theory, we present the optimization of multi-disc friction clutches for maximum torque transmission capacity. The uniform wear theory have used to explain the optimal values for multi-plate clutches. Techniques aimed at optimization were stochastic programming and geometric programming. In existing exercise, tolerances make design variables probabilistic. This gives a reasonable consideration when designing (Agrawal et al., 2014).

This study investigates the effects of mechanical vibration on driver health. In this study, the mean square value (RMS) of vibration for a specific period of engine operation was calculated. They investigated the effect of engine speed and load on engine vibration in two modes, with and without a balancer. As a result, they find that at full engine load, vibration increases in both observed modes with increasing engine speed. With a balancer, vibrations have reduced by an average of 22.3%.At constant speed, the oscillation increased in both observed modes as the load increased. By balancing with a speed of 1400 rpm and a torque of 125 Nm, the RMS secondary vibration has reduced by 38.9%. In addition, at 250 Nm, the RMS oscillation has reduced by 21.3% compared to the unbalanced mode. At full load and variable speed, the balancer reduced vibration by an average of 29%. Balancers have proven to be more efficient at low torque (Farrokhi et al., 2021).

In this study, Multi-plate clutches are widely used in high-speed and heavy-duty vehicles where high torque transmission is required and space is limited. This work illustrate, an empirical formula has used to construct a multi-disc clutch. A multi-plate clutch model was formed using CATIA V5 and bring it into ANSYS Workbench for Vehicle Uses. They performed a structural analysis by changing the friction surface material and using aluminum as the base material. Following the results, an analysis of the clutch has performed using ANSYS Workbench software to determine which materials were more effective in facing the friction surfaces, thus improving the multi-disc clutch face material. I made a distinction between both ingredients to justify. Analysis results show that the maximum shear stress, von Mises stress, and total strain values of the hybrid SF-BU are smaller than the corresponding LO31 results. Therefore, they decided that it was more advantageous to use a multi-disc clutch as the SF-BU hybrid friction material than to use LO31 as the friction material (Raut et al., 2013).

In this article on microstructure observation and study of the properties of friction and wear-resistant materials, the results show that the film and air cushion film undergo direct thermal decomposition, and that the transfer film has a positive effect on the coefficient of friction, thermal wear and abrasive wear. Mainly indicates adhesive wear when recording temperature conditions (Shi et al., 2018).

This paper discusses stress and deformation in coupled systems. (Pressure plate, clutch disc, flywheel) were examined based on the contact pressure of the diaphragm spring and the centrifugal force when the clutch disc is fully engaged (assuming no slippage on the contact surfaces). This study deals with the effect of the contact stiffness factor FKN on the pressure distribution, stress and deformation between the contact surfaces. Penalty and extended Lagrangian algorithms should be used to obtain the pressure distribution between the contact surfaces and numerical calculations should be performed in ANSYS13 software (Abdullah et al., 2013).

A transmission is a machine within a power transmission system that provides a controlled application of electrical power. Often the term gearbox simply refers to a gearbox that uses gears and gear trains to provide speed and torque conversion from one rotary power source to another. The transmission also offers a reverse gear to bring the vehicle backwards. A CVT provides the automatic ability to change gear ratios in response to different engine load conditions. Despite being an automatic transmission, the CVT has few moving parts and a simple and compact design. Metal belts and variable pulleys are one of the most common types of his CVTs widely used in automobiles because of their high low-speed gear ratios for good acceleration and low overdrive ratios for good fuel economy. CVTs have these advantages, but they produce less torque at lower engine speeds. This is because the belt slides on the conical surface of the variable pulley. Therefore, mechanisms with starting gears driving pulleys should be introduced and developed to reduce belt slippage and increase torque at low speeds to overcome this problem (Santosh S., 2019).

This article reviewed the simulation and analysis of single-plate clutches used in Tata Sumo vehicles to select suitable materials to reduce wear and increase clutch life. Static and dynamic analysis of the clutch disc has performed using Finite Element Analysis (FEA). The 3D solid model has created by CATIA V5 R16 and imported to ANSYS Workbench 19.0 for structural, thermal and modal analysis. Mathematical modeling was also performed using six different materials (e.g. steel, stainless steel, ceramic, Kevlar, aluminum alloy, and cast iron).A material comparison was then performed based on the results to demonstrate the improved lining material for clutch using ANSYS Workbench 19.0. Because of this study, the same compressive strength of 0.5 N/mm2 has obtained for different materials. Heat flow, total strain, stress, strain and first six mode frequencies have observed for various materials. By contrasting the presented value, it was obvious that ceramic had smaller warp and less modal frequencies than all other (Kedar, 2020).

Clutches are a very important part of the proper functioning of a vehicle's powertrain. Moreover, have subjected to high pressure, torsional and thermal loads. Therefore, it is necessary to select and design the clutch friction material. The goal is to select the optimal friction material. Performance has checked under ANSYS stress and thermal loads. A few materials have selected, some of which are old materials, and the performance of new materials has evaluated and compared to old materials. The first choice is the brand of the chosen vehicle and its clutch plates to create design limits. Various axial loads are then determined according to the theory of constant pressure and wear in a constant torque transmission state. FEM from ANSYS and solid models from Solid Works complete analysis. Finally, the results of the friction linings of various materials and their corresponding performance are organized and detailed, and at last, conclusion drawn as which materials are best suited for light commercial vehicle clutch friction linings. Identified methodology to extend research scope and findings to other vehicle models (Virmani et al., 2021).

A vibration analysis of friction disc were done to investigate effects of different factors such as lining thickness, type, and dimensionless radius ratio R on the natural frequencies of the clutch discs. Vibration characteristics were determined using a three-dimensional model. Related to the design and development of mechanical parts such as dry friction clutches, these parts have considered a key element in torque transmission from the engine to the transmission in order to advance ride and driving comfort of the vehicle. Finite element studies are used to model friction clutch disks and display their natural frequencies and mode shapes. Natural frequency calculations have developed for friction linings of various thicknesses and material morphologies. In addition, they investigate the consequence of R (found as the ratio of the inner and outer disc radii) on the vibration behavior. Numerical calculations have performed with ANSYS/WORKBENCH 13. As a result, it was found that the natural frequency rises with increasing R, and this increase frequency rate depends on the value of Young's modulus and the density of the friction material. As the thickness of the friction material increases, the natural frequency decreases due to the increased mass of the clutch disc. Also, as the number of modes increases, the gap between the natural frequencies increases (Abdullah & Schlattmann, 2012).

The section "Modeling and Analysis of Friction Clutch in Transmission to Suppress Jerk of Car at Startup" section analyzes the variable nature of the response of the clutch disc when starting the car. Based on the developed nonlinear multi-particle dynamic model of the friction clutch disk with four degrees of freedom, the self-excited vibration characteristics of the clutch disk have studied using the stick-slip-slip study and the Carnopp friction model. Self-excited oscillations cause negative damping due to negative friction gradients. When the clamp has forced to vibrate with the same function as the clutch disc, a resonance condition has created which causes the transmission to tilt. They concluded that vehicle sway could be suppress by improving the vehicle's friction surface and changing the transmission coefficient so that the natural frequency counteracts pressure fluctuations. According to their observation, vibration reduction is achieved to some extent by increasing the moment of inertia, torsional stiffness, viscous damping of the clutch disc, or by decreasing the axial stiffness of the waveform (Dhengre et al., 2018).

Wear maps for specific material combinations have used to indicate the prevailing wear processes and severity over a specific range of sliding conditions. Wet clutches are one application that can use these cards. In this operation, a copper-based friction material has slid over alloy steel in a ring-to-ring braking simulator. Wear maps based on the measured wear rates have divided into super soft, normal and heavy wear modes. The dominant wear mechanisms controlling these wear patterns are also discussed. Based on the data obtained, we constructed a linear equation representing the transition boundary between the wear modes (Gong et al., 2015).

Clutch charge control in clutch shift transmissions has a significant impact on shift quality. The oncoming clutch must be synchronize with the release of the oncoming clutch for smooth gear shifting. Therefore, when the allowable torque was close to zero at the end of the clutch-charging phase, the gap between the piston and the clutch disc must have be eliminated. Open loop control has usually implemented to fill the clutch due to the cost of the pressure transducer. Poor control accuracy can cause under fill or overfill, which reduces shift quality. This paper presents a mathematical model of an electro-hydraulic clutch switching control system. After that, special performance parameters have provided for optimal control of clutch charging. To eliminate obvious discrepancies between transmissions due to manufacturing or assembly errors, an automatic method for predicting initial charge control parameters have proposed. To prevent under fill and overfill, a fuzzy adaptive control method has proposed in which the clutch filling parameters are self-adaptive and continuously adjusted. Vehicle tests had shown that the use of fuzzy adaptation ensures that the quality of gear shifting remains constant even after a change in transmission condition (Guo et al., 2014)**.**

The characteristics of the coefficient of friction change associated with clutch engagement have explored. The damping coefficient of the transmission system with wet clutch, the moment of inertia of the drive disk, the stiffness of the transmission shaft, the law of change of the dynamic coefficient of friction during vibration and the effect on the meshing change have also analyzed. . It has been shown that change in oscillations occur and increase because of a fixed speed differential and a larger dynamic coefficient of friction gradient over time. Vibration has reduced by appropriately increasing the damping factor, the moment of inertia of the drive and driven disk, and the stiffness of the drive shaft (Zhigang, 2021).

The effect of heat on the clutch have investigated in this thesis. One of the major causes of clutch failure has identified as the significant thermal stresses that occur between the components because of frictional temperatures during slip. The finite element method has used to analyze the transient thermos elastic phenomena of dry clutch. They investigated how boundary conditions affect the contact pressure, temperature range, and heat flux distribution created along the friction surface. Analysis has performed using a two-dimensional axisymmetric model used to model the clutch element. An ANSYS program has used for numerical calculations. As a result, it has found that the maximum value of the contact pressure increased with time, while the contact area decreased with time. The maximum contact pressure values obtained were 3.38 MPa and 3.29 MPa, respectively, corresponding to the sides of the flywheel and pressure plate (Abdullah, 2014).

Development and validation of numerical tools that has used to model these abuse scenarios. We are investigating a scenario where the vehicle suddenly engages the clutch in first gear while it is stationary. The numerical model has been validated based on experimentally calculated torque data and shows the best agreement. A multi-parametric study has also performed using numerical tools to obtain the key transmission parameters that affect the amplitude of the generated torque (Bingham et al., 2016).

The axisymmetric finite element model has improved to obtain a numerical solution to the thermal complexity of the appropriate friction clutch, and various approaches have used to calculate the surface temperature of the friction disk. As a result, the maximum surface temperature has obtained at the contact of the friction surfaces with single bonding and frequent bonding. Two methods have used to model the thermal model of the automotive clutch to obtain the temperature field: the thermal separation method and the general thermal method. To investigate the thermal behavior of friction clutches under repeated actuation, an analysis has performed using an advanced axisymmetric finite element model. To demonstrate the accuracy of each approach, temperature distributions have compared based on the target approach. We found that the thermal distribution approach was not accurate for investigating thermal problems in clutches with multiple engagements (Abdullah et al., 2018).

Numerical simulations performed for specific types of vehicle clutch shifting based on the dynamic friction transmission mechanism of the wet clutch and the dynamic model of the vehicle's four-speed system. Degrees of freedom, influence of damping coefficient of wet clutch transmission system, moment of inertia of drive pulley, moment of inertia of driven pulley, stiffness of transmission shaft and effect on friction and layer interaction Law of dynamic coefficient variation. The amplitude of clutch shift vibration have effectively minimized to increase the damping coefficient, the moment of inertia of the drive and driven pulleys, and the rigidity of the drive shaft. If there is a large difference in the slope of the coefficient of dynamic friction with respect to time under predetermined switching conditions, turn-on oscillation occurs and the output signal increases. Dynamic friction coefficient studies can accurately analyze clutch engagement oscillations that are key to optimizing automatic transmissions (Zhang et al., 2021).

Single and double dry clutches are widely used in automotive transmissions due to their reliability and economy, low fuel consumption and pollutant emissions. A precondition for achieving the goal in automatic manual transmissions is the implementation of a "good" clutch model and the development of a stable control strategy. The purpose of this article is to study the clutch transmission models and mesh control strategies proposed in recent years. It provides an overview of dry clutch torque modeling and analyzes the main factors affecting torque transmission, including temperature, sliding speed, contact pressure, and wear. It then discusses strengths and weaknesses of common clutch actuator architectures and control strategies, as well as open questions. The survey ends with proposing some interesting topics for future research (Della et al., 2018).

To design and optimize coil springs Pareto Set software is used. Both conventional steel springs and composite springs are optimized and distinguished by different spring parameters (inner diameter, outer diameter, pitch, wire diameter, etc.). The algorithm has run on three different composites: carbon, Kevlar, fiberglass and epoxy. Composite design optimization considers constraints such as deflection, frequency, maximum stress, and loading conditions. Carbon fiber composites optimize both weight and stiffness, whereas glass fiber composites only optimize stiffness. Therefore, it is preferable to use composite springs over steel springs (Zebdi et al., 2019).

In powertrain modeling, torsional vibration analysis, and optimization of clutch damper factors to reduce gear rattle during vehicle creep conditions. The transient response predicted by the model indicates that the drive train has subjected to strong torsional vibrations and gear chatter phenomena. Analysis revealed that the clutch damper behaved like it jumped between the stiffness of the first stage and the stiffness of the second stage that causes this problem in creep conditions. In order to solve this problem, the innovative 3-stage rigid clutch damper has proposed. It has seen that the strong vibration of the drive train and the gear rattle phenomenon have effectively suppressed. Finally, conclude that Clutch damper settings can have a significant impact on powertrain vibration and gear chattering, and we used a clutch damper with three levels of rigidity to effectively eliminate gear chattering during vehicle slipping (Wu et al., 2016).

As demands for vehicle comfort, performance and fuel efficiency increase, transmission solutions become more complex. The solution is an automatic manual transmission (AMT). It works like a traditional manual transmission, but a computer controls clutch and gear selection. In this way, high efficiency with increased comfort and productivity has achieved. Therefore, the torque transferred by a slipping dry clutch has investigated in a test using a heavy truck (HDT). Material expansion with temperature has shown to describe torque differences up to 700 Nm where clutch actuator position is unchanged. The dynamic model was tested experimentally and the transmitted torque error decreased from 7% to 3% of the maximum motor torque compared to the static model (Myklebust, 2013).

Transient dynamics mesh model that can used to analyze powertrain rotation under various mesh conditions have presented in this paper. Various release situations have simulated using mathematical model. This model used to calculate the angular acceleration of the clutch shaft based on the trajectory imposed on release bearing as well as the nonlinear disc spring behavior. This model can also use to determine clutch shaft angular velocity and displacement, total slip time, and clutch disc slip angle. By implementing this model, a full simulation of clutch engagement dynamics would be performed for various membrane spring characteristics and clutch release arcs (Zhao et al., 2014).

Mathematical model was developed for transient engagement dynamics that describes features of spring, clamp load, pressure plate travel and release bearing motion, clutch pedal kinematics while engaging, vehicle power through launch Parameters such as train dynamics are associated. Using this model, clutch engagement time has simulated along with building clamping force and torque transfer to the drive train. Simulation results have validated by real tests. This analysis helps design release mechanisms for smooth clutch engagement and compare slip times for different clutches (Dutta & Baruah, 2014).

In rotating systems, the frictional torques developed between the flywheel, clutch disc and the pressure plate are modeled separately. This new approach of developing separate friction models helps to understand the variations in torque capacity due to friction heat and friction lining temperature rise due to engine heat. This article proposed a rare method of modeling a dry plate clutch using Simulink and the Sims Cape workbench. The clutch model has divided into two subsystems: translation and rotation. Individual models of translational and rotational systems contribute to understanding the detailed dynamics and interactions within subsystems. A translational system is a linear system of a membrane and a damping spring as a system with two degrees of freedom. Based on the experimental data, the nonlinearities of the membrane and cushion spring were calculated. This allows simulating the change in friction torque when the clutch has engaged. The change in abrasion coefficient with temperature rise has considered depend on experimental facts. The simulated model was under a variety of conditions (normal and worst case driving conditions) resulting in clutch overheating after multiple starts at 30% slope, although the reduction in torque capacity is acceptable under normal driving conditions was shown (Penta et al., 2017).

Stress and deflection were determined during static and dynamic analysis of a single disc clutch. The analysis has performed using composite materials, but the materials currently used for friction discs are cast iron and aluminum alloys. Composite materials have considered due to their high strength-to-weight ratio. E Glass Epoxy and Aluminum Metal Matrix Composite were materials used in this work. The single disc clutch has designed and modeled in Creo 2.0 software. Static and dynamic analyzes of the couplings were performed on determining the stresses and deflections of gray cast iron, aluminum alloy 7075, E-glass epoxy, and aluminum metal matrix composites. Analysis has performed in ANSYS. A theoretical calculation has performed to determine the stress. Static analysis results indicated that the analyzed stress values were lower than the respective yield stress values of aluminum alloy 7075, aluminum MMC, and E-glass epoxy. The material is therefore safe to use. Comparing results between materials, E-Glass epoxy is advantageous over other materials due to its lightweight and high strength. Theoretical calculations have performed to determine the stresses of all materials. For all materials, the stress values are lower than their respective allowable stress results. Observing the E-Glass-Epoxy results show lower stress readings (Sreevani, 2015).

An efficient and reliable analytical technique for mechanical coupling design using computer modeling and numerical techniques has described in this article. This work involved a stress analysis of an automotive single-disc clutch and attempted to reduce the stresses and forces developed in the clutch using a software approach. When designing automotive friction clutches, knowledge of thermoelasticity during the initial design stages was invaluable. In particular, the design of mechanical couplings, due to their durability and compactness, requires accurate prediction techniques for maximum structural stress. Detailed clutch studies and Clutch modeling is done in Pro-e software and analysis is done in ANSYS software. Also in this work, an efficient and reliable construction of the mechanical clutch was found (Deshbhratar and Nagnath, 2013).

To improve the structural, thermal and vibration properties of friction linings; single disc clutch was modeled and analyzed using ANSYS. Thermal analysis to reduce heat generated between friction surfaces. In addition, to reduce temperature rise during steady state periods. Structural analysis has performed to minimize stresses due to load contact between friction surfaces. Modal analysis has performed to optimize the frequency range of the engine and the natural frequency of the friction disk to avoid resonance. System optimization has performed in two ways to obtain a set of Pareto optimal points. Verifiable outcomes have obtained using multi-target optimization, multi-target genetic algorithm (MOGA), and single-target optimization, nonlinear programming with second-order Lagrangian (NLPQL). The result is a 27.61% improvement in output frequency outside the motor's frequency band. (Venkiteswaran et al.,).

$$q(t) = \frac{\emptyset(t)}{s} \quad (2.1)$$

Where: Φ(t): The per unit time by the heat of the heat transfer area

S: The thermal area;

q (t): The unit area per unit time heat flow through

Simplifying the calculation, the relationship between the dynamic friction force and the heat flux density at a certain point of the friction plate in the process of engaging the clutch when starting is as follows (Wang Ark., 2014):

$$q(t) = \left(\frac{3r}{2\pi({r_2}^3 - {r_1}^3)}\right)N(t) \quad (2.2)$$

Where: r1 and r2 = Inner and outer diameters of plate

R= the radius of the study points

N (t) = the sliding friction power in a function of time

An axisymmetric model of a single-plate friction clutch has improved considering different assumptions. This result demonstrates the transient thermal behavior of a friction clutch system during the engagement (heating) phase when the clutch begins to transmit torque. The analysis considers two types of stress (heat flow) based on friction clutch design theory. These theories have called even pressure and even wear. The results show the temperature field of a friction clutch disc under the assumption of uniform pressure and uniform wear. Specification of temperature field results and distribution in case of error (supposing uniform wear between contact faces). If uniform wear has assumed, the heat flow has always evenly dispersed on the friction faces of the clutch disc. The temperature output is depend on this assumption is around the temperature output at the center disc radius if the pressures between the friction surfaces are considered equal. This hypothetical output does not show the actual value of the maximum temperature and the change in temperature with disk radius (Schlattmann, 2016).

On the other hand, calculating the disk temperature as the restraining pressure increases the heat flux proportional to the radius of the disk. The lowest temperature at the inner radius of the disc and the highest temperature at the outer radius of the disc have displayed at any time during the slide (Abdullah et al., 2018).

When the clutch starts to engage, slip occurs between the contacts faces due to the speed difference (slip period) between the contact surfaces. After this period, all contact parts rotate at the same speed without slipping (full mating period). According to the first law of thermodynamics, most of the kinetic energy at the interface has converted to thermal energy during the slip period, and the heat generated between the contact surfaces dissipated to the environment by heat conduction and convection between the friction clutch components. Sliding has different loading conditions, i.e. pressure contact between the contact surfaces. In the second stage, there are three types of load conditions: the temperature distribution of the previous time (slip period), the pressure between the contact surfaces by the axial force of the diaphragm spring, and the centrifugal force by the rotation of contact part. Figure 3.1 shows the load conditions during the clutch engagement cycle. Where ts is the slip time and T is the torque delivered by the clutch. (Ibrahhim & Schlattmann, 2012).

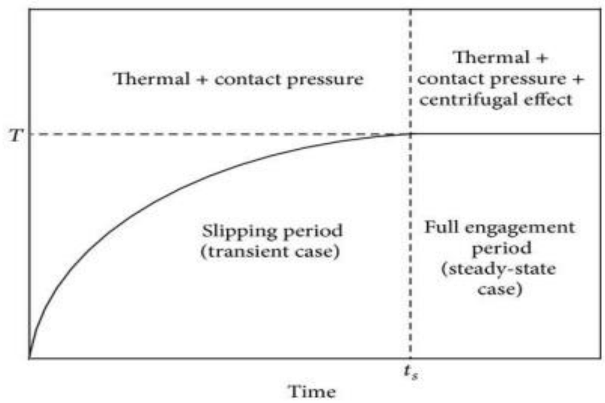

Figure 2.1. The load conditions during the engagement cycle of the clutch

Heat Generation during Engagement

The thermal properties of the material have assumed isotropic and independent of temperature. The actual contact area is equal to the nominal contact area. Based on the basic design theory of friction clutches, two types of pressure distributions, uniform pressure distribution and linear pressure distribution, have given between the contact surfaces. Assuming that all frictional energy has converted to heat, the total heat generated by sliding is:

$$Q(r,t) = Q_{gen.f} + Q_{gen.c} \tag{3.1}$$

$$= Q_{gen.p} + Q_{gen.c}$$

$$= \mu\, p\, V_s; 0 < t < t_s \tag{3.2}$$

Where, Q gen. f, Q gen. c, Q gen .p and Vs (Vs= ωsr) are Heat generated from the flywheel, heat generated from the clutch disc, heat generated from the pressure plate, and sliding speed, ωs is the sliding angular velocity (rad/sec), respectively. Assume that the sliding angular velocity decreases linearly with time as

$$\omega(t) = \omega o(1 - t/ts), 0 \le t \le ts \tag{3.3}$$

Where ωo is the initial sliding angular velocity at which the clutch starts sliding (t=0). Assuming that the pressure distribution across the contact surfaces is uniform now of sliding, the total heat generated between the contact surfaces is,

$$Qt,u(r,t) = \mu\, p\, r\, \omega o(1 - t/ts), 0 \le t \le ts \tag{3.4}$$

The total heat generated between the contact surfaces has given by assuming that the pressure distribution across the contact surfaces at any instant of slip is linear with respect to the disc radius (load B):

$$Qt,I(t) = \mu\, C\, \omega o(1 - t/ts), 0 \le t \le ts \tag{3.5}$$

Where: C = Pmax.ri.

The heat conduction equation for an axisymmetric problem in the cylindrical coordinate (r, z) used to obtained temperature distributions with time for the friction clutch system.

$$\frac{\partial}{\partial r}\left(K\frac{\partial T}{\partial r}\right)+\frac{K}{r}\left(\frac{\partial T}{\partial r}\right)+\frac{\partial}{\partial r}\left(K\frac{\partial T}{\partial z}\right)=\rho\, c\left(\frac{\partial T}{\partial t}\right); t>0 \tag{3.6}$$

Where r is the radial coordinate, z is the axial coordinate, K is the thermal conductivity, ρ is the density, and c is the specific heat. There are two methods used to compute the temperature fields of automotive clutches and brakes.1) Calculate the heat output of each part individually using the heat distribution ratio.2) Apply the total amount of heat generated across the model using the contact model. The contact model approach has used in this work and assumes perfect thermal contact between the contact surfaces, i.e. the surface temperature at the interface is the same for both bodies.

2.4.1. Torque Transmission under Uniform Wear

This theory is because wear is evenly distribute over the surface of the friction disc. This assumption used for worn or old clutches. Axial wear of friction discs is proportional to friction work. The work done by friction is proportional to the friction force (μ· p) and the friction velocity (2· π . r . n) where n is the rotational speed of the disk (rpm/min). The constant pressure theory is applicable only when the friction lining is new. Friction linings wear out after long-term use. Most of the life of friction linings therefore falls under the even wear criteria. Therefore, unit wear theory has used for clutch design.

2.5. Finite Element Analysis of Clutch Assembly

Finite element analysis is becoming a widespread method of computational tools for engineering analysis. With solid modeling, the components have defined to the computer, and this definition provides enough geometric data to build a finite element modeling mesh. (Rahat, 2019) explained Finite Element Analysis of Clutch Assembly in their study with below orders.

(Rahat, 2019) The research results show that the developed friction clutch assembly is within the safety limits according to the finite element analysis data performed in the ANSYS program. Their study analyzed three major components: clutch discs, pressure plates and diaphragm springs. Finite element analysis consisted of three steps: pre-processing, solution, and post-processing. Graphs of equivalent von Mises stress, total deflection and tool stress (factor of safety) were calculated and analyzed.

FEM is used to determine the temperature distribution, heat generation, and contact pressure distribution of the friction surface, and a 3D model is used to simulate the thermal structural coupling of an automotive clutch (Zhao et al., 2016).

2.6. Literature Summary and Research Gap

2.6.1. Literature Summary

From the above literature reviews, it has observed that most of the study focuses on the analysis of the static structural and dynamic analysis of a single component by changing dimensions of clutch disc to reduce heat produced, changing seat of driver to increase comfort. Most of the research work uses implicit dynamic numerical approach throughout the process for comparing the output results, and different software's are used for the analysis like ANSYS, Pareto Set software, Simulink and Sims Cape, Creo 2.0, Hyper mesh and so on. In addition, different approaches have used for optimization like Coupled Field, Pin on Disc and multi-physics model.

2.6.2. Research Gap

As it is discussed from the above literature review, it is concluded that almost all researches have been studied the reduction of lining material effect on trucks and racing car at different loading condition well as at different disc radius configuration during engagement. However, few studies have been studied the material effect in heat dissipation and wear debris of single plate disc due to same pressure intensity for different materials condition in clutch. In addition to this, those studies focused on impact of heat effect on large radius, multi-plate and surface geometry. In this work, dynamics of clutch using different lining materials of Minidor three wheeler clutch assembly are studied. Finally, best material is selected using LS DYNA software simulation result to select best among them.

CHAPTER THREE

MATERIALS AND METHODS

3.1 Introduction

This chapter describes the materials and methodology exercised to complete single plate Bajaj clutch design and modeling thesis.

3.2 Material

The Materials required for execution of this thesis work and the engine specification of the Minidor, Force three-wheeler has shown in table 3.1 have given below.

3.2.1 Tools

Various software and devices required for this paper are also used here as tools for design, modeling and analysis.

- ❖ Vernier Caliper

A Vernier caliper is a measurement and layout tool typically used to measure linear dimensions. Accurately measure internal and external dimensions, depth and thickness. In this case, it has used to measure inner and outer diameter, depth and thickness of the coupling component.

- ❖ CATIA V5

CATIA V5(Computer-Aided Three-dimensional Interactive Application) software is a complete multi-stage solution for Computer-Aided Design (CAD), Computer-Aided Manufacturing (CAM), Computer-Aided Engineering (CAE), PLM and 3D. Established via French company Dassault Systems, this software is best for generating solids, surfaces, assemblies, drawings, manufacturing, and analyses. Computer-aided design platform software set used across industries from aerospace to defense to packaging design (Aysha, 2020).

- ❖ ANSYS 2022 R1

ANSYS is a worldwide finite element-modeling package for numerically solving many of mechanical problems. These problems include static/dynamic, structural analysis, heat transfer, fluid flow, acoustics and electromagnetic problems. There are two means to use ANSYS. One way is through the graphical user interface (GUI). This method follows general Windows and X Windows-based program conventions. Another way is to use a command file.

- ❖ LS DYNA

LS-DYNA is an advanced mixed-use multi-physics simulation software set developed by the previous Livermore Software Technology Corporation (LSTC), which has obtained by ANSYS in 2019. LS-DYNA is a versatile dynamic finite element program for unsteady processes capable of simulating complex real-world problems. Enhanced for UNIX, Linux, and Windows platforms with shared and devoted memory. This is an explicit 3D finite element program for analyzing the dynamic response of elastomeric and inelastic bodies and structures to large deformations. The program is widely used by many major automotive, aerospace and research institutions. A variety of material types and interfaces provide efficient mathematical modeling for different engineering difficulties (Ilie & Cristescu, 2022).

3.3 Methods

Applying well-developed methodologies to solve the general and specific problems of this paper. Various steps included in the methodologies have listed below and summarized in figure 3.1. Among the procedures, the modeling and analysis stage have a more detail explanation and it has stated in detail on chapter four.

3.3.1 Literature Review and Problem Identification

A literature review of clutch response during engagement and disengagement is a key methodology for this paper, helping others find out what they are doing and where limits exist, so this work builds on research gaps. The latest reviews and research in the areas of clutch development, modification, construction, analysis and optimization for a better life of the owner and the comfort of the passengers have collected and studied.

3.3.2 Data Collection

To perform the numerical analysis, the necessary data have collected on an existing Minidor Force tricycle hitch. In order to obtain reliable information and necessary data about Minidor, Force Bajaj is collected from the Adama research area using primary data collection methods. Taken from interviews with the Baja owner, this Bajaj assembler in Mojo Town, and various workshops. Secondary data collection by visiting various websites. Various data are collected, and you can understand the current state of research and methodology of Force Bajaj, a Minidor that is also useful for clutch development and modification.

3.3.3 Conceptual Design

Various concepts of the existing Force Minidor Bajaj clutch have presented. In this way, ideas have generated to overcome or minimize these problems and improve comfort development through material modification methods.

3.3.4 Modelling and Analysis of the Existing Model

The 3D modeling of the parts and the subsequent mini-doll, Force Bajaj assembly process have performed in CATIA V5, and finally the mechanical simulation has performed in CATIA V5. Once the 3D modeling of the clutch components is completed, vibration and thermal analyzes are performed using ANSYS and LS DYNA software respectively.

3.3.5 Modification Analysis

After careful observation of the vibration, thermal and wear behavior of the existing model, modifications and construction have carried out at key points of the vehicle. We then analyzed the modified parts separately.

3.3.6 Discussion

At this stage, the response of modifications has examined using engineering analysis and discussions. If the result were satisfactory, the next stage of the research will take place but if not, the modification is to be re-designed and repeat the steps.

3.3.7 Design and Analysis of the New Model

Safety developments or modifications that improve driver and clutch comfort and durability are incorporate into existing models and further analyzed in ANSYS and LD DYNA. Numerical comparisons has done between the existing and modified models using various parameters such as frequency, temperature and wear rate.

3.3.8 Verification

Validity of values in the absence of experimental data is obtained by computational models is accurately represented through a validation process. For ANSYS simulations, verification would be done by taking advantage of extensive acceleration and environmental testing capabilities to check the reliability simulation validation set. These include high temperature service life (to predict electro migration), temperature cycling (for solder fatigue), temperature/humidity bias (THB) and highly accelerated stress testing (HAST), random and sinusoidal vibration, mechanical shock, and drop tests. (*Simulation Validation and Verification Testing _ Ansys*, 2022).

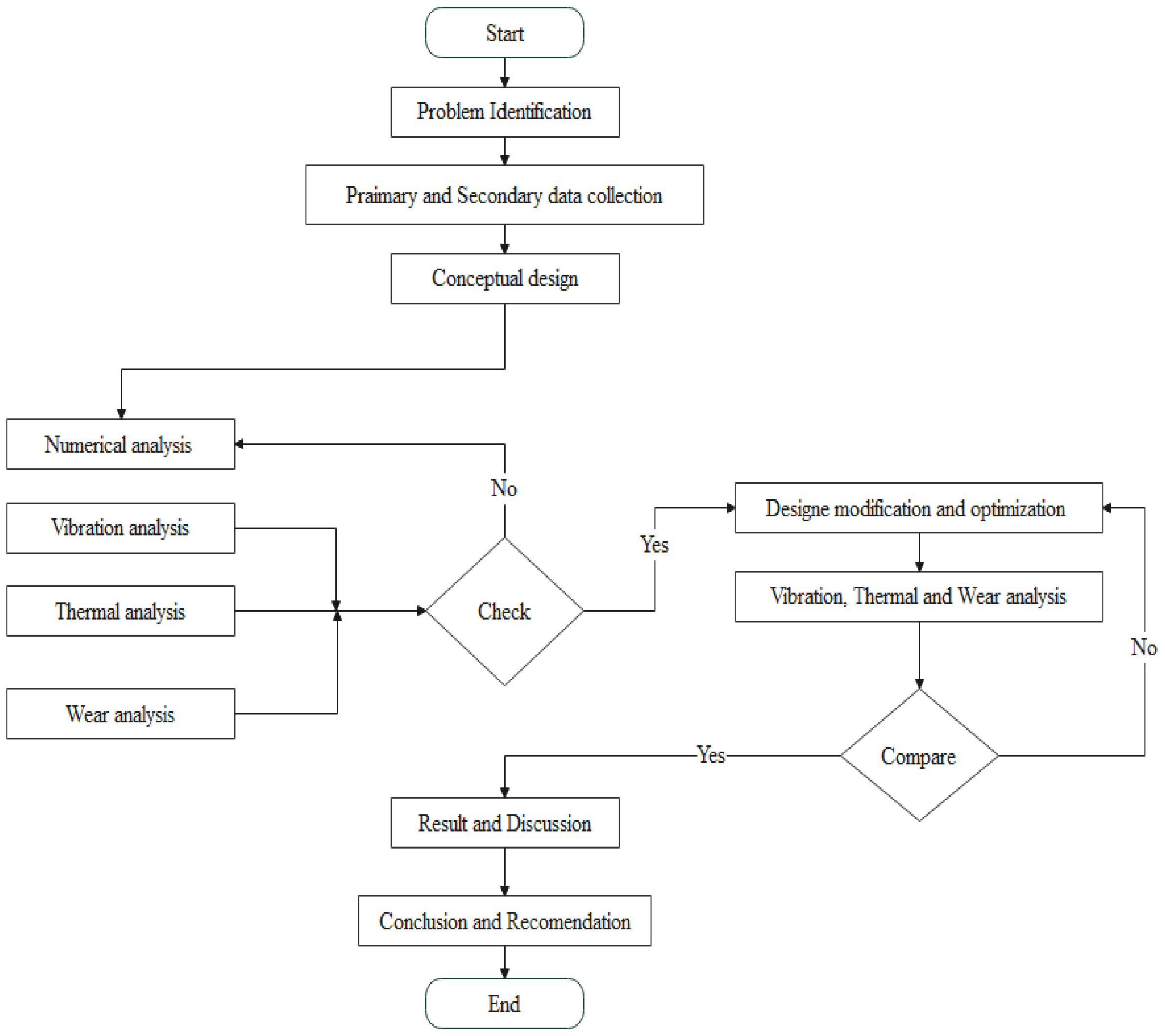

Figure 3.1. Research Methodology

3.3.9 Design Calculations

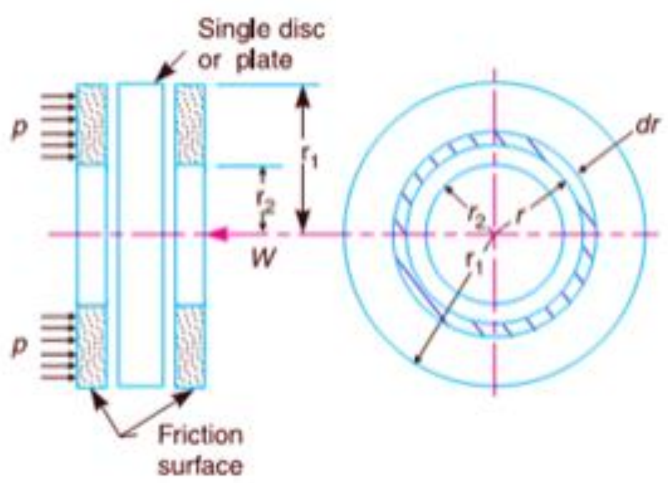

Figure 3.2. Clutch lining terminology (Narayan et al., 2018)

Specification

Max Power =7.2kW (ISO) @ 2800-3000rpm

Max Torque =28Nm @1800-2000rpm

Number of contact surface (n)

n=2

R_m=mean radius of the friction surface

Outer radius (r_o) and inner radius (r_i)

r_o=0.07831m r_i=0.05331m

A. Considering uniform pressure

When the applied pressure is uniformly, distribute over the whole space of abrasion surface.

$$P = \frac{load}{contact\ surface\ area} = \frac{W}{\pi({R_o}^2 - {R_i}^2)} \tag{3.7}$$

Where: W=Axial trust with friction surface

Friction torque acting on the friction surface is included by,

$$T = n\,\mu\,w\,R_m \tag{3.8}$$

$$R_m = {}^2\!/_3\,\frac{{r_0}^3 - {r_i}^3}{{r_0}^2 - {r_i}^2} \tag{3.9}$$

$$= 0.666m$$

i. Lining material: kevlar49

Coefficient of friction $\mu = 0.5$

W = 420.42 N

p = 0.0407 N/mm^2

ii. Lining material: aluminum alloy A360

Coefficient of friction $\mu = 0.23$

W = 913.96 N

p = 0.0884 N/mm^2

iii. Lining material: alumina

Coefficient of friction $\mu = 0.6$

W = 350.35 N

p = 0.0339 N/mm^2

B. Considering uniform axial wear

Friction torque acting on the friction surface has included by equation 3.9

$$R_m = \frac{r_o + r_i}{2} \tag{3.10}$$

$$= 0.06581m$$

Axial force is required to engage the clutch

$$W = 2\,\pi\,C\,(r_o - r_i) \tag{3.11}$$

$$C = P\,r \quad , (C = constant) \tag{3.12}$$

The maximum intensity pressure occurs at inner radius of friction surface

$$C = P_{max} * r_i \tag{3.13}$$

$$C = \frac{W}{2\pi(r_0 - r_i)} \tag{3.14}$$

$$P_{max} = \frac{C}{r_i} \tag{3.15}$$

The minimum intensity pressure occur at outer radius of friction surface.

$$P_{min} = \frac{C}{r_o} \tag{3.16}$$

The average pressure on the friction surface

$$P_{avg} = \frac{Total\ force\ on\ the\ friction\ surface}{Crossection\ area\ of\ friction\ surface} \tag{3.17}$$

$$P_{avg} = \frac{W}{\pi({r_o}^2 - {r_i}^2)} \tag{3.18}$$

iv. Lining material: kevlar49

Coefficient of friction μ = 0.5

W = 425.47 N

p = 0.0411 N/mm^2

v. Lining material: aluminum alloy A360

Coefficient of friction $\mu = 0.23$

$W = 924.93$ N

$p = 0.0894$ N/mm^2

vi. Lining material: alumina

Coefficient of friction $\mu = 0.6$

$W = 354.56$ N

$p = 0.0346$ N/mm^2

Table 3.1. The working pressure and axial force in each clutch plate

Material	At constant pressure		At constant wear	
	Working Pressure (N/mm^2)	Axial Force (N)	Working Pressure (N/mm^2)	Axial Force (N)
kevlar49	0.0407	420.42	0.0411	425.47
aluminium alloy A360	0.0884	913.96	0.0894	924.93
alumina	0.0339	350.35	0.0346	354.56

CHAPTER FOUR

MODELING AND ANALYSIS

4.1. Introduction

This chapter describes the methods used to analyze and modify existing Minidor Bajaj single disc clutches. The workflow used has shown in Figure 4.1. These procedures used to analyze the transmission of vibrations to the gearbox, heat and wear of existing and modified clutch discs.

4.2. Work Flow of Modeling and Analysis

For the design and analysis of the Minidor Bajaj single disc clutch, CATIA V5 has used for modeling and the model was import into ANSYS and LS DYNA. Model surface cleaning, meshing, and other parameters have performed using ANSYS Workbench in the PREPOST processes. Clutch dynamic analysis was done in ANSYS and LS DYNA post-processing. Details of each step was shown in Figure 4.1 below.

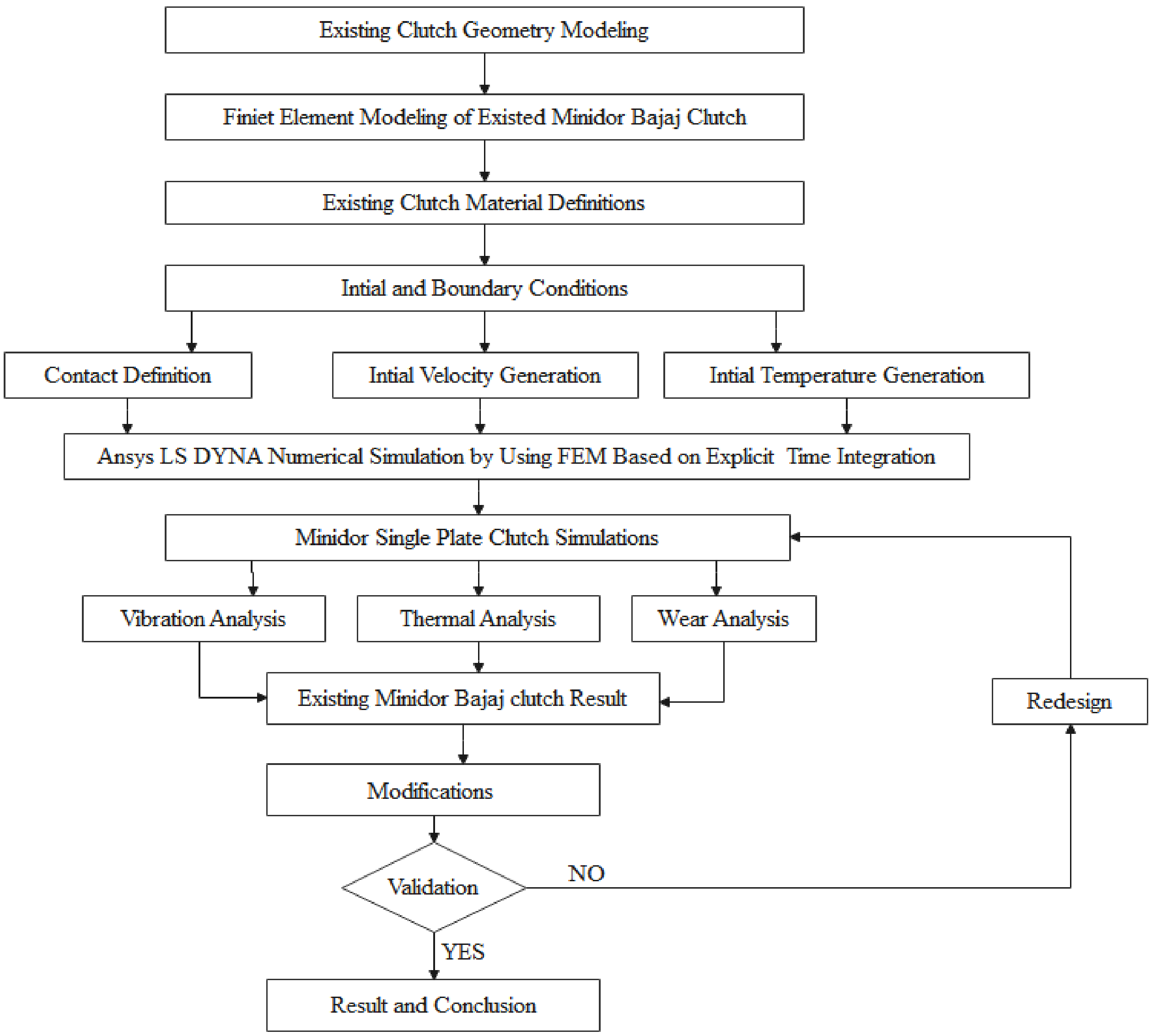

Figure 4.1. Workflow for modelling and analysis

4.3. Modeling and analyzing of the existing structure

4.3.1. Modeling of Single Plate Minidor, Force Bajaj Clutch

Geometry model of Single plate force Bajaj clutch is modeled based on specification obtained from data collection. Before attaching the geometry to ANSYS and LS DYNA, several steps are perform during modeling in CATIA V5. Sketcher is the initial stage of modeling in which the basic profile or part of the single plate clutch. After that, the surface has generated, and the corresponding extruding (pad) thickness has given for each part. Finally, the parts are assemble for checking for dimension error. The parts have named separately in CATIA; these steps are shown on Figure 4.2, and the lists of parts modeled assembled are listed below:

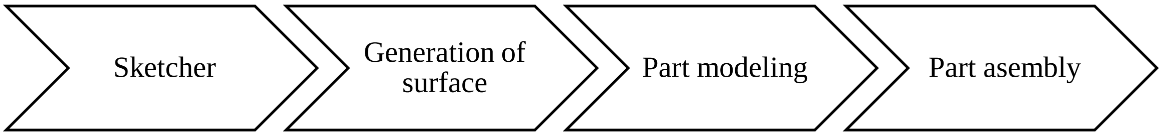

Figure 4.2. Modelling procedure

1. Flywheel
2. Clutch disc assembly: damper spring, cushion spring ,friction lining
3. Pressure plate assembly: pressure plate, diaphragm spring, fork, transmission input shaft

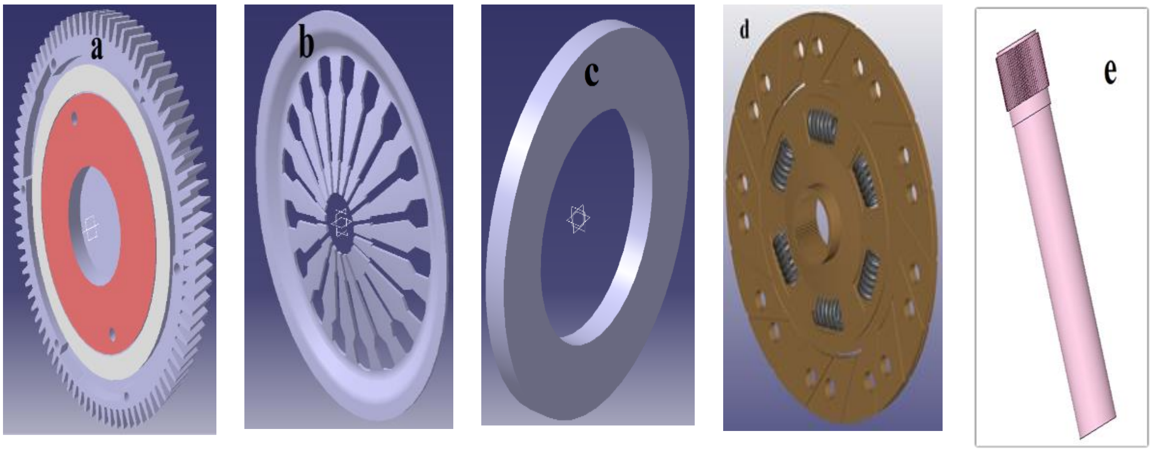

Figure 4.3. (a) flywheel (b) diaphragm spring (c) pressure plate (d) friction disc assembly (e) input shaft

The geometry is then export into ANSYS 2022 R1 Design-Modeler. Figure 4.4 shows, the geometry after being import to the ANSYS workbench in STP format and assembled.

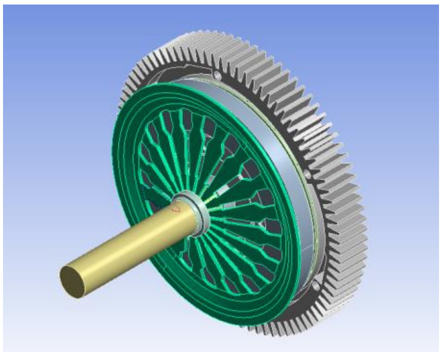

Figure 4.4 Geometry after being import to ANSYS workbench

4.3.2. Model Check and Surface Clean

After modeling, the next step is model validation. Correct model acquisition, or model validation, consists of three basic phases: before analysis, during analysis, and after analysis, as shown in Figure 4.5.

After Modeling Getting the model "right", or model checking, consists of three basic phases: pre-analysis, during analysis, and post-analysis (Krishnamoorthy et al., 2011).

Pre-Analysis Checks: All the checks that LS-DYNA needs to run before running an analysis.

Checks During Analysis: Checks that may be perform while the model is running.

Post Analysis Review: Review the model after completing the analysis. This includes feedback on accessing initial model data.

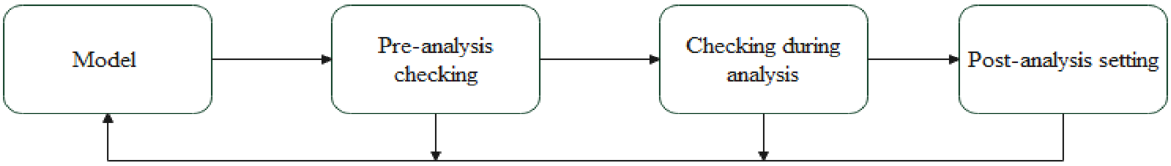

Figure 4.5. Model checking procedure

4.3.3. Pre-analysis Checking

Before meshing: the Computer Aided Design (CAD) of a Minidor, Force single plate clutch model has converted by ANSYS software in to an Initial Graphics Exchange Specification (IGES) model. Then, the model has cheeked for whether modeling errors are available or not. Duplicate faces between parts, unwanted lines, edges, intersections, etc. have flanged and removed from the imported model. The next step is to mesh the model before and after investigation and perform more, thorough checks before analysis.

4.3.4. Mesh Generation

Once the domain has created, the next step is networking. Run Paraphraser Again. To use a numerical equation, divide the area into small cells called grids. The mesh used in ANSYS Mechanical has created with ANSYS Meshing. The domain has meshed with the Influence Bodies feature to achieve refinement around the component. Mesh density focused on specific regions of the domain. Aids reduce the time and effort spent getting accurate outcomes (Frisk & Tegehall, 2015). To focus on certain regions of the domain. A fine mesh has used as shown in Figure 4.6 the mesh near contact surface is very fine to get an accurate result. The outer volume has meshed with coarse elements fine around surface.

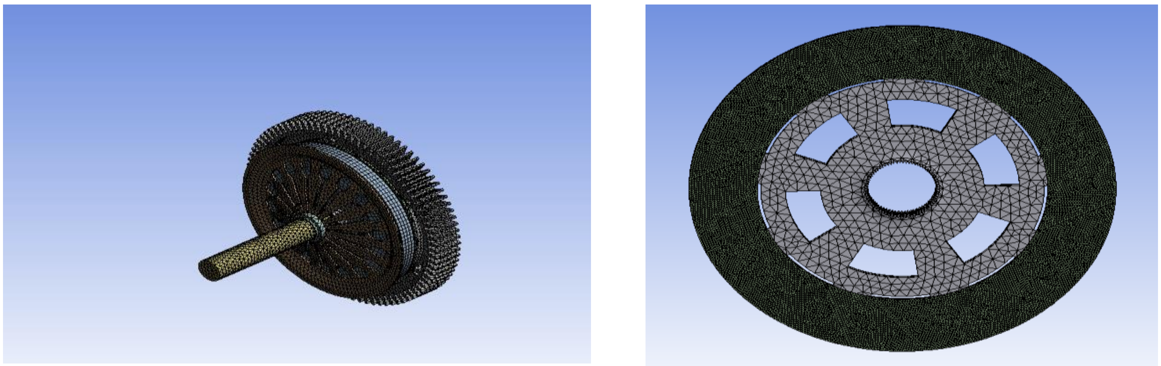

Figure 4.6. Fine mesh generation on the clutch component and contact surface

According to the User's Guide for ANSYS mechanical, Mesh quality is determine by the minimum orthogonal quality. Orthogonal quality ratings range from 0 to 1, with smaller values signifying worse quality cells. The minimal orthogonal value should not be less than 0.01, with the average value being much higher, as shown below in Figure 4.7 the mesh quality is greater than 0.01.

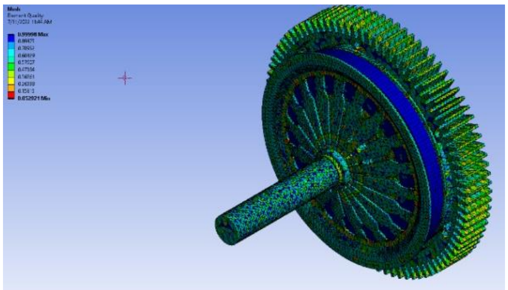

Figure 4.7. Quality of mesh for the clutch

4.3.5. Grid Independence Test (GCI)

Grid independence should be tested using mesh convergence studies. In other words, it check that the quality of the mesh was not sufficient to affect the solution; it is verified through the GCI. GCI is an indicator used to determine the optimal mesh by calculating the mesh convergence error based on the Richardson extrapolation method. As an indicator to quantify the error of a coarser mesh used to save computational cost, this mesh type is provide results with acceptable accuracy.

A value greater than 1.3 is recommended for the mesh refinement factor to distinguish discrete errors from other errors (Lee et al., 2020). In this study, the optimal grid resolution derived through the grid independence test has defined as the medium grid. Using this grid as the reference, the coarse and fine grids among the grid resolutions satisfy the grid refinement ratio have defined. The GCI has calculated according to Richardson's extrapolation with

$$GCI = F_s \frac{\varepsilon}{r^p - 1}, \tag{4.1}$$

Where F_s is the safety factor, p is the order of convergence, and ε is the relative error of two grid conditions in the simulation. The value of 1.25 is use for F_s when comparing three or more grids. p is calculated as follows:

$$p = \frac{\ln[(f_{coarse} - f_{medium})/(f_{medium} - f_{fine})]}{\ln r} \tag{4.2}$$

Results found in grid independency test is presented in table 4.1 that shows the amount of errors found in choosing mesh size of components.

Table 4.1. Grid independence test

No. Element			Grid ratio		Parametric result		
No.E/t1	No.E/t2	No.E/t3	R21	R32	Max.deff. 1 (mm)	Max.deff. 3 (mm)	Max.deff. 3 (mm)
41924	54831	12040	1.094	0.603	8.63e-1	8.19e-1	8.06e-1

Normal error		S.F	Grid convergence Index	
Err 21	Err 32	Fs	GCI 21%	GCI 32%
5.4e-2	1.5e-2	1.25	2.56%	0.71%

From the three mesh size (2mm, 4mm and 8mm) less error is found between 2 and 4mm. if fine mesh is used the computational time is very high. So medium size mesh has chosen for the simulation, which is 4mm.

4.3.6. During Analysis

Under this section, penetrations and modeling error etc., were reported. So that a user can fix the problem by reading Warning in message file or on the running LS DYNA command window.

Messages

	Text	Association	Timestamp
Warninc	Modal analysis used may have not found all the modes in the harmonic frequency sweep	Project>Model>Harmonic Response>Analysis Settings	Wednesday, May 25, 2022 9:13:26 AM
Warninc	During this solution, the elapsed time exceeded the CPU time by an excessive margin. Oft	Project>Model>Harmonic Response>Solution	Wednesday, May 25, 2022 9:13:19 AM
Warninc	One or more contact regions has been defined as nonlinear contact. However, an eigenv	Project>Model>Harmonic Response>Solution	Wednesday, May 25, 2022 9:06:54 AM
Info	This solution was solved with less than 4 cores. Up to 4 cores can be used for the solutio	Project>Model>Modal>Solution	Wednesday, May 25, 2022 8:52:16 AM
Warninc	During this solution, the elapsed time exceeded the CPU time by an excessive margin. Oft	Project>Model>Modal>Solution	Wednesday, May 25, 2022 8:51:54 AM
Warninc	One or more contact regions has been defined as nonlinear contact. However, an eigenv	Project>Model>Modal>Solution	Wednesday, May 25, 2022 8:24:27 AM

Figure 4.8. Warning during analysis

4.4. Analysis Setup

4.4.1. Selection of Constitutive Material Models Used

Vehicle material types and properties are the most important factors, which effect significantly the accuracy of the impact simulation. Moreover, material types and properties should fulfil the automotive criteria, such as safety, environment, lightweight, fuel consumption, cost and design. Mostly, the clutch model consists of solid, which does not need to identify thicknesses for every single shell besides mechanical material properties.Constitutive material models used in this research along with the list of components modelled using given material definition is listed below in table 4.2.

Table 4.2. Constitutive material models used in FE models of existed Minidor single plate clutch

Material Model	clutch components
001 *MAT_THERMAL_ISOTROPIC	Pressure plate, flywheel and clutch disc
020 *MAT_RIGID	Pressure plate and flywheel
024 *MAT_PIECEWISE_LINEAR_PLASTICITY	Clutch disc assembly

MAT_RIGID

MAT_RIGID presents a very convenient way of defining parts within the model as rigid bodies. In some applications it is a good choice to approximate a part of the model as a rigid body, since its definition is bypassed in the element processing and results in increased calculation speed (Hallquist, 2007). Rigid bodies are also commonly used in LS-DYNA for joint definition such as JOINT_REVOLUTE and JOINT_CYLINDRICAL keywords. Pressure plate and flywheel, used for thermal test procedure, was modeled using the material rigid definition.

MAT_THERMAL_ISOTROPIC

It has used to define material thermal properties like heat capacity and thermal conductivity. The pressure plate, flywheel and cutch disc used for the test procedure was modeled as thermal isotropic.

MAT_PIECEWISE_LINEAR_PLASTICITY

Most of the steel, alloy and aluminum structural elements in the developed FE models were modelled using MAT_PIECEWISE_LINEAR_PLASTICITY material definition. Elements of the clutch, such as clutch lining and cushion spring, were defined as MAT_024 on the existed clutch as listed in table 4.3 below (Hallquist, 2007). The mechanical properties of major clutch components, which is useful for the analysis, was described in table 4.3.

Table 4.3. Material mechanical properties for clutch part set

Clutch parts	Mass density (kg/m3)	Young's Modulus (Pa)	Poisson's ratio	Thermal conductivity(w/m ºC)	Specific heat capacity (J/kg K)
Flywheel	7850	2e+11	0.3	60.5	420
Dumper spring	7850	2e+11	0.3	60.5	420
Friction disc	2800	1.65e+11	0.28	0.07	816
Cushion spring	7850	2e+11	0.3	60.5	420
Pressure plate	7200	1.1e+11	0.28	53	460
Diaphragm spring	8000	2.05e+11	0.303	50	420
Input shaft	8000	2.05e+11	0.303	50	420

4.1.1 Contact Definition

The keyword *CONTACT provides a way of treating interaction between disjoint parts. During FEM thermal calculations, it is often the case that modelled parts come in contact. In order to prevent two objects penetrating each other, a contact handling algorithm is necessary to be implemented into the FEM software. Contact treatment algorithms are critical for large deformation problems, and accurate contact modelling is very important. Many contact types are currently available in commercial FEM software. Contact algorithms in LSDYNA can be separated into two groups; penalty based contacts and constrained based contacts (LSTC, 2014)

Most of the contacts algorithms, used for thermal applications, are penalty based contacts. The principle of classical penalty contact definition in LS-DYNA requires the user to define “slave” nodes (ex. node sets, parts, part sets) that should be prevented from penetrating “master” segments (ex. segment set, parts, part sets). A search algorithm is implemented in LS-DYNA software in search for possible penetrations. Once a penetration is detected, a penalty force, proportional to the depth of the penetration is applied to the “slave” node in order to eliminate detected penetration (LSTC, 2014).

Since the penalty force is proportional to the depth of the penetration, it is often described as a tension-only spring, attached to the penetrating “slave” node. The resultant reaction force, coming from the contact spring, is also distributed over neighboring nodes that belong to the “master” segment in order to follow the laws of conservation of momentum. The contact spring stiffness is a product of a user defined penalty factor and a stiffness value, defined as a minimum stiffness from either master segment or slave node (Du Bois, 2010).

Currently, AUTOMATIC_SINGLE_SURFACE contact algorithm is the most commonly used in impact simulations. It considers contact between all parts defined within the slave part set, as well as their self-contact. This contact is considered to be reliable and accurate (LSTC, 2014). Since location of parts relative to each other cannot always be predicted as the model experiences enormous deformations.

*CONTACT_AUTOMATIC_SINGLE_SURFACE contact algorithm was used to define contact between all parts in developed FE models. Friction coefficient for this contact type was set equal to 0.15 representing steel to steel contact. (LSTC, 2014).

*CONTACT_AUTOMATIC_SURFACE_TO_SURFACE is a suggested contact form since, in thermal simulations, the location of parts relative to each other is predicted as the model experiences enormous deformations. As mentioned before, automatic contacts check for penetration on either side of a shell or solid element. A contact between flywheel and clutch disc. A separate contact entity was created for clutch disc and pressure plate contact with a friction coefficient set to 0.3 representing lining to cast iron shown in table 4.6 below. The whole clutch parts with each other used this contact type for the simulation.

Table 4.4. Contact master and slave

No.	Contact type	Slave	Master
1.	Automatic surface to surface	Clutch disc	Flywheel
2.	Automatic surface to surface	Pressure plate	Clutch

4.1.2 Constraints

The joining process of the existing Minidor clutch system are usually arc welding , river and bolt. After meshing the individual parts of single plate clutch model, interactions have been defined between them. These connections were defined among the surfaces of dissimilar parts and control the transmission of forces and moments between separate members. Kinematic linkages have been well-defined for different parts of the clutch. The constraint between two deformable parts was given by the keyword CONSTRAINED_NODAL_RIGID_BODY in Entity creation. Also to connect rigid to deformable body CONSTRAINED_EXTRA-NODE_SET is used by creating node sets from deformable body. Constrained spot-weld and joint generalized was also used for this project to joint two separate parts.

4.1.3 Boundary Conditions and Simulation Environment

The function of the boundary conditions is to create and define constraints and loads on finite element models. To simulate a clutch dynamics, all loads and boundary conditions that occur in the actual dynamics event needs modeling. Just as a clutch disc is subjected pressure loads during engagement in real life, the simulated model should have a representative pressure applied. Friction forces between the clutch disc and the flywheel surface play an important role in how the clutch behaves during engagement and disengagement, so these have to be account for in the simulation. The angular velocity has applied to the flywheel in a manner as to not impart any unrealistic acceleration or cause the simulation to run for an extended amount of time. Fortunately, Ls-Dyna provides methods to simulate all of these requirements (Liu, 2013).

Research presented in this thesis has been carried out on Intel(R) Core(TM) i7-8700 CPU @ 3.20GHz 3.19 GHz processor and RAM 8 GB Computing systems. Clutch transient simulations presented in this thesis have been completed using HP desktop at the Adama Science and Technology University (ASTU) Automotive Laboratory, Ethiopia.

Due to the transient, nonlinear and explicit character of the thermmal test simulation explicit time integration solver in LS-DYNA was used for rollover simulations. LS DYNA R11.1.0 version released at 2019 used for this simulation and the simulation runs for 72 hours for total 0.7 sec termination time the automatic deformable to rigid switch up to 0.92 sec, the automatically the material switch to deformable.

In this section the setups for the simulation of vibration and thermal has presented. The Boundary condition and set up follows the standards indicted on literature. The detail of set ups and boundary condition in each of the analyses are presented as follows. In this study, environment temperature has considered as 293.44 °K before starting torque transmission. The rotational velocity of the clutch disc is 3000rpm because the temperature increases with engine rpm this will increase frictional heating. The simulation has adjusted for 700ms.

The following boundary conditions should be fulfilled to accomplish the material test for lining of minidor clutch.

- ❖ The CONTROL_TERMINATION time is set as 0.1 sec, Settings of several control cards are also necessary to be addressed in composite beam material test are;
- ❖ CONTROL_ACCURACY, INN=4: The invariant node numbering for shell and solid elements are toggled on. Setting INN=4 minimize the sensitivity of updating of the orientation of the material coordinate system, as the material coordinate system is automatically updated following the rotation of element coordinate system.
- ❖ CONTROL_THERMAL_TIMESTEP in a coupled thermal-stress analysis, the thermal time step is independent from the mechanical time step. Use the keyword *CONTROL_THERMAL_TIMESTEP to set the value. For most problems, the implicit thermal time step is chosen equal to the implicit mechanical time step, or 10 to 100 times greater than the explicit mechanical time step. The rate of mechanical motion, mechanical deformation, and rate of heat transfer must all be considered in selecting an appropriate time step in the thermal-stress calculation procedure.
- ❖ CONTROL_THERMAL_SOLVER defines parameters to perform the numerical integration.

- ❖ CONTROL_THERMAL_TIMSTEP defines parameters for the time integration method used for the 1st term.

4.1.4 Database Options

Database options are given to obtain the output i.e., to generate results and to interpret plots. Database used to define the expected results using American Standard Code for Information Interchange (ASCII) to define specific functions such as NODOUT, JNFORC, JSTIFR and DEFORC (Kunle et al., 2019). Generally, they have used to analyze the sliding energy; temperature etc… are discuss in next chapter on result and discussions. Some of the database plots used are:

D3PLOT (database for complete output states and some default results)

D3DUMP (complete database for restart when interruption occurs on running due to power or other)

ASCII options (absorption energies (GLSTAT), material energies (MATSUM), output temperature (TPRINT), Resultant contact forces (RCFORC) and so on.

4.2 Analytical Analysis of Wear

Wear is a dynamical process related to changes in the surfaces of bodies moving relative to one another because of mechanical interaction between them. This process depends on many factors and parameters (geometry of contacting surfaces, normal applied force, relative velocity, material hardness, etc.). Wear of mechanical parts in most cases is considered to be the main cause of the deterioration of the quality of operation and performance of a device (Grzelczyk & Awrejcewicz, 2015).

The volume lost allows calculating the wear rate of the material. Since the action performed on all samples is identical, the wear rate could be used as a quantitative comparative value for wear resistance. Damages of contact surfaces are results of wear. Wear Coefficients for both the pin and sample are calculated from the volume of material lost during a specific friction run .This method is based on Archard’s equation (Shriwas et al., 2015).

The Archard wear equation is a simple model used to describe sliding wear and is based around the theory of asperity contact. It concludes that the volume of the removed debris due to wear is proportional to the work done by friction forces. A modified form of ARCHARD'S equation is used here to predict the local wear depth increment for a given point within the contact as shown below:

$$V = \frac{K\ W\ L}{H} \tag{4.3}$$

Where: V is the total volume of wear debris produced

K is a dimensionless constant

P is the total normal load

L is the sliding distance

H is the hardness of the softest contacting surfaces

$$dhs = K\ p\ ds \tag{4.4}$$

Where: K is the dimensional wear coefficient (mm^2N/m)

hs is the wear depth by effect brake pressure (mm), & s is sliding distance

Substituting$ds = v(t)dt$, in to equation (4.4) in order to use ARCHARD'S equation to relate the problem.

$$dhs = p\ c\ k\ \omega(t)\ r\ dt \tag{4.5}$$

Where: $\omega(t)$ is the angular velocity of disc brake with time

Wear coefficient should be noted that the wear coefficient k is not an intrinsic material property but is also dependent on the operating condition. The value of k for a specific operating condition and given pair of materials may be obtain by experiments. Also worth noting, is that measured values of wear coefficients usually have large scatter and may affect wear predictions significantly. Care should thus be take in obtaining the values K is the wear coefficient which distinguish between the wear mechanisms by considering the area subjected to wear it is possible to express the wear displacement in terms of the contact pressure and it is often called the specific wear rate and quoted in units of mm3 N−1 m−1. The numerical value of k expressed in mm^3 N−1 m−1 is the same as the value of K. Under unlubricated sliding conditions (so-called dry sliding), it can be as high as 10−2, although it can also be as low as 10−8. Often two distinct regimes of wear are distinguish, termed 'severe' and 'mild'. In metals, 'severe' sliding wear is associated with relatively large particles of metallic debris, while in 'mild' wear the debris is finer and formed of oxide particles. In the case of ceramics, the ‘severe’ wear regime is associated with brittle fracture, whereas ‘mild’ wear results from the removal of reacted (often-hydrated) surface material. When hard particles are present and the wear process involves abrasion (by sliding or rolling particles) or erosion (by the impact of particles), then the highest values of K occur (Du et al., 2022).

4.3 Modification on the Existing Single Plate Minidor, Force Bajaj clutch

4.3.1 Introduction

Asbestos has properties suitable for use as the main material for friction linings, but is harmful to health. It is carcinogenic in nature. Therefore, there is an opportunity to replace it, and some researchers are proposing materials to replace asbestos as the main material for brake lining materials. Brake lining materials must have good mechanical properties such as compressive strength and tensile strength to withstand high loads. However, these alternative materials can be systematically investigate for their friction and mechanical properties while changing their composition. (Shinde & Mistry, 2017). Modifications has made on the friction lining material by keeping the thermal property and minimizing the effect on human health.

- Very high power dissipation.
- More heat-resistant properties.
- Low wear properties.
- High durability.
- High coefficient of friction.
- Stable friction properties.

4.4 Friction Disc Design

In designing friction disc two theories are used this are

The annular plate with surface of friction material has forced against a metal by means of spring. During this time, the friction disc rub with the flywheel to stope its motion, high frictional heating has produced at the contact area. Therefore, to with stand this temperature the material should with stand the heat to work properly and have low wear rate.

To explore the consequence of friction lining material on heat dissipation and holding ability, different friction disc lining material have designed and compared by LS DYNA software. The heat transfer to the pressure plate and flywheel has measured by heat flux. The effect of lining material type on heat dissipation evaluated at the contact.

4.4.1. Friction Lining Material

A friction material is a substance that creates friction between hard surfaces to control or stop forward or backward movement. Friction materials have important properties and properties that are necessary to provide high-quality performance. The properties that manufacturers include in their products include heat resistance, high coefficient of friction, energy absorption, durability and wear resistance. Therefore, to design friction lining, three materials has chosen and compared to get better heat dissipation based on cost, availability and durability. These materials are alumina porcelain, aluminum alloy, and Kevlar49.

The Alumina porcelain, Al_2O_3 is the main building material. Its excellent mechanical and electrical properties combine to enable use in a variety of applications. Alumina can be produced in a variety of purities with additives designed to improve properties. A wide range of ceramic machining techniques, including machining or mesh forming, can be applied to produce parts of various sizes and shapes. It can also be easily bonded to metals or other ceramics using plating and soldering techniques. Alumina-based ceramics are by far the largest range of modern ceramics manufactured by Morgan Technical Ceramics. Due to the significant combination of properties. Aluminum oxide is used because of its hardness and strength. The strength and abrasive properties are due to the high hardness of aluminum oxide (Modepalli, 2015).

Kevlar 49 is friction material introduced by DuPont in the 1970s. It is an organic fiber with sufficient tensile strength and modulus of elasticity for use. Originally developed to replace steel in radial tires, Kevlar is now used for a variety of purposes. Exhibit low creep and low water absorption and low wear rate (Fink, 2014).

Aluminum alloy Aluminum-Silicon (Al-Si) alloys are the most flexible materials, accounting for 85-90% of all aluminum body parts produced for the automotive industry. With the recent development of diesel engines and direct injection gasoline engines with high power density, the combustion pressure and piston temperature increase, which has a great influence on the performance of piston materials. At the same time, wear resistance is usually related to the surface hardness due to the properties of the matrix, and the wear resistance of these alloys is due to the presence of hard particles of primary silicon in the microstructure of a large volume fraction. The popularity of these alloys has accelerated in recent years. It provides strong bonding, good corrosion resistance, good wettability, low density and high flexibility, improved wear resistance (Viswabharathy et al., 2017).

Table 4.5. shows the mechanical properties of different lining materials used for the simulation of single plate clutch.

Table 4.5. Properties of friction lining material

Material name	alumina	Kevlar 49	Aluminium alloy
Density (kg/m3)	3700	1440	2680
Young's modulus (pa)	3.2 e +11	1.21e+11	7.1 e +10
Poisons ratio	0.23	0.36	0.33
Friction coefficient	0.6	0.5	0.23
Yield strength(GPa)	15.4	1.24	0.165
Hardness (brinell)	1100	68	75
Heat capacity (J/kg ^{o}C)	930	1420	963
Thermal conductivity (w/m ^{o}C)	3	0.04	113

CHAPTER FIVE

RESULT AND DISCUSSION

5.1. Introduction

This chapter presents the results simulation of thermal analysis of Minidor, Force single pate clutch was reported and comparative analysis carried out between the modified and existing vehicle model was also made. In addition, the detail discussion on the results was presented. Before entering into the report or result, the verification method for ANSYS and LS-DYNA simulation results was discussed below.

As indicated in the introduction part, the main objective of this thesis work was to investigate different lining material of single plate Minidor, Force Bajaj clutch. Before inter in to the modification the required data about the vehicle was collected. Then the analysis of the existing clutch has done with different boundary conditions. In doing so CATIA V5 and LS DYNA software used for 3D modeling and analysis of Clutch respectively. After analyzing the existing clutch for thermal cases, weak and strong parts have identified and modification was done based on this. Modification was done on friction lining parts of the single plate clutch. The material properties used was selected based on their cases.

Transient thermal analysis of dry friction clutch disc for repeated engagements based on the uniform wear and uniform pressure theory was performed .Two dimensional axisymmetric model was built to obtain the numerical simulation for friction clutch elements during the slipping. The sliding speed plays an important role in determining the amount of heat generated between contact surfaces; to select the suitable friction material to withstand the high temperature, which produces by frictional heating during the slipping. In wear analysis the value of coefficient of friction with respect to time, load and velocity for all materials in numerous value and graphical value for comparative study of all materials for selecting best of them because of clutch material should able to with stand at high temperature and high speed. For this reason, Alumina, Aluminum alloy A360 and Kevlar49 is used, and analysis was done with the same as the existing.

5.2. Result and discussion of existing clutch model

5.2.1. Effective Von Misses Stress

Von Mises stress is a value used to determine if a given material will yield or fracture. It is used mostly for ductile materials, such as metals. The von Misses yield criterion states that if the von Mises stress of a material under load is equal or greater than the yield limit of the same material under simple tension then the material will yield. When a body, in an initial state of equilibrium or undeformed state, is subjected to a body force or a surface force, the body deforms correspondingly until it reaches a new state of mechanical equilibrium or deformed state. The inner body forces are the result of a force field such as gravity, while the surface forces are forces applied on the body through contact with other bodies.

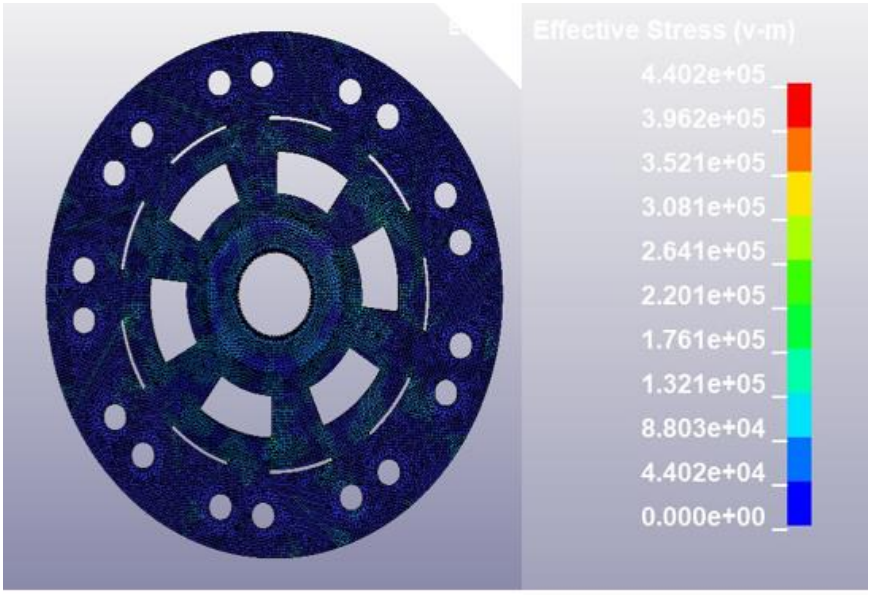

Figure 5.1. Von misses stress results of asbestos

Figure 5.1. shows von misses stress with temperature effect done in LS DYNA workbench software over clutch disc in engaged state. As shown the contour plot, maximum von misses stress is indicating by red color, which has value of 440.2kPa.

5.2.2. Total Energy-balance Graph

The law of conservation of energy states that energy cannot be created or destroyed and can be transformed from one form of energy to another. Applying the same principle to thermal analysis, the amount of kinetic energy lost during bonding must be converted into other forms of energy such as internal energy, sliding energy and external work energy.

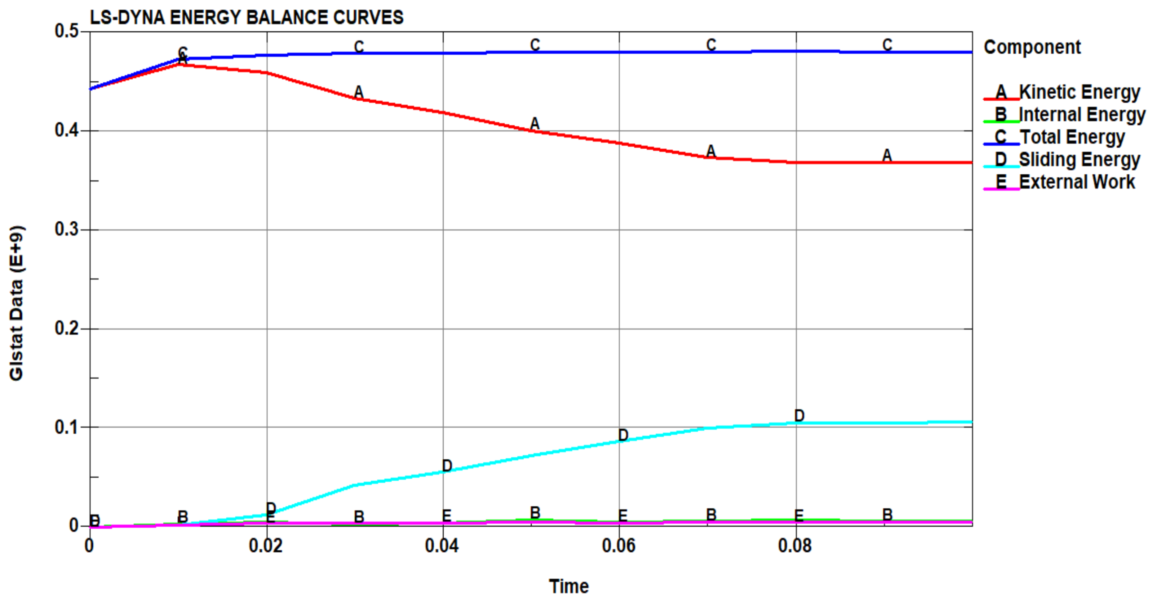

Figure 5.1. Energy balance curve

From Figure 5.2. It has seen that, at the start the kinetic energy that is high at the beginning of the impact is equal with the total energy with value equal to 0.481 GJ. As the engaging event happens, the system kinetic energy starts to slowly being reduce, converted to other forms of energy, and then finally reaches to 0.368 GJ of energy. From this difference, it can be observed that 0.113 GJ of energy is absorbed and converted to internal energy, sliding energy, heat energy and hourglass energy.

5.2.3. Energy Converted to Heat

Among the loss of kinetic energy 0.106 GJ or 93.8 % of energy was converted in the form of sliding energy, which results frictional heating, as shown on Figure 5.13 and the remaining 6.2% energy was dissipated in the form of external work and internal energy.

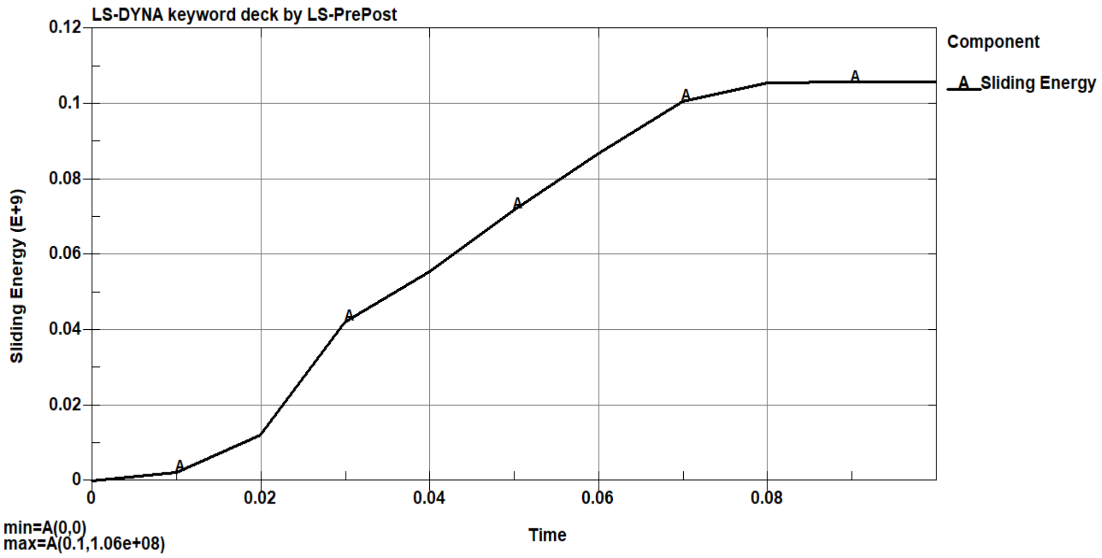

Figure 5.2. Sliding energy

5.2.4. Temperature distribution

During sliding kinetic energy converted to frictional energy and causes heating. This heat generate temperature rise around the friction disc.

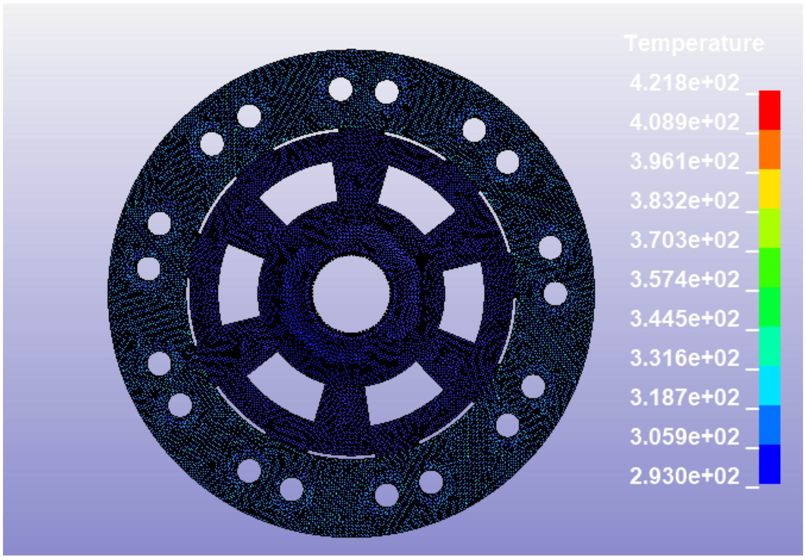

Figure 5.3. Temperature distribution of asbestos lining

From the above Figure 5.4. Liner asbestos reaches a maximum temperature T = 421.8 °K at end of sliding, t=10 s and at the mid of the period of sliding T = 360.9 °K.

5.2.5. Heat Flux

Heat flux is the rate of heat energy transfer in per unit surface through a given surface. The heat generated by slipping absorbed by the pressure plate and flywheel. The heat flux at the time t from the center of the friction disc is as follows:

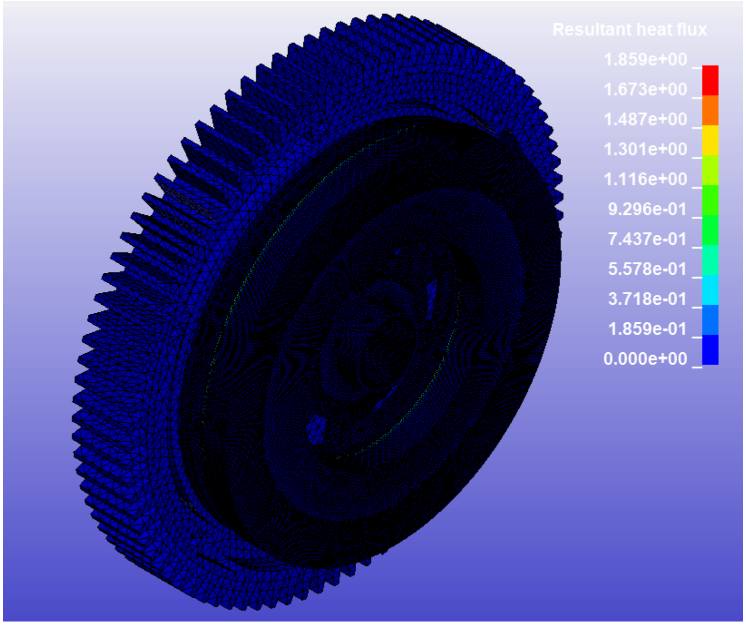

Figure 5.4. Heat flux

The above Figures 5.5. Shows the change in heat flow as a function of the radius of the clutch disk for both sides of the clutch disk at the selected time interval. You can see it at the beginning of the clutch engagement at (t=0.02s). The maximum value of the heat flux occurs near ro and the minimum value occurs at ri in this cases. After the start of engagement, thermal deformation affects the contact pressure distribution. As a result, the heat flux distribution also changes. The heat flow area decreases over time. The maximum value of the heat flux generated between the flywheel, pressure plate and friction plate is 1.859 MW/m^2.

5.3. Result and Discussion of Modified Clutch

In this section, the result of the modified Minidor clutch transient analysis was discussed.

5.3.1. Effective von misses stress

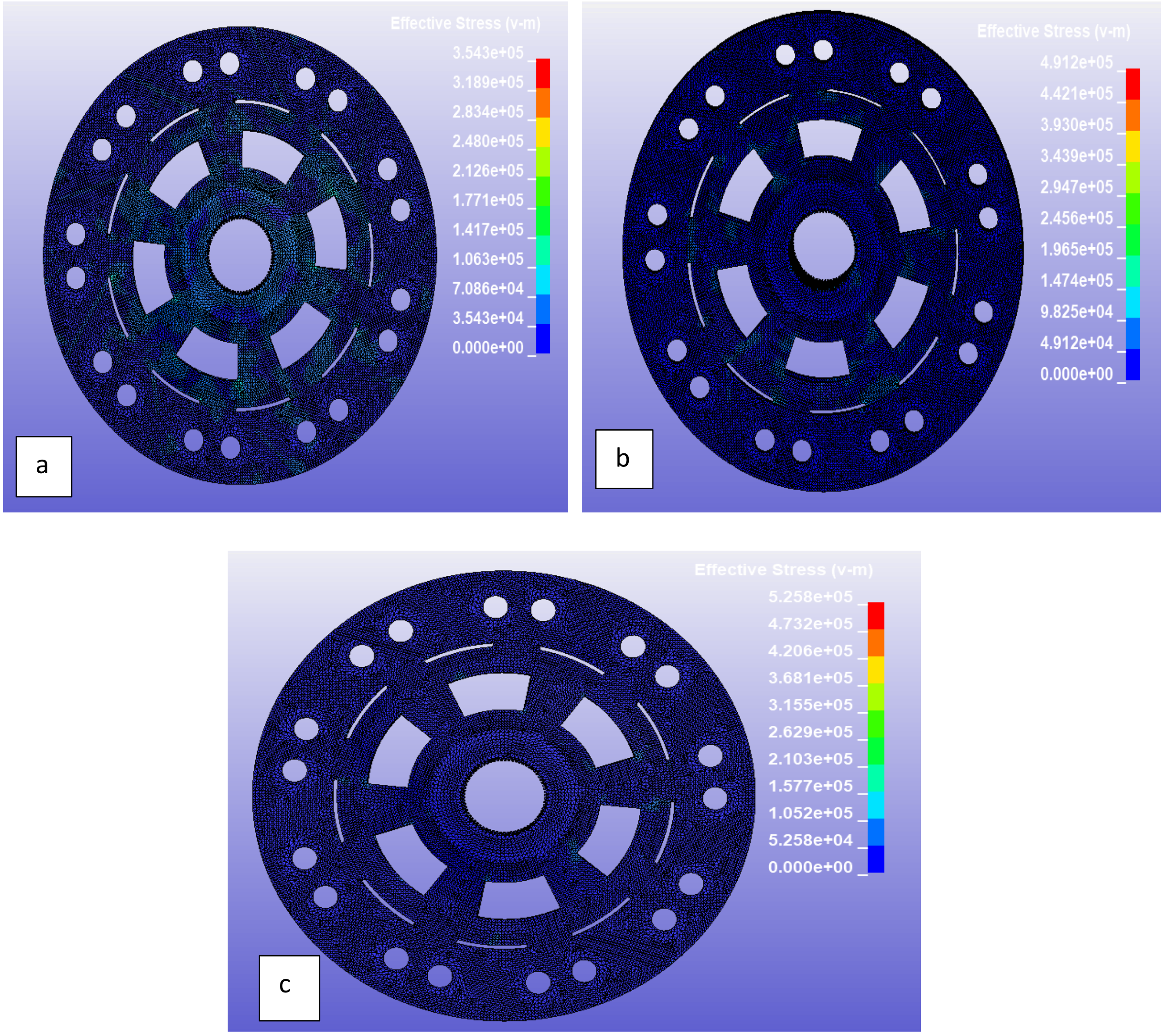

Figure 5.5. Von misses stress results of (a)alumina (b)aluminium alloy A360 (c) Kevlar 49

The above Figure 5.6 shows von misses stress with temperature effect done in LS DYNA workbench software over clutch disc in engaged state. As shown the contour plot, maximum von misses stress is indicating by red color, which has value of 354.3kPa for Alumina lining. In addition, the figure depicted that the von misses stress is high around the lip of the disc in contact with pressure plate. Same procedure used for Aluminum alloy A360 and Kevlar49 and recorded von misses.

Stress with respect to each applied boundary condition, is 419.2kPa and 528.8kPa. and also the comparison between the materials shows maximum von misses stress the result is recorded in Kevlar49.

5.3.2. Total Energy-balance graph

The law of conservation of energy states that energy cannot be created or destroyed and can be transformed from one form of energy to another. Applying the same principle to thermal analysis, the amount of kinetic energy lost during bonding must be converted into other forms of energy such as internal energy, sliding energy and external work energy.

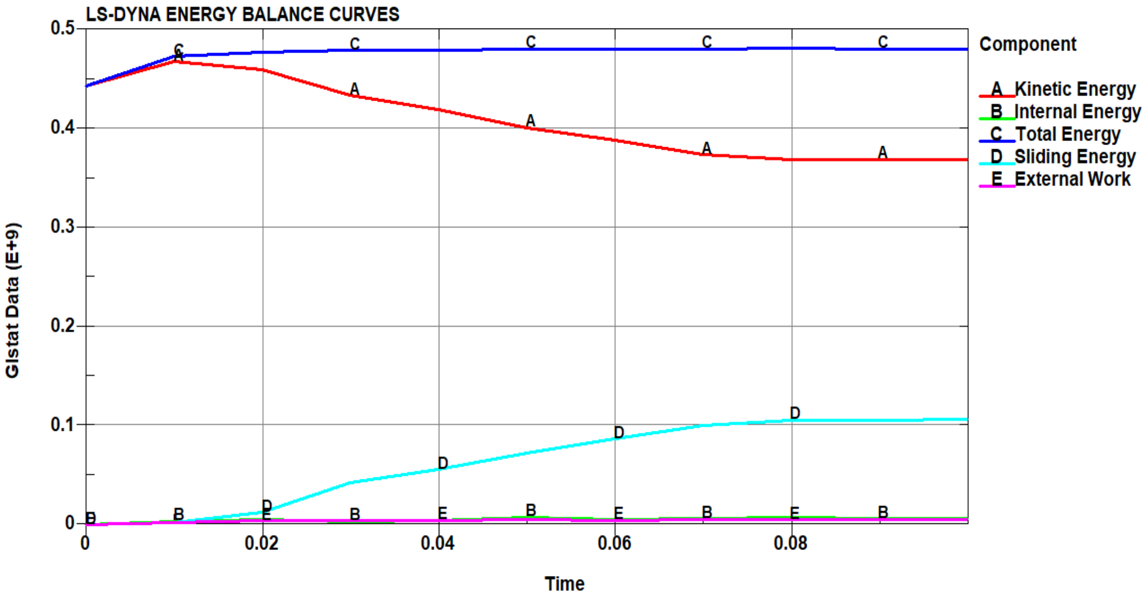

Figure 5.6. Energy balance curve

From figure 5.7. It has seen that, at the start the kinetic energy that is high at the beginning of the impact is equal with the total energy with value equal to 0.481 GJ. As the engaging event happens, the system kinetic energy starts to slowly being reduce, converted to other forms of energy, and then finally reaches to 0.368 GJ of energy. From this difference, it can be observed that 0.113 GJ of energy is absorbed and converted to internal energy, sliding energy, heat energy and hourglass energy.

5.3.3. Energy Converted to Heat

Among the loss of kinetic energy 0.106 GJ or 93.8 % of energy was converted in the form of sliding energy, which results frictional heating, as shown on Figure 5.13 and the remaining 6.2% energy was dissipated in the form of external work and internal energy.

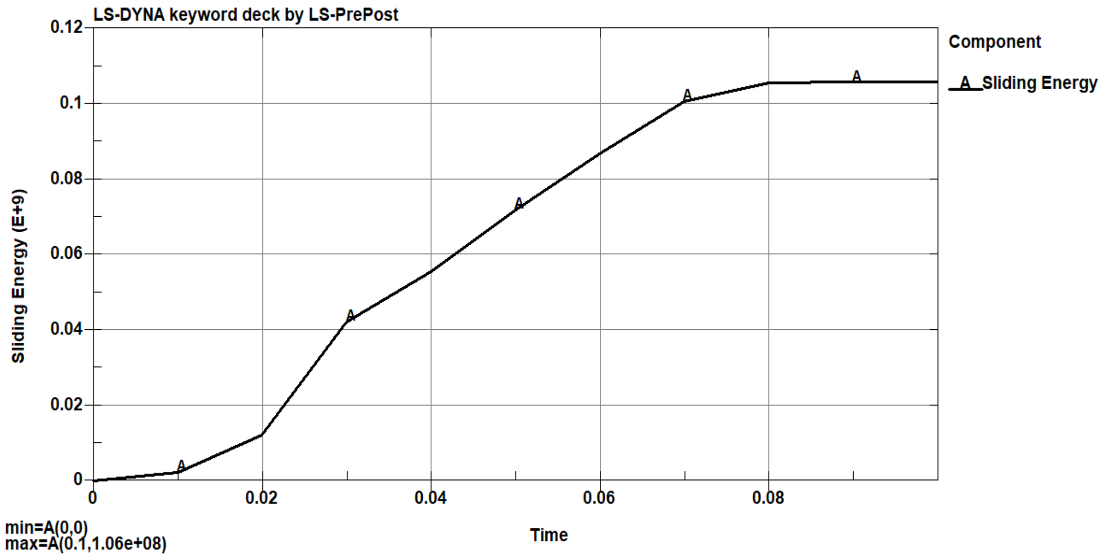

Figure 5.7 Sliding energy

5.3.4. Effect of the Friction Material on the Thermal Behavior of the Clutch

As for the case of clutch disc, the choice of friction material has a positive effect on the thermal and tribological behavior of the clutch elements. In this section, I try to compare the thermal behavior of three different materials of a single disc clutch linings. The chosen materials are aluminum alloy A360, alumina Al2O3 and kevlar49. They are generally used in the tribological and thermomechanical domain because of their good friction and wear behavior and resistance to thermal stresses. From Figure 5.14, the temperature of the liner kevlar49 during the sliding phase is much larger than the other two types of aluminum alloy A360 and alumina linings.

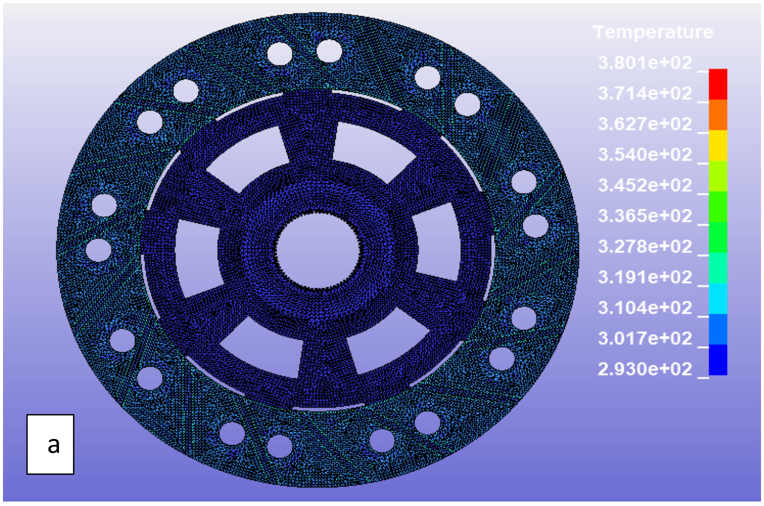

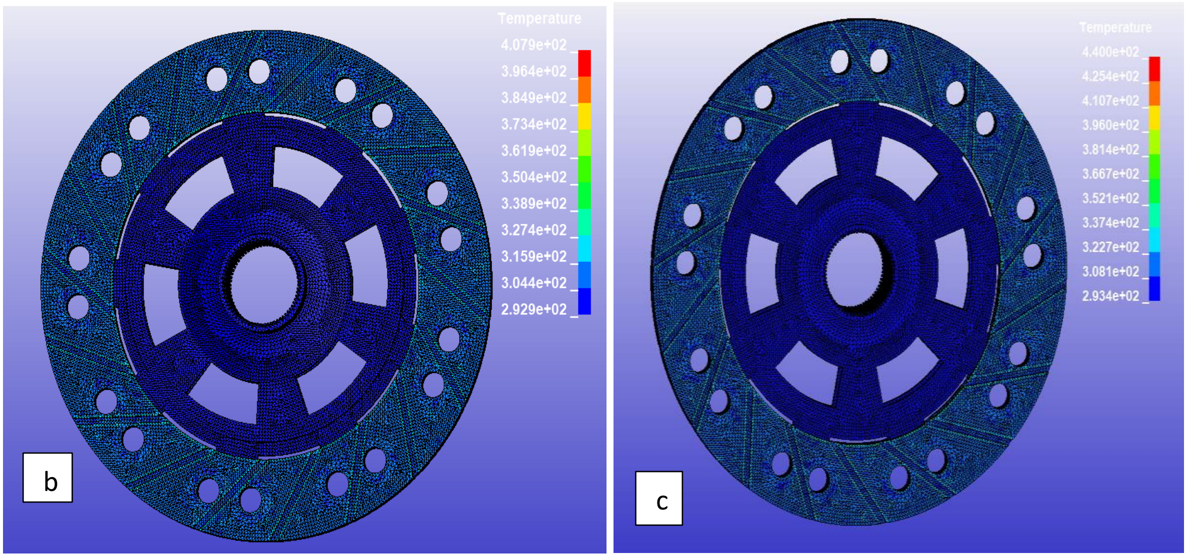

Figure 5.8. Temperature distribution of (a) Alumina (b) Aluminium alloy (c) Kevlar49

The liner kevlar49 reaches a maximum temperature T = 440 °K at end of sliding, t=10 s and at the mid of the period of sliding T = 362.9 °K, while for the material of alumina Al2O3 is T = 334.26 °K at t = 5 s and T =380.1°k to t = 10 s. The maximum variation in temperature at t = 5 s is 28.64 °K and at t = 10 s it is 59.9 °K. In case of the lining of aluminum alloy A360, the maximum temperature at the instant t = 0.5 s is T = 347.8°K and passes at T 407.9°K at t = 10. The sliding time affect frictional heating. From the thermal point of view, the best alternative is the lining of alumina Al2O3.

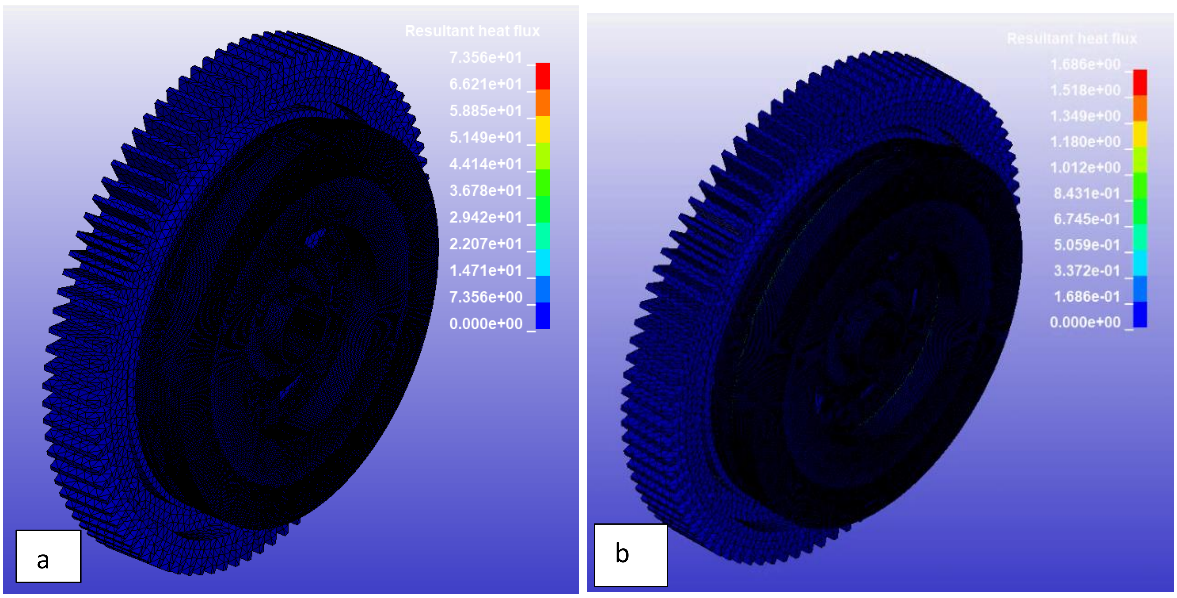

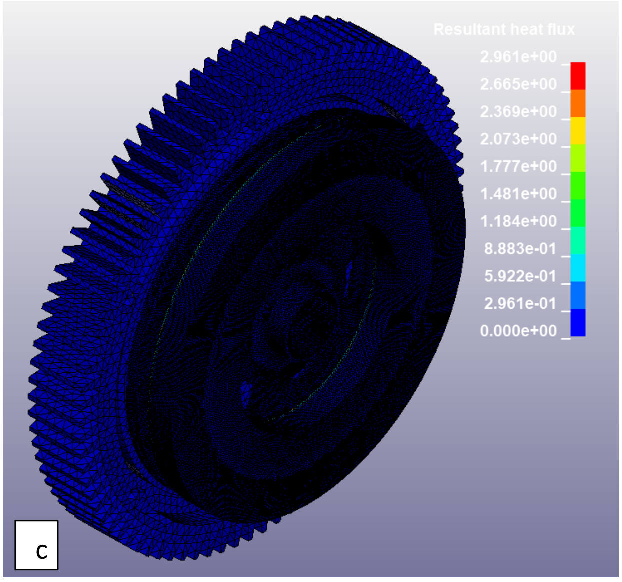

Figure 5.9. Heat flux of (a) Alumina (b) Aluminium alloy A360 (c) Kevlar49

Figures 5.10. Shows the change in heat flow as a function of the radius of the clutch disk for both sides of the clutch disk at the selected time interval. You can see it at the beginning of the clutch engagement at (t=0.02s). The maximum value of the heat flux occurs near ro and the minimum value occurs at ri in all cases. Shortly after the start of bonding, thermal deformation affects the contact pressure distribution. As a result, the heat flux distribution also changes. The heat flow area decreases over time in all cases, but for alumina the heat flow area is much smaller than in the other cases. The maximum value of the heat flux for all cases corresponds to the outer radius and turns out to be 1.686 MW/m2, 2.961 MW/m2 and 73.56 MW/m2 corresponds to the Alumina, Kevlar49 and Aluminum alloy A360 respectively

5.3.5. Inner and Outer Node Temperature

The temperature at the inner and outer node of friction lining was determined, to indicate at what direction, dose temperature dissipate quickly and which side was exposed to high heat.

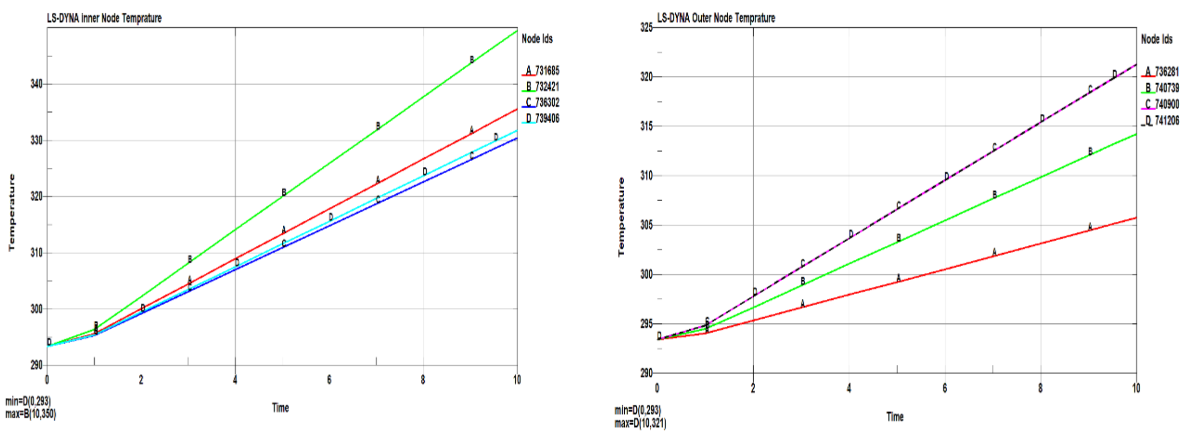

Figure 5.10. Inner and outer node temperature distribution of Aluminium alloy A360 lining

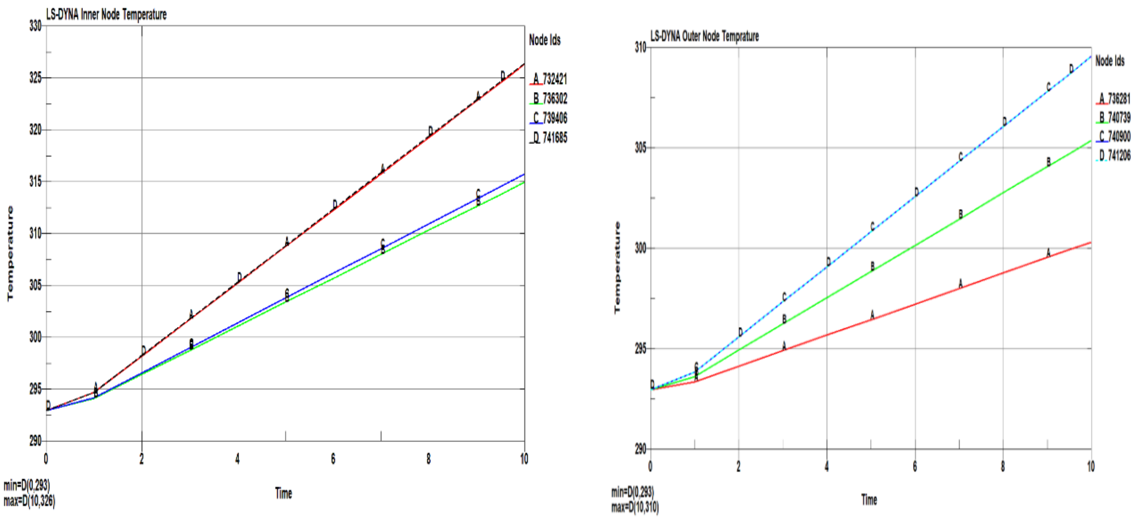

Figure 5.11. Inner and outer node temperature distribution of Alumina lining

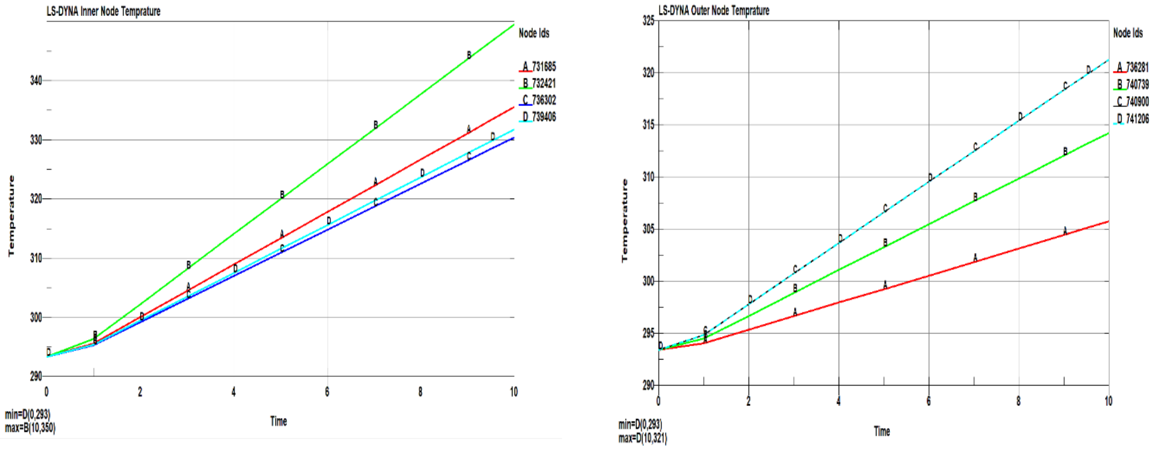

Figure 5.12. Inner and outer node temperature distribution of Kevlar49 lining

Figure (5.11-5.13) shows the temperature change with the radius of the disk. It has seen that the temperature increases almost linearly in the radial direction of the disk. This means that the temperature is maximum at the inner edge of the disk and minimum around the disk. For discs made of Kevlar49 and aluminum alloy A360, the temperature rises from T = 321 °K at the outer radius to T = 350 °K at the inner radius, the difference being 29 °K in a linear fashion. For discs with aluminum surfaces, the temperature is maximum at the inner end of the disc with T = 326 °K and at the outer axial disc at 310 °K. Due to the convective action of these regions, the temperature change in the regions located at the outer and inner radii of the clutch disk decreases with increasing radius and has an inverse relationship.

5.3.6. Wear volume

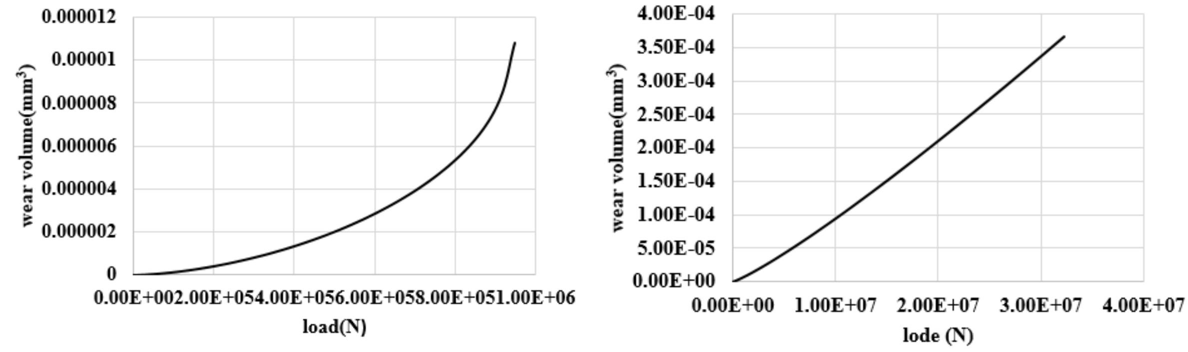

Figure 5.13. Aluminum alloy A360 wear volume at contact side of pressure plate and flywheel respectively

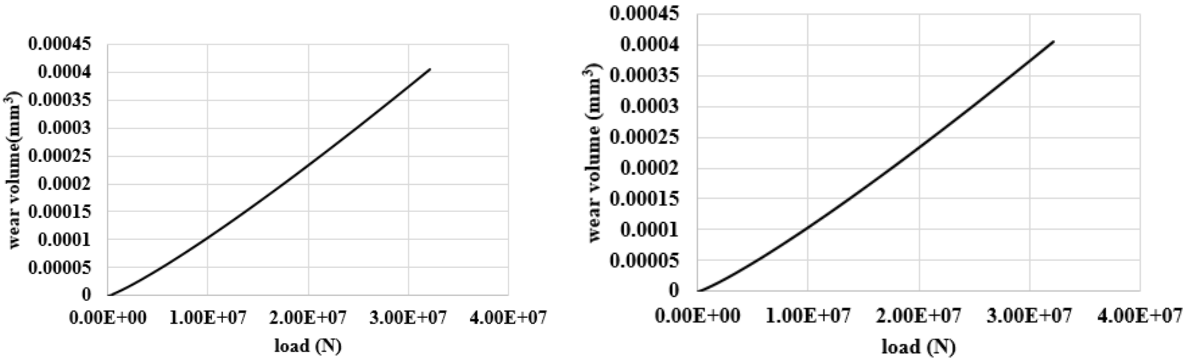

Figure 5.14. Kevlar49 wear volume at contact side of pressure plate and flywheel respectively

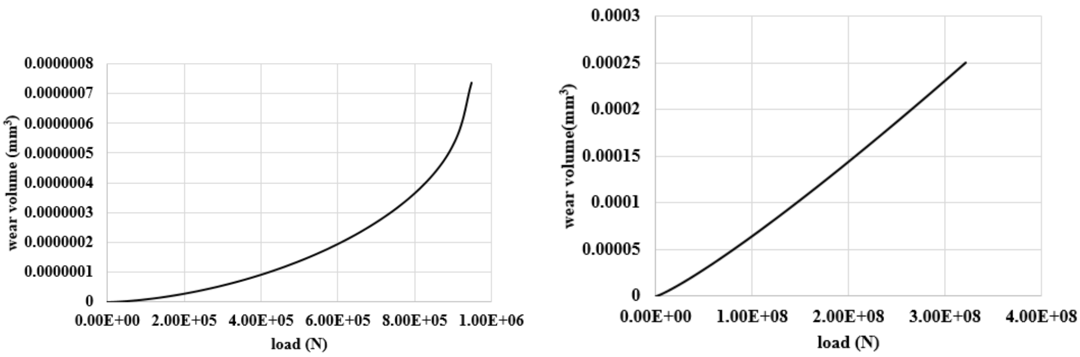

Figure 5.15. Alumina wear volume at contact side of pressure plate and flywheel respectively

Figure (5.14-5.16) shows the relationship between the wear volume and the load. The wear volume increases linearly with an increase in load. the change in the amount of wear along the disk radius. When load increases the wear resistance decreases and volume increases For aluminum alloy A360, the amount of wear debris at both contact is 0.00912 mm. the amount of alumina lining removed is 0.00319mm and for Kevlar49 the volume is 0.01mm. The wear volume of Kevlar49is much larger than the other two lining. Therefor alumina is chosen for less volume.

5.3.7. Wear depth

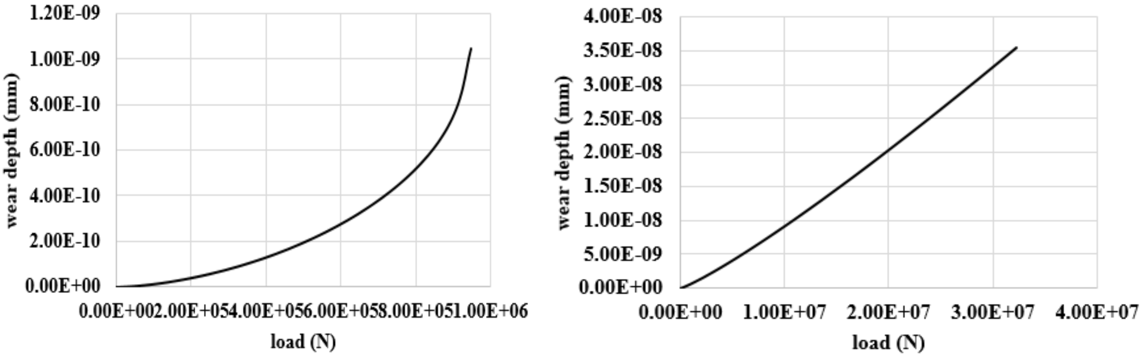

Figure 5.16. Aluminium alloy A360 wear depth at contact side of pressure plate and flywheel respectively

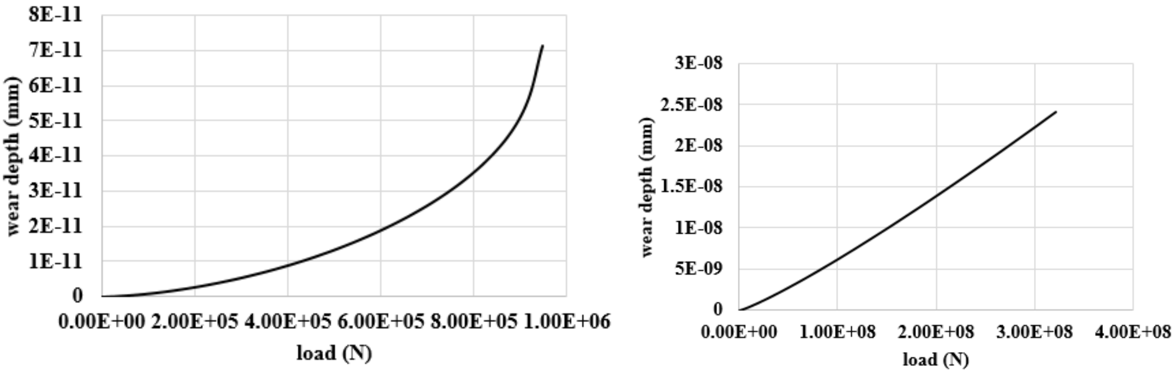

Figure 5.17. Alumina wear depth at contact side of pressure plate and flywheel respectively

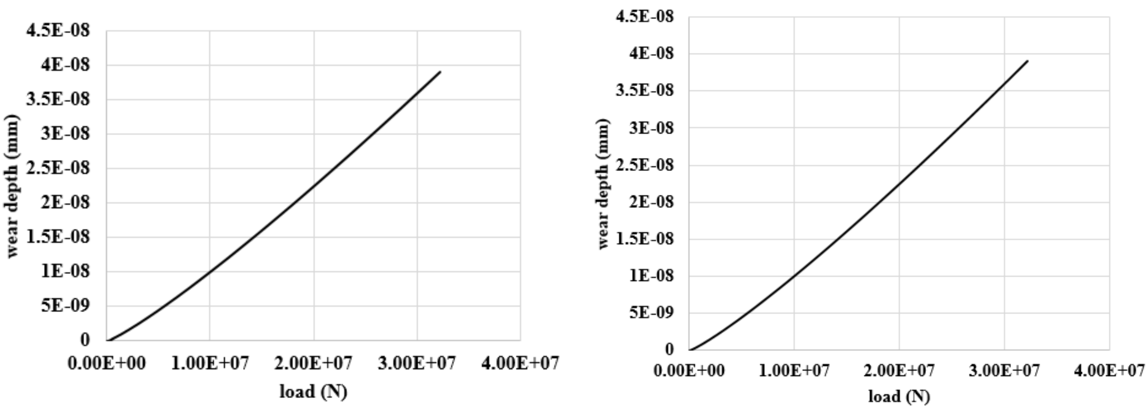

Figure 5.18. Kevlar49 wear depth at contact side of pressure plate and flywheel respectively

From figure (5.17-5.19) shows the variation of the wear depth along the contact surface at both sides. From the above figure, wear depth and load are directly proportional. When load increases wear volume, also increase linearly. It has found that the depth increases in an almost linear manner in the flywheel direction of the disc. This means that the depth at the flywheel direction of the disc are maximum and minimum on the pressure plate and flywheel direction of the disc. For kevlar49 wear depth at flywheel side is h=4.94 e-7 mm and at the pressure plate side is h=4.97 e-7 mm. For aluminum alloy A360 disc, the wear depth is h=4.47 e-7 mm at the flywheel and h=4.34 e-8 mm in pressure plate side. For the disc with alumina surfaces, the wear depth is maximum at flywheel side of the disc with h=3.05 e-7 mm and in the pressure plate side of the axial disc h=2.96 e-9 mm. The depth variation in regions which located at flywheel and pressure plate side of clutch disc because of the effect of load and sliding distance on these regions, when hardness of material increases volume reduced, they have invers relation.

5.4. Comparison Between Existed and Modified Single Plate Clutch

Comparisons were used to evaluate and compare values between two or more viewpoints. The existing and modified single plate of Minidor clutch simulation results were compared using the following parameters

- ❖ Stress
- ❖ Temperature
- ❖ Heat flux
- ❖ Wear volume

Table 5.1 Summary of comparison between existing and modified clutch model

Material	Stress (kPa)	Temperature (°K)	Heat flux (MW/m2)	Wear volume(mm3)
Alumina	354.3	380.1	1.686	0.00319
Aluminium alloy A360	418.2	407.9	73.56	0.00912
Kevlar49	528.8	440	2.961	0.01
Asbestos	440.2	421.8	1.859	0.00951

5.5. Verification

Validation is to verify how accurately the model reflects reality. Notice that there are two alternative methods. The first one is to compare the simulation results with the experimental results, and the other one is to crosscheck with the existing mechanical studies confirmed by the experimental data.

Since the clutch model selected in this study has made for low-income countries, it is difficult to verify it with previous studies on other vehicles. In addition, the validation of numerical results is limited by the work of previous researchers because the experimental budget allocated to this study becomes an obstacle to conduct new experimental setting and research.

As a result that the validation of mechanical model merely referring to the suitability of aforementioned vibration and thermal model for clutch performance analysis. In numerous clutch performance study mechanical model is utilized and have shown a very good correlation with experimental findings (Clifton et al., 2018) (Erdiwansyah et al., 2019) (Modepalli, 2015). Based on that the finding of this study is well constructed and verified.

According to the stability of the clutch the von misses stress is 354.3 kPa less than the yield strength. This is a decent agreement that the designed clutch is safe for a full load on the numerical technique of stability analysis.

(O.Dabas, 2018) evaluates the wear volume, wear depth and wear rate of friction lining at different load and speed. wear tests were carried out at a sliding distance of 11 m, a speed of 0.36 m/s, a duration of 30 s and loads in the range 3-11 N. The effect of load and speed on wear volume and wear depth of friction lining was increased when load and speed increases. The following figure shows wear volume and depth graph found by O.Dabas.

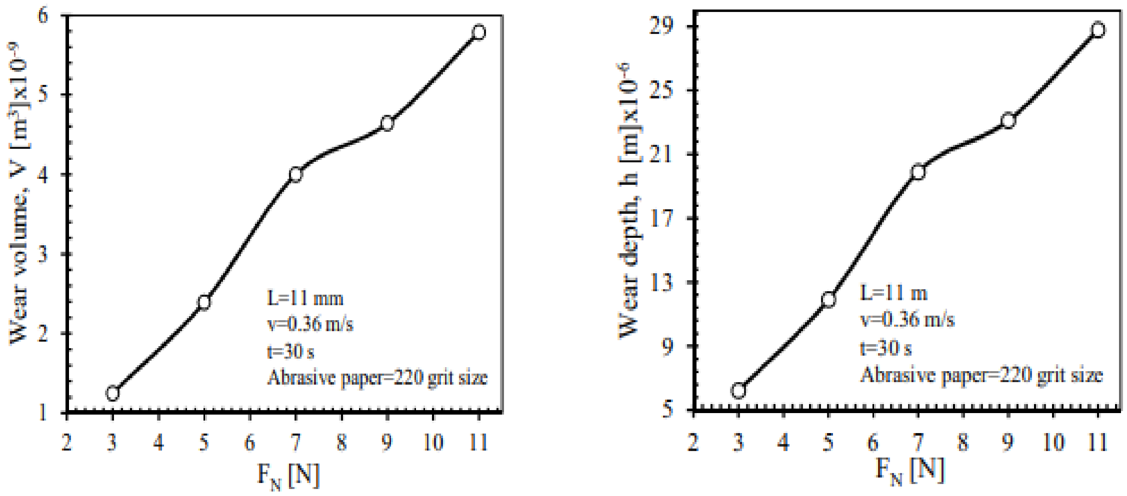

CHAPTER SIX

CONCLUSION AND RECOMMENDATION

6.1. Conclusion

Transient thermal analysis of three different non asbestos-based clutch lining replacement materials was performed. Analysis is performed to ensure a longer life and more reliable operation of the clutch disc and ultimately the clutch itself. Simulation results successfully show that the best friction lining material based on temperature, heat dissipation, stress, amount of wear debris to reduce temperature rise and maximize heat dissipation compared to asbestos-based friction linings. From the comparison alumina has good heat dissipation, low stress, low temperature and low wear volume.

The percent reduction in temperature distribution became 11.03% alumina, 4.52% aluminum alloy A360 but kevlar49 show 3% increment in heat generation than the existed. Therefore, alumina has better heat dissipation than the other two. The amount of wear debris of alumina lining removed is 0.00319mm and for Kevlar49 the volume is 0.01mm. Alumina has better heat dissipation and wear resistance than the other two. So alumina can substitute asbestos lining.

6.2. Recommendation

Based on the studies done on this thesis work the following points are recommended:

- ❖ It can be observed that with little modification the comfort of the current Minidor, force three wheeler can be improved, so that the owners and manufacturers shall implement some of the comfort developments concepts discussed on this thesis work to improve the comfort and life of the Bajaj.
- ❖ As the study shows even with average and less speed the Minidor, Force Bajaj has causing more sever vibration and health hazard, so it is better if the government and concerning bodies implement the comfort and health regulation for three wheelers which are play a crucial role on the economy of our country.
- ❖ The consequence of road and driver profile simulation should be included.

6.3. Future scope of the work

Considering the review of the existing research limitations and results the motivations for future research are suggested as follows:

- The present work evaluated the vibration behavior of existing Minidor three-wheeler by considering the response of the structure and this work can be extended to evaluating the response and resonance level to occupants at different road conditions.
- This action does not include road and driver profile effects. Therefore, the effects of road and driver profile modeling should be included and can be explored in the future.
- Future investigation will attempt to develop a system that will take initial design parameters and material properties of friction lining as an input, analyze clutch disc (structurally and thermally) and will give optimized design parameters and friction lining material for general purpose. You can also compare other non-asbestos materials for specific applications.

REFERENCE

Abdullah, O. I., Schlattmann, J., Majeed, M. H., & Sabri, L. A. (2018). The temperatures distributions of a single-disc clutches using heat partitioning and total heat generated approaches. *Case Studies in Thermal Engineering*, *11*, 43–54. https://doi.org/10.1016/j.csite.2017.12.003

Agrawal, A., Verma, A. K., & Dhagat, S. K. (2014). Optimization of multi plate friction clutch for maximum torque transmitting capacity using uniform wear theory. *Procedia Engineering*, *97*(August 2019), 1089–1096. https://doi.org/10.1016/j.proeng.2014.12.387

Banker, S., Lathiya, K. C., & Rathod, H. D. (2020). *Design modification and Failure Analysis of Damper Spring of 310 D.P.A of Single Plate Clutch System*.

Belhocine, A., & Omar, W. Z. W. (2016). A numerical parametric study of mechanical behavior of dry contact slipping on the disc-pads interface. *Alexandria Engineering Journal*, *55*(2), 1127–1141. https://doi.org/10.1016/j.aej.2016.03.025

Bhorkade, P. B., & Kakade, A. B. (2020). *Tribological behavior of Clutch Plate Material in Laboratory Simulated Conditions*. www.ijert.org

Bingham, P., Theodossiades, S., & Daubney, R. (2016). A study on automotive drivetrain transient response to "clutch abuse" events. *Proceedings of the Institution of Mechanical Engineers, Part D: Journal of Automobile Engineering*, *230*(10), 1403–1416. https://doi.org/10.1177/0954407015611293

Clifton, G. C., Abu, A., Gillies, A. G., Mago, N., & Cowie, K. (2018). Fire engineering design of composite floor systems for two way response in severe fires. *Applications of Fire Engineering - Proceedings of the International Conference of Applications of Structural Fire Engineering, ASFE 2017*, *March 2018*, 367–377. https://doi.org/10.1201/9781315107202-39

Della Gatta, A., Iannelli, L., Pisaturo, M., Senatore, A., & Vasca, F. (2018). A survey on modeling and engagement control for automotive dry clutch. In *Mechatronics* (Vol. 55, pp. 63–75). Elsevier Ltd. https://doi.org/10.1016/j.mechatronics.2018.08.002

Dhengre, N., Mogra, A., & Gupta, A. (2018). *Investigating Behaviour of Multi-Clutch Plate*

Frictional Materials using Investigating Behaviour of Multi-Clutch Plate Frictional Materials using ANSYS. *October 2020*.

Du Bois, P. &. (2010). Modeling & Simulation with LS-DYNA, Class material.

Du, D., Zhang, W., & An, J. (2022). Two Types of Wear Mechanisms Governing Transition between Mild and Severe Wear in Ti-6Al-4V Alloy during Dry Sliding at Temperatures of 20–250 °C. *Materials*, *15*(4). https://doi.org/10.3390/ma15041416

Dutta, T., & Baruah, L. (2014). *Engagement Model of Dry Friction Clutch with Diaphragm Spring*.

Dyna support, s. (2021). https://www.dynasupport.com/howtos/element/hourglass. Retrieved April 29, 2022, from https://www.dynasupport.com: https://www.dynasupport.com/howtos

Erdiwansyah, M.S.M. Sani1, R. Mamat, J.M. Zikri1, N. F. . R. and M. (2019). Experimental investigation of vibrations and noise characterization for spark ignition engine Experimental investigation of vibrations characterization for spark ignition engine and. *Journal of Physics*. https://doi.org/10.1088/1742-6596/1262/1/012014

Farrokhi, Z. N., Shahgholi;Gholamhossein, & , Agh, S. (2021). Studying the effect of balancer on engine vibration of massey ferguson 285 tractor. *Acta Technologica Agriculturae*, *24*(1), 14–19. https://doi.org/10.2478/ata-2021-0003

Fink, J. K. (2014). Aramids. *High Performance Polymers*, 301–320. https://doi.org/10.1016/b978-0-323-31222-6.00013-3

Frisk, D., & Tegehall, L. (2015). Planing Hull Cfd. *Chalmer University of Thechnology*.

Glodová, I., Lipták, T., & Bocko, J. (2014). Usage of finite element method for motion and thermal analysis of a specific object in SolidWorks environment. *Procedia Engineering*, *96*(April 2015), 131–135. https://doi.org/10.1016/j.proeng.2014.12.131

Gong, T., Yao, P., Xiao, Y., Fan, K., & Deng, M. (2015). Wear map for a copper-based friction clutch material under oil lubrication. *Wear*, *328–329*, 270–276. https://doi.org/10.1016/j.wear.2015.02.055

Grzelczyk, D., & Awrejcewicz, J. (2015). Wear processes in a mechanical friction clutch:

Theoretical, numerical, and experimental studies. *Mathematical Problems in Engineering*, *2015*. https://doi.org/10.1155/2015/725685

Guneş, F. E. (2015). Thermal Modeling and Simulation of Dry Friction Clutches in Heavy Duty Trucks. *Istanbul Technical University, June*.

Guo, W., Liu, Y., Zhang, J., & Xu, X. (2014). Dynamic analysis and control of the clutch filling process in clutch-to-clutch transmissions. *Mathematical Problems in Engineering*, *2014*(1). https://doi.org/10.1155/2014/293637

Ilie, F., & Cristescu, A. (2022). Tribological Behavior of Friction Materials of a Disk-Brake Pad Braking System Affected by Structural Changes — A Review. *MDPI, Basel, Switzerland*.

Kharat, R. M. (2015). Effect Of Vibration On The Health Of Driver Of Three Wheeler Using Iso. 2, 5029–5033. *Https://Doi.Org/10.15680/Ijirset.2016.0504192*

Kumbhalkar, M. A., Bhope, D. V., & Vanalkar, A. V. (2017). Evaluation Of Frequency Excitation Of Helical Suspension Spring Using Finite Element Analysis. *International Journal Of Computer Aided Engineering And Technology*, 9(4), 420–433. Https://Doi.Org/10.1504/Ijcaet.2017.086921

Lee, M., Park, G., Park, C., & Kim, C. (2020). Improvement of Grid Independence Test for Computational Fluid Dynamics Model of Building Based on Grid Resolution. *Advances in Civil Engineering*, *2020*. https://doi.org/10.1155/2020/8827936

Liu, Y. P. (2013). Simulation of vehicle's frontal crash with dummy inside. *Advanced Materials Research*, *760–762*(Iccsee), 1244–1249. https://doi.org/10.4028/www.scientific.net/AMR.760-762.1244

Luniya, T. A. (2019). Design of a Diaphragm Spring Clutch. *International Journal of Engineering Research and Technology (IJERT)*, *8*(11), 41–46. https://www.ijert.org

Mahendra. S and A.K.Jain. (2018). Design and Structural Analysis of Single Plate Clutch

By FEA. *International Journal for Research Trends and Innovation*, (www.ijrti.org).

ISSN: 2456-3315

M Akshay Shenoy. (2018). What-is-the-material-used-for-making-clutch-plates. In *Quora*.

Modepalli, G. (2015). Clutch Assembly Modeling and Dynamic Analysis. *International Journal of Mechanical And Production Engineering, 3,* 2320–2092. http://www.iraj.in/journal/journal_file/journal_pdf/2-197-1448169697102-107.pdf

Mr. Vishal J., Deshbhratar, and Mr. Nagnath, U. K. (2013). Design and structural analysis of single plate clutch. *International Journal of Engineering Research & Technology (IJERT)*, *10*(2), 411–414.

Myklebust, A. (2013). Modeling and Estimation for Dry Clutch Control. *Linkoping University Institute of Technology*, *1616*, 41.

Narayan, S., Grujić, I., Stojanović, N., Muhammad Usman, K., Shitu, A., & Mahroogi, F. (2018). DESIGN AND ANALYSIS OF AN AUTOMOTIVE SINGLE PLATE CLUTCH. *Mobility and Vehicle Mechanics*, *44*(1), 13–28. https://doi.org/10.24874/mvm.2018.44.01.02

Odabas, D. (2018). Effects of Load and Speed on Wear Rate of Abrasive Wear for 2014 Al Alloy. *IOP Conference Series: Materials Science and Engineering*.

Penta, A., Warule, P., Patel, S., & Dhamija, L. (2017). Development of High Fidelity Dynamic Model with Thermal Response for Single Plate Dry Clutch. *SAE International Journal of Passenger Cars - Mechanical Systems*, *10*(1), 378–384. https://doi.org/10.4271/2017-26-0260

Porwal, A., Tripathi, A., Agrawal, T., & Baskar, P. (2018). Optimal design of clutch plate based on heat and structural parameters using cfd and fea. *International Journal of Mechanical Engineering and Technology*, *9*(5), 717–724.

Process Industry Forum. (2014). Advantages And Disadvantages Of Metals Commonly Used In Manufacturing. In August 20, 2014 (Pp. 1–4). Http://Www.Processindustryforum.Com/Article/Advantages-Disadvantages-Metals-Commonly-Used-Manufacturing

Purohit, R., Khitoliya, P., & Koli, D. K. (2014). Design and Finite Element Analysis of an Automotive Clutch Assembly. *Procedia Materials Science*, *6*(Icmpc), 490–502.

https://doi.org/10.1016/j.mspro.2014.07.063

Rahat, T. (2019). Modelling and simulation of thermal strength of clutch pressure plate and flywheel with numerical analysis techniques. *BURSA ULUDAĞ ÜNİVERSİTESİ FEN BİLİMLERİ ENSTİTÜSÜ*.

Raut, G., Manjare, A., & Bhaskar, P. (2013). Analysis of Multidisc Clutch Using FEA. *International Journal of Engineering Trends and Technology*, *6*(1), 6–9. http://www.ijettjournal.org

Rupnar, A., Babar, A., Karale, A., & Gundawar, S. (2016). Design and Analysis of Diaphragm Spring of a Single Plate Dry Clutch. In *IJSTE-International Journal of Science Technology & Engineering* | (Vol. 2). www.ijste.org

Santosh Soman, K. (2019). Design and development of continuous variable transmission with launch gear. In *International Journal of Advance Research*. www.IJARIIT.com

Shi, L. M., Feng, S. L., Wang, Z. H., & Jian, X. C. (2018). The optimization design and research of CX20 clutch friction plate. *Advanced Materials Research*, *900*, 781–786. https://doi.org/10.4028/www.scientific.net/AMR.900.781

Shinde, D., & Mistry, K. N. (2017). Asbestos base and asbestos free brake lining materials : comparative study. *International Journal of Scientific World*, *5*(1), 47. https://doi.org/10.14419/ijsw.v5i1.7082

Shriwas, P. ;Kumar S., Guruprasad;, & Sahu, G. (2015). A Review on Wear Analysis and Heat Generation in Dry Friction Clutch. *IJSTE-International Journal of Science Technology & Engineering |*, *2*(3), 71–75. www.ijste.org

Simulation Validation and Verification Testing _ Ansys. (2022).

Tang, J. (2012). Design of Automobile Clutch Plate Test System Based on Kalman Filter. *Energy Procedia*, *17*, 311–318. https://doi.org/10.1016/j.egypro.2012.02.100

P. Rajesh., Ribeiro, J. F and Madhogaria, T. (2014). Design and finite element analysis of an automotive clutch assembly. *Procedia Materials Science*, 6- 490 – 502.

Ravikiran M. and S. H. Sarje (2015). Design and Analysis of Clutch Plate for Automatic Single Plate Clutch. I*JSRD- International Journal for Scientific Research & Development*, 3.09.

Teixeira, R. L., Neto, F. P. L., & Ribeiro, J. F. (20016). Modelling And Experimental Investigation Of An Active Damper. Shock And Vibration, 13(4–5), 343–354. Https://Doi.Org/10.1155/2006/486719

Thacker, V., & Vijayaragavan, E. (2018). Design optimization of clutch cushion disc with the integration of finite element analysis and design of experiments. *IOP Conference Series: Materials Science and Engineering*, *402*(1). https://doi.org/10.1088/1757-899X/402/1/012053

Triana, C. A., & Fajardo, F. (2013). Experimental study of simple harmonic motion of a spring-mass system as a function of spring diameter. *Revista Brasileira De Ensino De Fisica*, 35(4). Https://Doi.Org/10.1590/S1806-11172013000400005

Uginox. (2021). The Advantages Of Stainless Steel In Roofing. Http://Www.Aperam.Com/Uploads/Stainlesseurope/Technicalpublications/Advantages Of Stainless Steel/Aperam-Leaflet-Roofing-Eng.Pdf

Venkiteswaran, A., Muralikrishna, S. V, & Subramoniam, V. *Optimal Design of A Single Plate Clutch Friction Disc Using ANSYS*.

Virmani, K., Madhogaria, T., & Baskar, P. (2021). Design optimization of friction lining of a clutch plate. *Materials Today: Proceedings*, *46*, 8009–8024. https://doi.org/10.1016/j.matpr.2021.02.775

Viswabharathy, P., Vigneshwar, G., Pragadhishwaran, M., & Gopalakrishnan, M. (2017). Static and Dynamic Analysis of Single Plate Clutch in Four Wheeler Application Using ANSYS. *International Journal of Emerging Technologies in Engineering Research (IJETER)*, *5*(3), 222–233. www.ijeter.everscience.org

Waghade, A. A., Bansod, G. V, & Mankar, N. N. (2014). Experimental And Harmonic Analysis Of Helical Suspension Spring Gauge : *Umrer College Of Engineering, Umrer, Dist. Nagpur, India*, 19(59).

Wu, H., & Wu, G. (2016). Driveline Torsional Analysis and Clutch Damper Optimization for Reducing Gear Rattle. *Shock and Vibration*, *2016*. https://doi.org/10.1155/2016/8434625

Yasmeen, S. A., Abhijit, A., & Rao, D. S. (2014). Dynamic Characteristic Estimation Of Structural Materials By Modal Analysis Using Ansys. *International Journal Of Advance Research In Science And Engineering*, 3(7), 197–204. Https://Drive.Google.Com/File/D/1e2qb_Mqeniscbzl1y0mlmk5d5aic4e96/View?Usp=Sharing

Zebdi, O., Boukhili, R., & Trochu, F. (2019). Optimum design of a composite helical spring by multi-criteria optimization. *Journal of Reinforced Plastics and Composites*, *28*(14), 1713–1732. https://doi.org/10.1177/0731684408090370

Zhang, Z., Zou, L., & Qing, H. (2021). Analysis of Factors Affecting Vibration during Wet Clutch Engagement. *IEEE Access*, *9*, 34298–34306. https://doi.org/10.1109/ACCESS.2021.3061009

Zhao, J., Chen, Z., Yang, H., & Yi, Y. (2016). *Finite element analysis of thermal buckling in automotive clutch plates*. *5739*(March). https://doi.org/10.1080/01495739.2015.1123590

Zhao, X., Wang, X., & Wang, Y. (2014). Analysis on the influence of the strength and stiffness under the contact conditions for friction plate. *Key Engineering Materials*, *579–580*, 523–529. https://doi.org/10.4028/www.scientific.net/KEM.579-580.523

Appendix – A

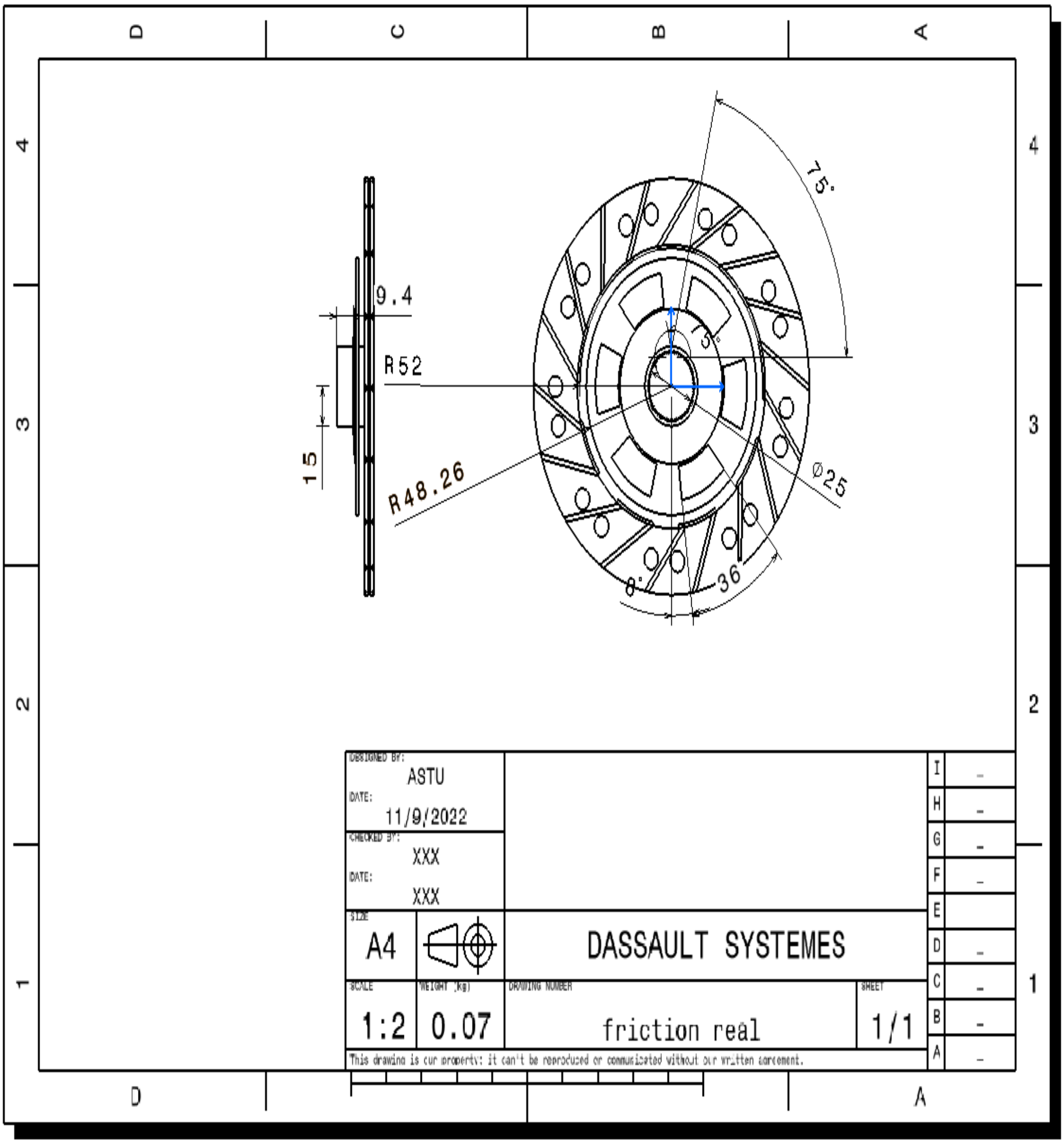

75°
9.4
R52
15°
15
R48.26
Ø25
36
8°
DESIGNED BY:
ASTU
DATE:
11/9/2022
CHECKED BY:
XXX
DATE:
XXX
SIZE
A4
DASSAULT SYSTEMES
SCALE
1:2
WEIGHT (kg)
0.07
DRAWING NUMBER
friction real
SHEET
1/1
This drawing is our property; it can't be reproduced or communicated without our written agreement.

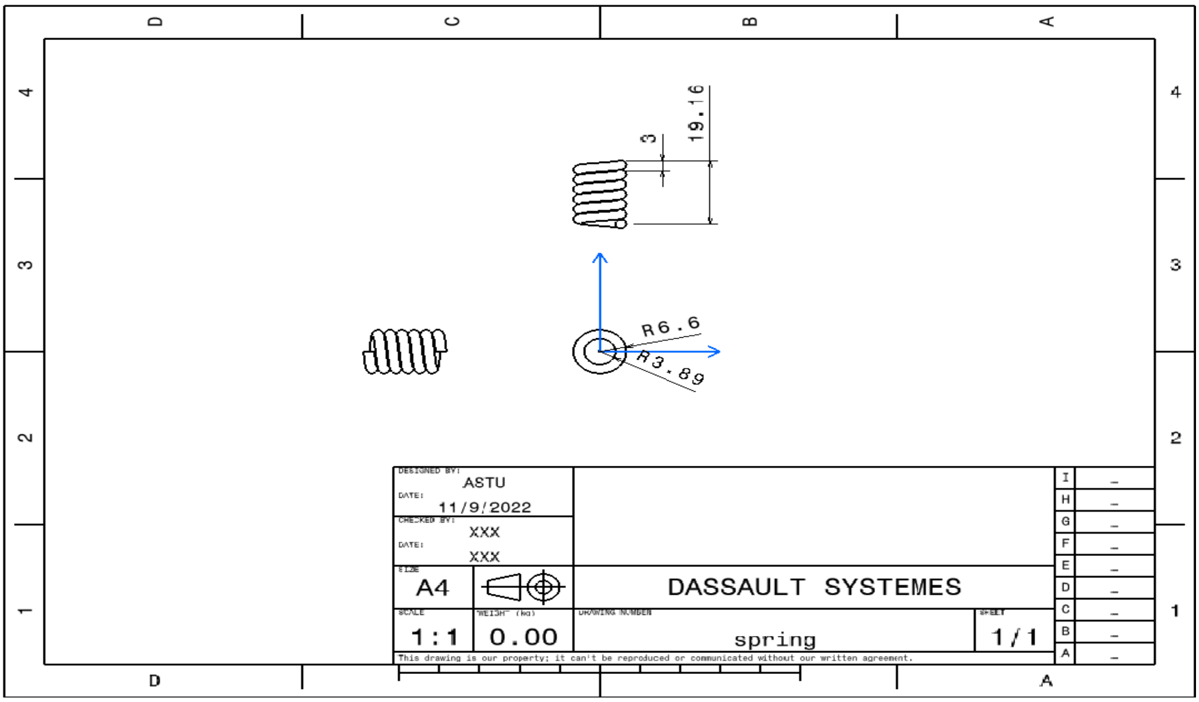
19.16
3
R6.6
R3.89
DESIGNED BY: ASTU
DATE: 11/9/2022
CHECKED BY: XXX
DATE: XXX
SIZE A4
DASSAULT SYSTEMES
SCALE 1:1
WEIGHT (kg) 0.00
DRAWING NUMBER spring
SHEET 1/1
This drawing is our property; it can't be reproduced or communicated without our written agreement.

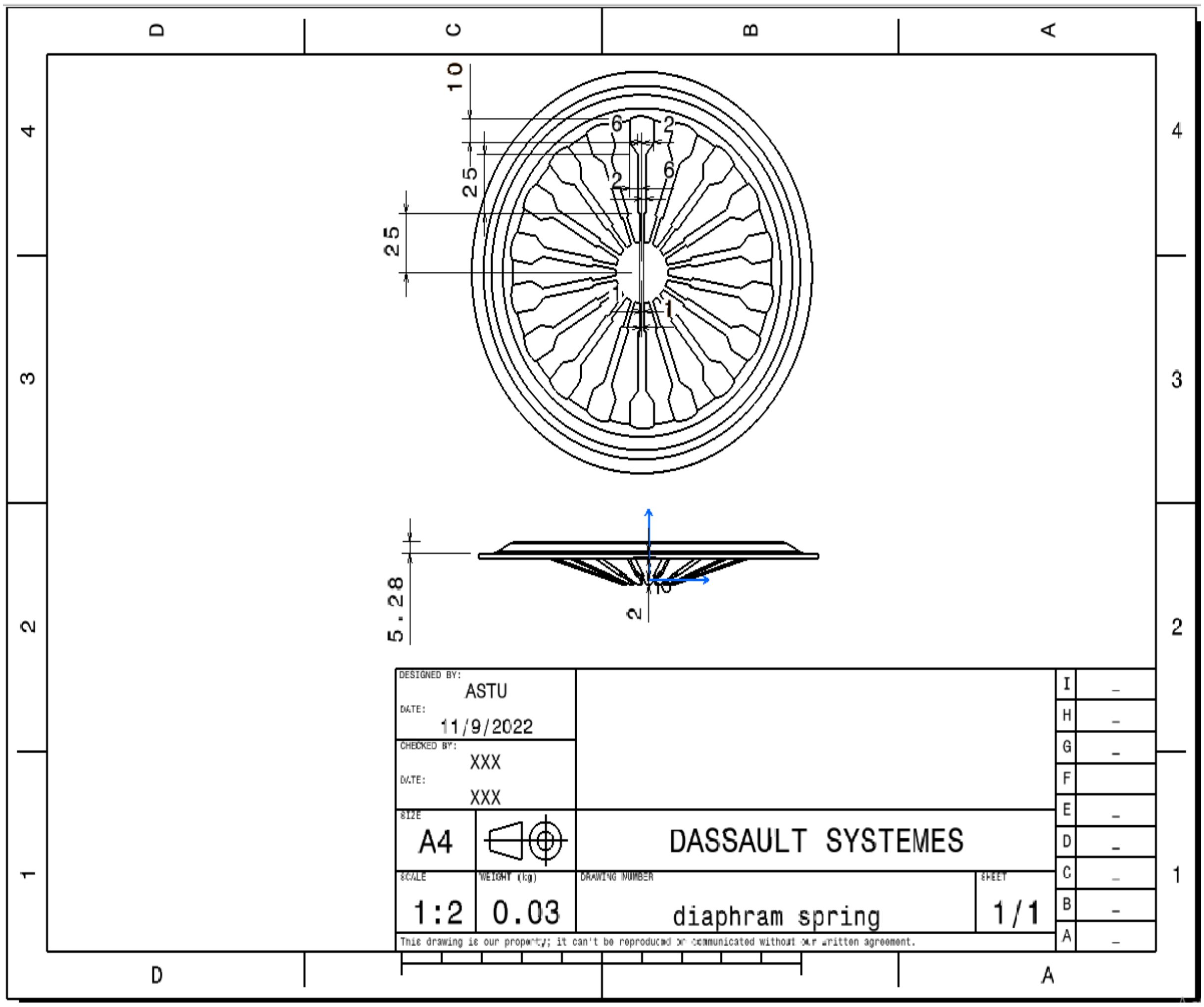
10
25
25
6
2
6
2
1
5.28
2
10
DESIGNED BY: ASTU
DATE: 11/9/2022
CHECKED BY: XXX
DATE: XXX
SIZE A4
DASSAULT SYSTEMES
SCALE 1:2
WEIGHT (kg) 0.03
DRAWING NUMBER diaphram spring
SHEET 1/1
This drawing is our property; it can't be reproduced or communicated without our written agreement.

Appendix – B

Results for existing

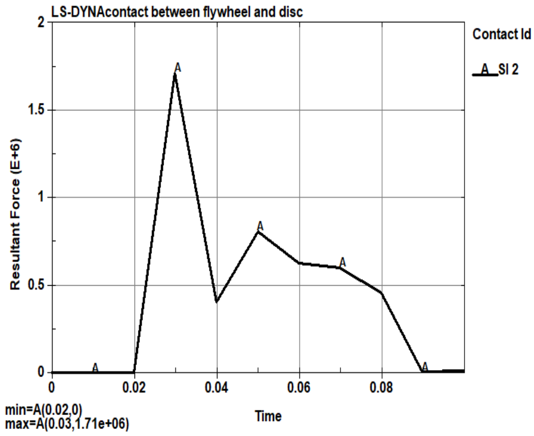

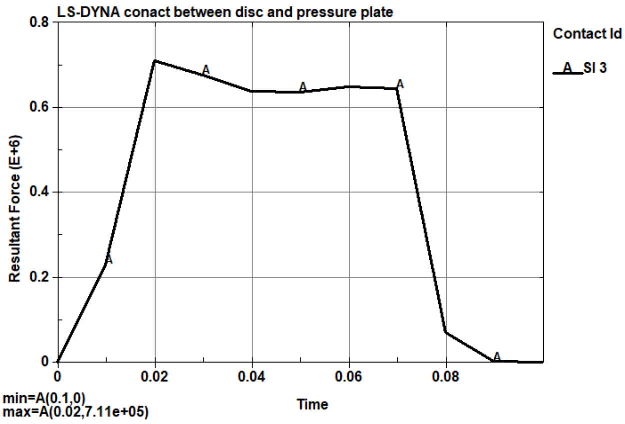

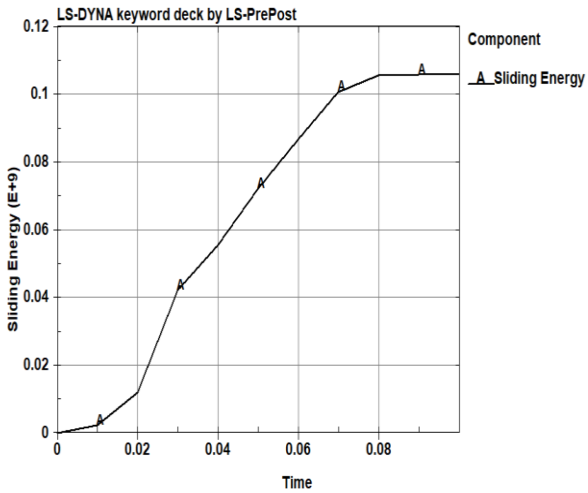

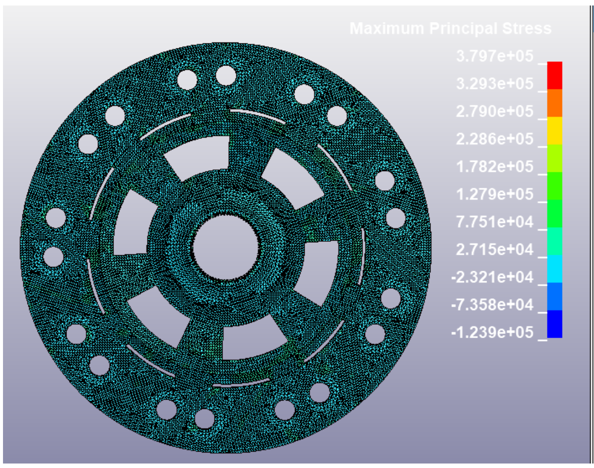

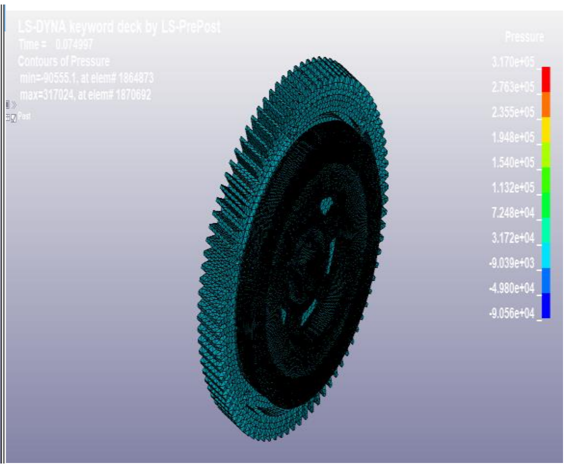

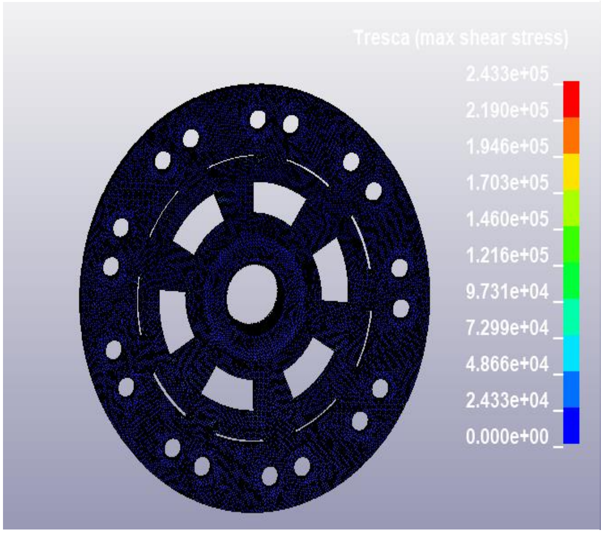

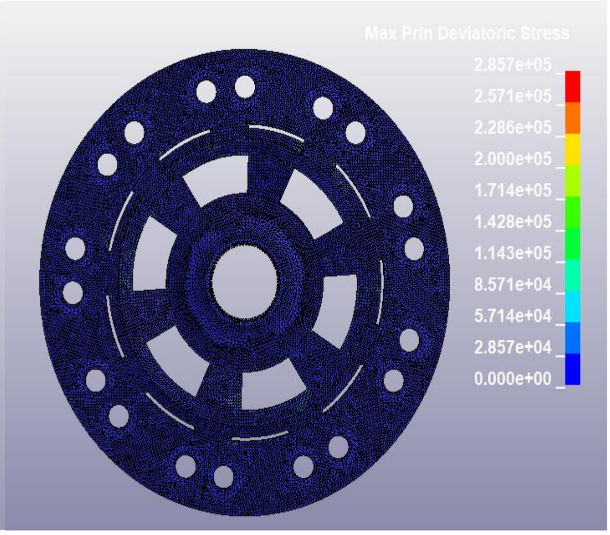

Results for modified

Alumina

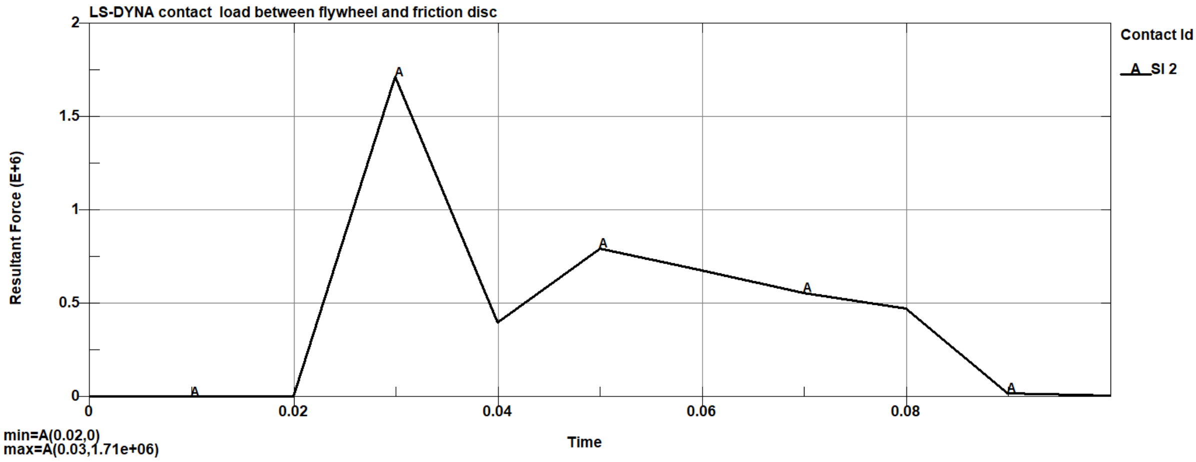

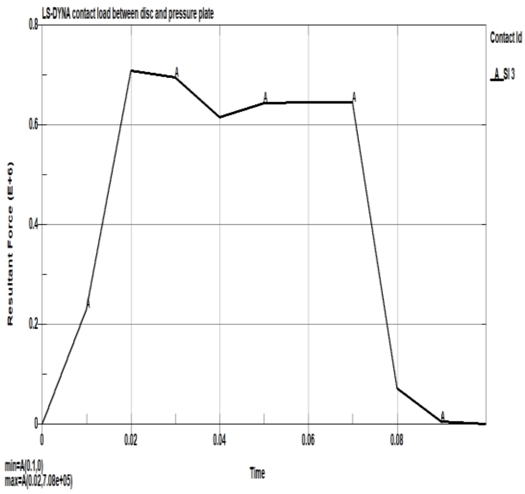

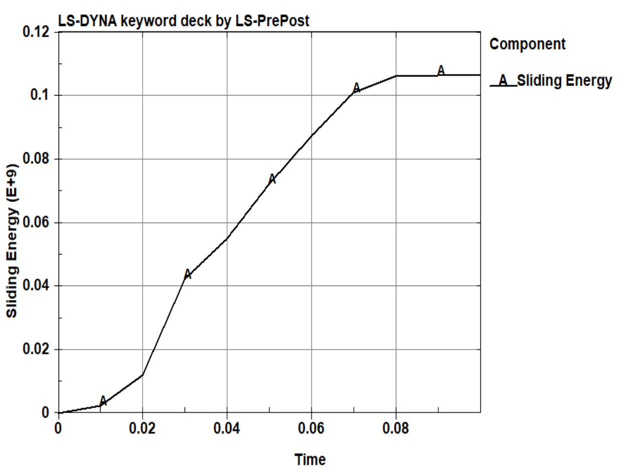

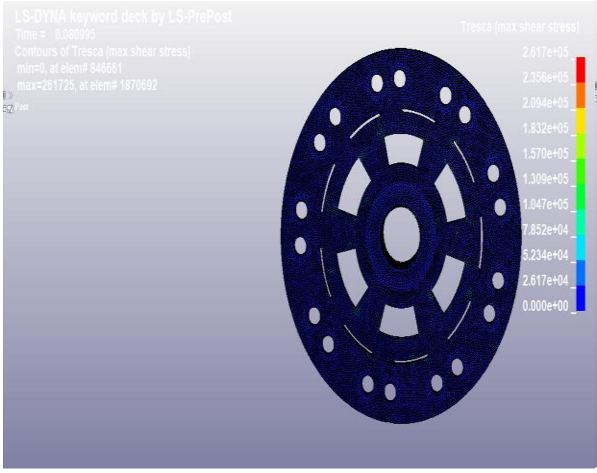
LS-DYNA keyword deck by LS-PrePost
Time = 0.080995
Contours of Tresca (max shear stress)
min=0, at elem# 846661
max=261725, at elem# 1870692
Tresca (max shear stress)
2.617e+05
2.356e+05
2.094e+05
1.832e+05
1.570e+05
1.309e+05
1.047e+05
7.852e+04
5.234e+04
2.617e+04
0.000e+00

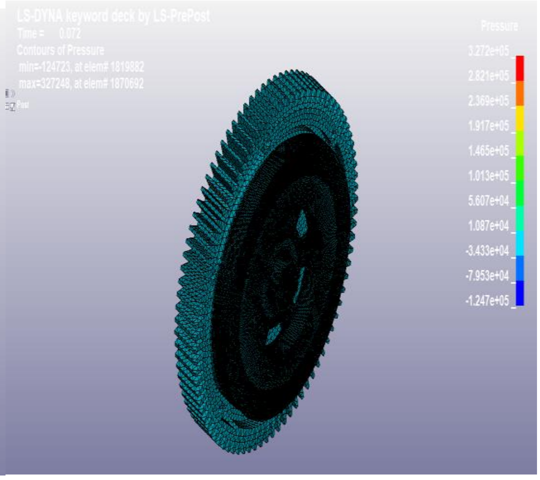
LS-DYNA keyword deck by LS-PrePost
Time = 0.072
Contours of Pressure
min=-124723, at elem# 1819882
max=327248, at elem# 1870692
Pressure
3.272e+05
2.821e+05
2.369e+05
1.917e+05
1.465e+05
1.013e+05
5.607e+04
1.087e+04
-3.433e+04
-7.953e+04
-1.247e+05

Kevlar 49

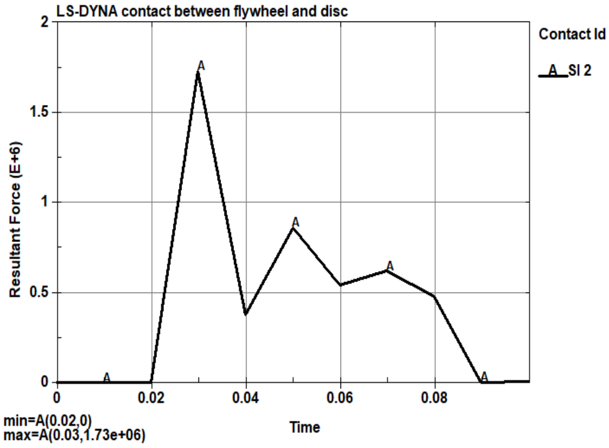
LS-DYNA contact between flywheel and disc
Contact Id
A SI 2
Resultant Force (E+6)
2
1.5
1
0.5
0
0
0.02
0.04
0.06
0.08
Time
min=A(0.02,0)
max=A(0.03,1.73e+06)

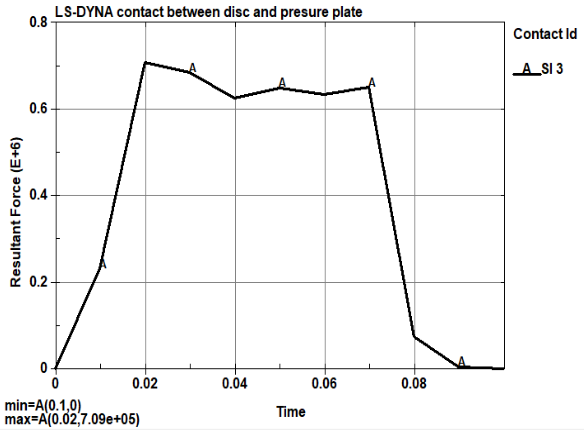
LS-DYNA contact between disc and presure plate
Contact Id
A SI 3
Resultant Force (E+6)
0.8
0.6
0.4
0.2
0
0
0.02
0.04
0.06
0.08
Time
min=A(0.1,0)
max=A(0.02,7.09e+05)

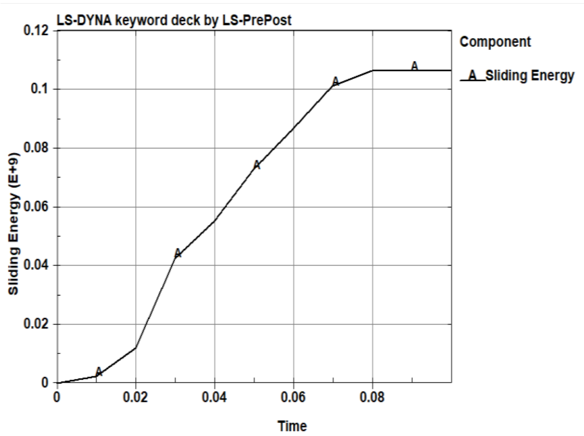
LS-DYNA keyword deck by LS-PrePost
Component
A Sliding Energy
Sliding Energy (E+9)
0.12
0.1
0.08
0.06
0.04
0.02
0
0
0.02
0.04
0.06
0.08
Time

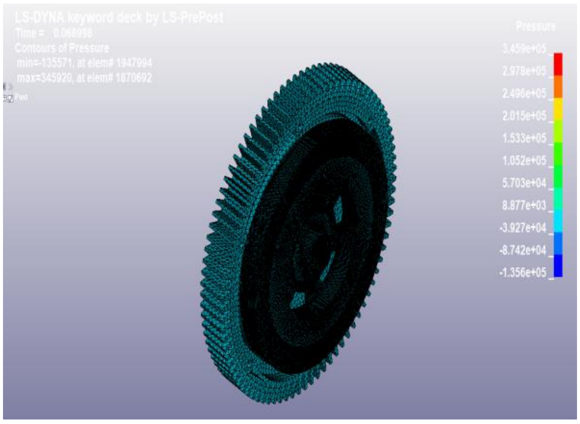
LS-DYNA keyword deck by LS-PrePost
Pressure

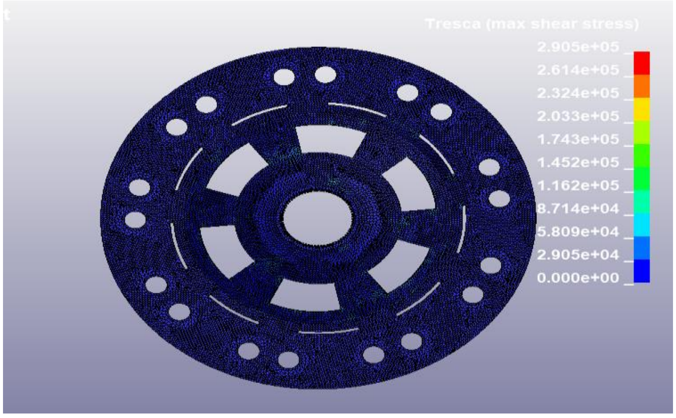

Aluminum alloy a360

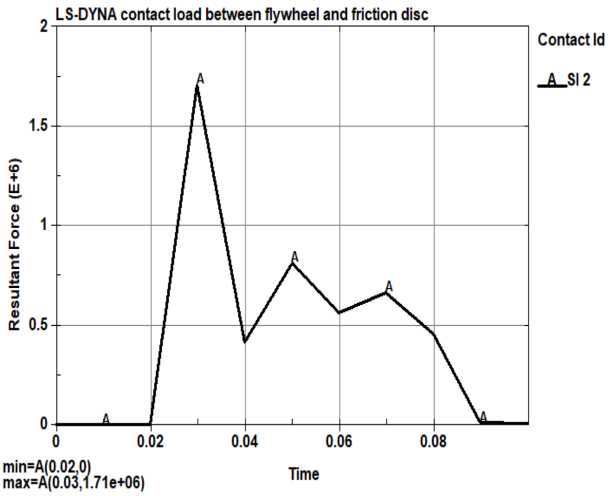

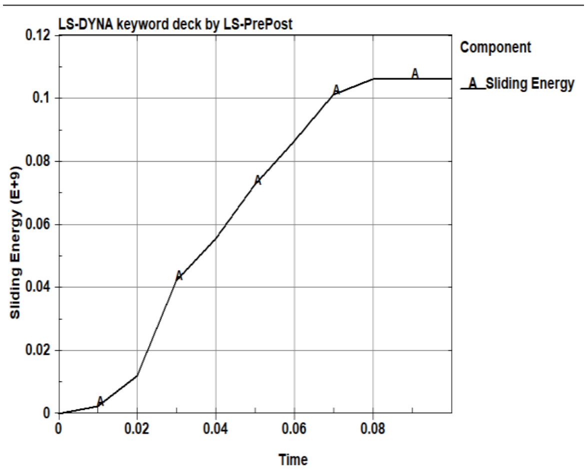

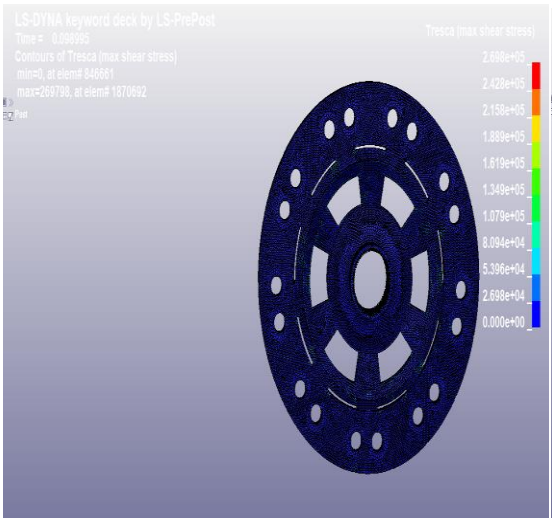

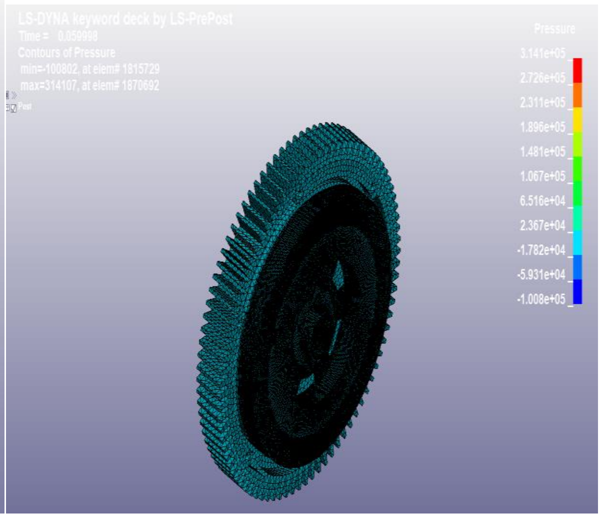

Appendix – C

Data collected from pilot study at Posta bet

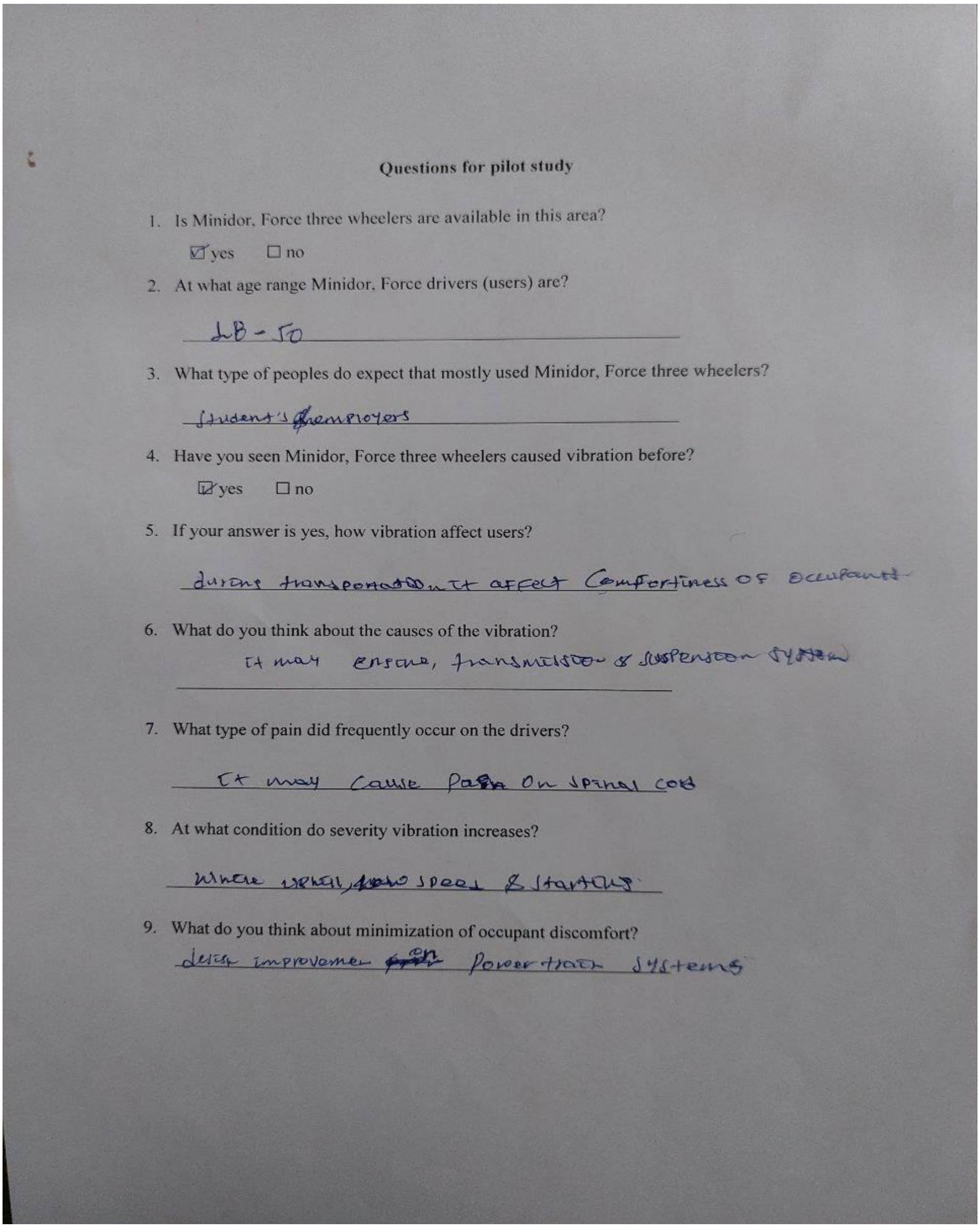

Questions for pilot study

1. Is Minidor, Force three wheelers are available in this area?

   ☑ yes ☐ no

2. At what age range Minidor, Force drivers (users) are?

   28 - 50

3. What type of peoples do expect that mostly used Minidor, Force three wheelers?

   Student's employers

4. Have you seen Minidor, Force three wheelers caused vibration before?

   ☑ yes ☐ no

5. If your answer is yes, how vibration affect users?

   during transportation it affect comfortiness of occupant

6. What do you think about the causes of the vibration?

   It may engine, transmission & suspension system

7. What type of pain did frequently occur on the drivers?

   It may cause pain on spinal cord

8. At what condition do severity vibration increases?

   Where uneven, ~~high~~ speed & starting

9. What do you think about minimization of occupant discomfort?

   design improvement on power train systems

Data collected from pilot study at National

Questions for pilot study

1. Is Minidor, Force three wheelers are available in this area?
   ☑ yes ☐ no
2. At what age range Minidor, Force drivers (users) are?
   From 18 years to 60 years drivers are available
3. What type of peoples do expect that mostly used Minidor, Force three wheelers?
   Every types of people specially younger community use it.
4. Have you seen Minidor, Force three wheelers caused vibration before?
   ☑ yes ☐ no
5. If your answer is yes, how vibration affect users?
   The vibration and sound of mindor bajaj are unpleasant
6. What do you think about the causes of the vibration?
   I think the causes of vibration are engine and suspension
7. What type of pain did frequently occur on the drivers?
   The Most frequently the vibration result to headache
8. At what condition do severity vibration increases?
   At Uncomfortable road type the vibration increases.
9. What do you think about minimization of occupant discomfort?
   Minidor bajar does not allow passenger a comfortable travel.

Data collected from pilot study at Gendehara

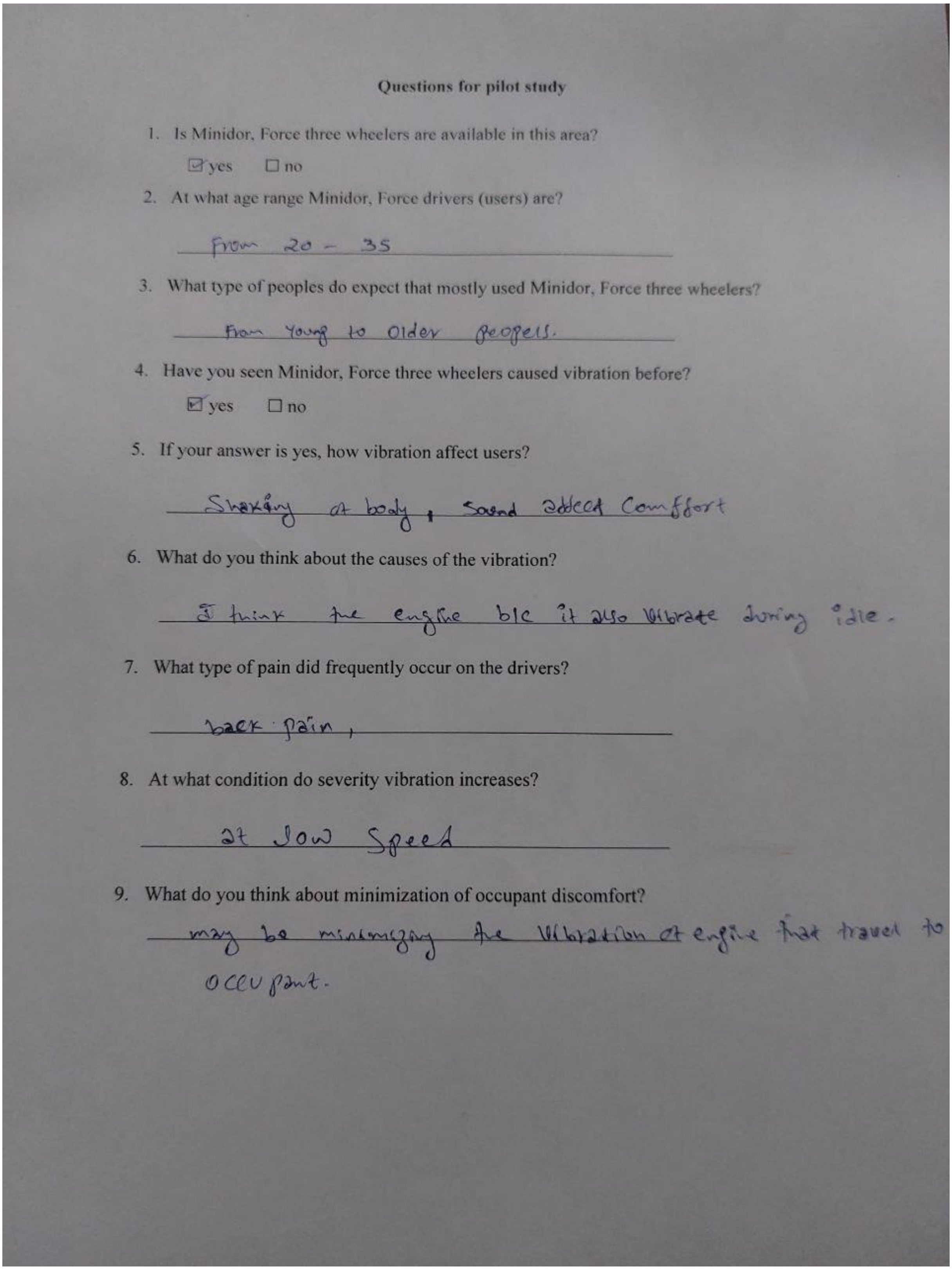

Questions for pilot study

1. Is Minidor, Force three wheelers are available in this area?

   ☑ yes ☐ no

2. At what age range Minidor, Force drivers (users) are?

   from 20 - 35

3. What type of peoples do expect that mostly used Minidor, Force three wheelers?

   From Young to Older peopels.

4. Have you seen Minidor, Force three wheelers caused vibration before?

   ☑ yes ☐ no

5. If your answer is yes, how vibration affect users?

   Shaking at body, Sound affect Comffort

6. What do you think about the causes of the vibration?

   I think the engine b/c it also vibrate during idle.

7. What type of pain did frequently occur on the drivers?

   back pain,

8. At what condition do severity vibration increases?

   at low Speed

9. What do you think about minimization of occupant discomfort?

   may be minimizing the vibration of engine that travel to occupant.

Appendix – D

Data collected from Federal Transport Minister

From Information Communication Technology Directorate

Type of Vehicles and Number in the Regions (up to Sene 2009) Registration												
Description	**AA**	**AM**	**AF**	**BN**	**DD**	**SO**	**TG**	**GM**	**HA**	**SN**	**OR**	**Total**
Ambulance	180	0	34	27	9	2	69	0	4	7	165	**497**
Automobile	171523	1485	55	34	1967	558	927	228	1275	51	6376	**184479**
Bajaj	0	2132	2302	0	0	0		0	536	4671	5152	**14793**
Tri Cyle	0	40	0	0	0	0	0	0	0	27	16861	**16928**
Bus(< 12 Seats)	25929	7146	442	260	1376	755	2799	0	0	50	126	**38883**
Bus(> 11 Seats)	14524	9747	372	229	457	537	1521	1375	357	178	2126	**31423**
Combiner	10	17	0	0	1	2	8	0	357	0	6322	**6717**
Dozer	0	0	3	0	0	1	5	0	20	0	252	**281**
Dry Cargo(<=10 Quintals)	34446	1602	273	94	847	953	733	0	176	95	1067	**40286**
Dry Cargo(>10 Quintals)	105150	4099	224	92	3916	2152	4372	0	2	15	527	**120549**
Dual Purpose Vehicle	43253	3443	339	255	1104	515	1665	0	36	21	131	**50762**
Field Vehicle	43681	1590	298	138	426	912	1034	0	445	16	7168	**55708**
Grader	5	2	0	0	1	1		0	3	0	17517	**17529**
Forklift	145	0	3	0	6	0	2	0	317	0	19880	**20353**
Not Specified	18370	8121	25	16	214	263	187		0	50762	13480	**91438**
Gotach	5178	0	0	0	57	0	308	0	1699	0	1305	**8547**
Liquid Cargo	5057	272	34	2	203	114	621	0	7	65	358	**6733**
Liquid Trailer	0	11	0	0	0	0		0	336	0	2189	**2536**
Motor Bicycle	21509	26442	1048	3237	5761	1157	5705	2166	0	4	642	**67671**
Other	9766	442	35	1	89	33	524	1353	72	22	3	**12340**
Three wheel dry load	8	0	0	6	2	166	65	0	1	0	263	**511**
Three wheel public load	506	0	0	1508	299	5145	5046	0	0	0	7	**12511**
Tractor	1027	281	46	124	20	0	184	0	0	1	239	**1922**
Trailer	23810	292	8	1	379	1	2485	0	0	0	13	**26989**
Vehicle with Machinery	367	135	14	1	109	27	62	0	0	0	164	**879**
Total	**524444**	**67299**	**5555**	**6025**	**17243**	**13294**	**28322**	**5122**	**5643**	**55985**	**102333**	**831265**

From Information Communication Technology Directorate

Type of Vehicles and Number in the Regions (up to Sene 30.2010) Registration												
Description	**AA**	**AM**	**AF**	**BN**	**DD**	**SO**	**TG**	**GM**	**HA**	**SN**	**OR**	**Total**
Ambulance	198	0	37	35	9	2	91	0	4	25	238	639
Automobile	184227	1485	59	49	2057	558	1421	228	1275	16162	4796	212317
Bajaj	0	2132	2644	0	289	0	0	0	536	8721	34339	48661
Tri Cyle	0	40	0	0	0	0	0	0	0	27	0	67
Bus(< 12 Seats)	26408	7146	448	324	1468	755	4768	0	0	709	14174	56200
Bus(> 11 Seats)	15242	9747	449	325	514	537	3335	1375	357	1144	22772	55797
Combiner	20	17	0	0	1	2	5	0	357	0	75	477
Dozer	16	0	3	3	0	1	5	0	20	0	0	48
Dry Cargo(<=10 Quintals)	37384	1602	289	101	890	953	1069	0	176	3070	7063	52597
Dry Cargo(>10 Quintals)	109952	4099	229	98	4089	2152	4886	0	2	1195	1810	128512
Dual Purpose Vehicle	44954	3443	348	301	1157	515	2063	0	36	1435	372	54624
Field Vehicle	45081	1590	303	148	447	912	1185	0	445	117	5421	55649
Grader	7	2	0	0	1	1	4	0	3	0	1	19
Forklift	188	0	4	1	6	0	13	0	317	0	2	531
Not Specified	18154	8121	32	25	222	263	602	0	0	1534	6020	34973
Gotach	5598	0	0	0	59	0	572	0	1699	0	0	7928
Liquid Cargo	6341	272	35	2	206	114	645	0	7	65	189	7876
Liquid Trailer	0	11	0	0	0	0	0	0	336	0	117	464
Motor Bicycle	22931	26442	1152	4129	5891	1157	10744	2166	0	49409	29378	153399
Other	9912	442	36	1	88	33	494	1353	72	36	1763	14230
Three wheel dry load	12	0	0	24	2	166	888	0	1	0	4	1097
Three wheel public load	375	0	0	1909	0	5145	9962	0	0	0	0	17391
Tractor	1059	281	46	134	21	0	265	0	0	7	503	2316
Trailer	25336	292	8	1	394	1	2793	0	0	0	302	29127
Vehicle with Machinery	543	135	15	1	113	27	115	0	0	0	0	949
Total	**553938**	**67299**	**6137**	**7611**	**17924**	**13294**	**45925**	**5122**	**5643**	**83656**	**129339**	**935888**

From Information Communication Technology Directorate

Type of Vehicles and Number in the Regions (up to Sene 30.2011) Registration

Description	AA	AM	AF	BN	DD	SO	TG	GM	HA	SN	OR	Total
Ambulance	253	0	38	44	7	14	164	0	4	28	365	917
Automobile	205773	1701	66	49	2246	609	1660	228	1275	80	6012	219699
Bajaj	0	4722	2889	0	2318	0	0	0	536	9307	48822	68594
Tri Cyle	0	37	0	0	0	0	0	0	0	27	0	64
Bus(< 12 Seats)	27357	8805	465	347	1607	837	5201	0	0	12503	3024	60146
Bus(> 11 Seats)	16698	12840	532	378	681	677	3886	1375	357	10029	38439	85892
Combiner	23	53	0	0	1	2	5	0	357	0	78	519
Dozer	17	0	3	3	0	1	5	0	20	0	0	49
Dry Cargo(<=10 Quintals)	41333	2396	301	102	993	1036	1163	0	176	102	1868	49470
Dry Cargo(>10 Quintals)	115023	4591	240	103	4313	2348	5030	0	2	153	7188	138991
Dual Purpose Vehicle	47278	3907	380	310	1370	684	2188	0	36	1438	97	57688
Field Vehicle	47059	1767	318	153	487	1037	1228	0	445	123	3299	55916
Grader	6	2	0	0	2	1	4	0	3	0	2	20
Forklift	237	0	4	1	8	0	18	0	317	0	2	587
Not Specified	18943	1462	34	48	248	0	396	436	1179	3118	7929	33793
Gotach	5756	0	0	0	67	2	613	0	1699	0	0	8137
Liquid Cargo	6703	318	35	2	226	148	650	0	7	65	437	8591
Liquid Trailer	0	14	0	0	0	0	0	0	336	0	187	537
Motor Bicycle	24700	40229	1181	4865	6689	1366	12358	2166	1178	54084	49903	198719
Other	10279	643	36	1	105	33	485	1353	72	38	2905	15950
Three wheel dry load	15	9625	0	39	7	233	1417	0	1	0	4	11341
Three wheel public load	368	0	0	2259	0	6106	12953	0	0	0	0	21686
Tractor	1199	392	51	136	21	0	304	0	0	10	530	2643
Trailer	26326	349	8	1	417	1	2891	0	0	0	217	30210
Vehicle with Machinery	738	148	17	1	125	25	132	0	0	0	0	1186
Total	**596084**	**94001**	**6598**	**8842**	**21938**	**15160**	**52751**	**5558**	**8000**	**91105**	**171308**	**1071345**

From Information Communication Technology Directorate

Type of Vehicles and Number in the Regions (up to sene 30.2012) Registration												
Description	**AA**	**AM**	**AF**	**BN**	**DD**	**SO**	**TG**	**GM**	**HA**	**SN**	**OR**	**Total**
Ambulance	303	0	82	55	6	45	187	0	4	58	438	1178
Automobile	222683	1786	83	53	2360	648	1994	322	1303	98	5258	236588
Bajaj	0	9308	3925	0	3086	0	0	0	4909	11325	55462	88015
Tri Cyle	0	0	0	0	0	0	0	0	0	0	0	0
Bus(< 12 Seats)	28432	9197	493	375	1656	979	5656	2125	80	13300	27315	89608
Bus(> 11 Seats)	17707	13953	678	467	786	871	4473	859	3000	9617	32289	84700
Combiner	27	54	0	0	1	1	5	0	0	0	79	167
Dozer	16	0	3	3	0	1	4	0	0	0	0	27
Dry Cargo(<=10 Quintals)	44898	3597	338	105	1041	1104	1298	0	0	1577	1839	55797
Dry Cargo(>10 Quintals)	119032	3653	259	108	4522	2604	5148	0	0	3612	7325	146263
Dual Purpose Vehicle	49234	4068	461	330	1569	989	2266	0	56	1701	2889	63563
Field Vehicle	48837	1835	371	160	507	1148	1282	330	300	149	3037	57956
Grader	5	2	0	0	2	1	4	0	0	0	2	16
Forklift	281	0	4	1	9	1	18	0	0	0	2	316
Not Specified	19955	1532	71	56	283	511	397	231	0	295	1650	24981
Gotach	5854	0	0	0	66	5	624	0	0	0	0	6549
Liquid Cargo	6866	313	37	2	241	186	658	0	0	67	181	8551
Liquid Trailer	0	14	0	0	0	0	0	0	0	0	171	185
Motor Bicycle	25726	45137	1355	6108	7656	1651	14405	2370	1076	76565	61386	243435
Other	10786	718	35	30	124	33	485	0	0	43	3796	16050
Three wheel dry load	16	42	0	50	9	250	1874	0	0	0	4	2245
Three wheel public load	356	10311	0	2612	0	8523	16647	0	0	0	0	38449
Tractor	1325	401	54	138	21	0	317	0	0	16	526	2798
Trailer	27266	360	8	1	431	1	2913	0	0	1	377	31358
Vehicle with Machinery	835	153	20	1	134	27	145	0	0	0	0	1315
Total	**630440**	**106434**	**8277**	**10655**	**24510**	**19579**	**60800**	**6237**	**10728**	**118424**	**204026**	**1200110**

From Information Communication Technology Directorate

Type of Vehicles and Number in the Regions (up to sene 30.2013) Registration												
Description	**AA**	**AM**	**AF**	**BN**	**DD**	**SO**	**TG**	**GM**	**HA**	**SN**	**OR**	**Total**
Ambulance	322	0	90	56	6	45	187	0	4	65	590	1365
Automobile	255793	1834	86	56	2413	648	1994	0	1303	104	5758	269989
Bajaj	0	11381	4608	0	3302	0	0	1439	4909	12901	65218	103758
Tri Cyle	0	0	0	0	0	0	0	0	0	0	0	0
Bus(< 12 Seats)	31330	9787	494	393	1666	979	5656	2125	80	13874	29068	95452
Bus(> 11 Seats)	19206	14802	713	526	860	871	4473	859	3000	12579	39631	97520
Combiner	106	61	0	0	2	1	5	0	0	0	78	253
Dozer	16	1	3	3	0	1	4	0	0	0	0	28
Dry Cargo(<=10 Quintals)	52338	3825	351	109	1083	1104	1298	0	0	176	2187	62471
Dry Cargo(>10 Quintals)	139376	3767	267	117	4670	2604	5148	0	0	233	8201	164383
Dual Purpose Vehicle	56063	4258	486	343	1704	989	2266	0	56	1712	3028	70905
Field Vehicle	53233	2066	389	164	524	1148	1282	0	300	206	3266	62578
Grader	6	2	0	0	2	1	4	0	0	0	2	17
Forklift	351	0	4	1	10	1	18	0	0	0	2	387
Not Specified	21185	1621	72	57	327	511	397	0	0	2540	2293	29003
Gotach	7235	0	0	0	67	5	624	0	0	0	0	7931
Liquid Cargo	8307	331	39	2	244	186	658	0	0	67	184	10018
Liquid Trailer	0	14	0	0	0	0	0	0	0	0	0	14
Motor Bicycle	28235	48997	1454	7385	8111	1651	14405	2643	1076	80466	63359	257782
Other	12526	778	35	39	137	33	485	0	0	44	4304	18381
Three wheel dry load	17	281	0	56	10	250	1874	0	0	0	9	2497
Three wheel public load	350	13807	0	3111	0	8523	16647	0	0	0	0	42438
Tractor	1505	415	54	146	21	0	317	0	0	33	1015	3506
Trailer	32676	381	8	1	450	1	2913	0	0	1	408	36839
Vehicle with Machinery	1004	158	21	1	134	27	145	0	0	0	0	1490
Total	**721180**	**118567**	**9174**	**12566**	**25743**	**19579**	**60800**	**7066**	**10728**	**125001**	**228601**	**1339005**

ማሳሰቢያ፡- የአዲስ አበባ ተሽከርካሪ ከሁሉም ክፍለከተሞች የተሰበሰበው መረጃ መርጅ በሚደረግበት ጊዜ ካለፈው ቁጥር ጋር ሲነፃፀር ዝቅ በማለቱ ከ6ወር በፊት በተሰጠው መረጃ መሰረት እንዲሆን እንገልፃለን፡፡